

Catalog No. L52280



**In-Situ Measurement of Pipeline Mechanical Properties Using
Stress-Strain Microprobe –
Validation of Data for Increased Confidence & Accuracy**

Contract PR-345-063517

**Prepared for the
Materials**

of

Pipeline Research Council International, Inc.

**Prepared by the following Research Agencies:
Advanced Technology Corporation**

Authors:

Fahmy M. Haggag

Publication Date:

April 1, 2007

“This report is furnished to Pipeline Research Council International, Inc. (PRCI) under the terms of PRCI PR-345-063517, between PRCI and Advanced Technology Corporation. The contents of this report are published as received from Advanced Technology Corporation. The opinions, findings, and conclusions expressed in the report are those of the authors and not necessarily those of PRCI, its member companies, or their representatives. Publication and dissemination of this report by PRCI should not be considered an endorsement by PRCI or Advanced Technology Corporation, or the accuracy or validity of any opinions, findings, or conclusions expressed herein.

In publishing this report, PRCI makes no warranty or representation, expressed or implied, with respect to the accuracy, completeness, usefulness, or fitness for purpose of the information contained herein, or that the use of any information, method, process, or apparatus disclosed in this report may not infringe on privately owned rights. PRCI assumes no liability with respect to the use of, or for damages resulting from the use of, any information, method, process, or apparatus disclosed in this report.

The text of this publication, or any part thereof, may not be reproduced or transmitted in any form by any means, electronic or mechanical, including photocopying, recording, storage in an information retrieval system, or otherwise, without the prior, written approval of PRCI.”

Pipeline Research Council International Catalog No. L52280

Copyright, 2007

All Rights Reserved by Pipeline Research Council International, Inc.

PRCI Reports are Published by **Technical Toolboxes, Inc.**



3801 Kirby Drive, Suite 340
Houston, Texas 77098
Tel: 713-630-0505
Fax: 713-630-0560
Email: info@toolboxes.com

Contents

Executive Summary	1
Acknowledgement	2
1.0 Introduction	2
2.0 Objectives	3
3.0 Testing Procedures	3
3.1 ABI Testing	3
3.2 Tensile Testing	4
3.3 Destructive Fracture Toughness Testing	4
3.4 Haggag Toughness Method (HTM)	4
3.4.1 The Critical Fracture Stress (σ_f)	5
3.4.2 Critical Fracture Strain Model	5
3.5 Tensile and Fracture Toughness Specimen Geometries and Test Setups	8
4.0 Results	10
4.1 ABI-Measured Tensile Properties and Comparisons with Results from Destructive Tensile Tests	13
4.2 ABI-Measured Fracture Toughness (K_{Jc}) Values and Comparisons with Results from Destructive Fracture Toughness Tests	20
4.3 ABI-Measured Tensile and Fracture Toughness Tests on Sections of Pipelines	21
4.4 Results from ABI tests and from 0.5T CT Fracture Toughness Specimens of BP Storage Tank Material	24
4.4.1 Discussion on Application of Critical Fracture Stress and Critical Fracture Strain Models	31
References	33
APPENDIX A	35
APPENDIX B	36
APPENDIX C	61
APPENDIX D	66
APPENDIX E	77

List of Tables

Table 1 Critical Fracture Stress of Ferritic Steels as a Function of Test Temperature.....	6
Table 2 Summary of tensile properties from the certificates of pipelines received from Shell.....	12
Table 3 Comparison between yield strength measured from ABI and tensile tests	16
Table 4 Comparison between tensile strength measured from ABI and tensile tests.....	18
Table 5 Comparison of fracture toughness values from ABI tests (conducted on end tabs of miniature tensile specimens using the Haggag Toughness Method) and from disk compact fracture toughness specimens	21
Table 6 Summary of ABI test results on pipeline sections (5 tests conducted on each material) .	22
Table 7 Summary of tensile test results	24
Table 8 Summary of results from 3 ABI test conducted on end tabs of the three tensile specimens	24
Table 9 Summary of all 15 ABI tests at room temperature (3 on mini-tensile and 12 on two fracture toughness specimens), English units	25
Table 10 Summary of all 15 ABI tests at room temperature (3 on mini-tensile and 12 on two fracture toughness specimens), SI units.....	25
Table 11 Summary of fracture toughness results from tests conducted at room temperature.....	26
Table 12 Fracture toughness results from tests conducted at low temperatures.....	28
Table 13 Summary of fracture toughness results from 9 ABI tests conducted at low temperatures	30
Table 14 ABI-measured tensile and fracture toughness properties from 6 ABI tests conducted ..	31
at -100°C	31

Table of Figures

Fig. 1 The testing head of the miniature SSM system (Model SSM-M1000) is mounted using electric magnets on steel pipelines.....	7
Fig. 2 The bench-top SSM system (Model SSM-B4000).....	7
Fig. 3 Dimensions of the miniature tensile specimen.....	8
Fig. 4 Dimensions of the 0.18T disk compact fracture toughness specimen (for all pipeline materials).....	8
Fig. 5 Dimensions of the 0.5T compact tension fracture toughness specimen (for BP tank steel).	9
Fig. 6 Destructive fracture toughness testing setup using the environmental chamber of the bench-top SSM system (Model SSM-M4000).	9
Fig. 7 Photo of the four pipelines received from Shell (grades X42, X52, X60, and X65).....	10
Fig. 8 Photo of all 9 pipeline sections.....	11
Fig. 9 Photographs of both surfaces of the 9-inch diameter steel trepan from a BP storage tank.	11
Fig. 10 Sample of the engineering stress-strain curves of five pipeline materials	12
Fig. 11 Sample of the true-stress versus true-plastic-strain curves (ASTM Standard E646) of five pipeline materials.....	13
Fig. 12 Sample of ABI force-depth data.....	14
Fig. 13 Sample of ABI-measured true-stress/true-plastic-strain curves	14
Fig. 14 Overlay of the true-stress/true-plastic-strain curves from ABI and tensile tests.....	15
Fig. 15 Overlay of the true-stress/true-plastic-strain curves from ABI and tensile tests.....	15

Fig. 16 Fracture surfaces of all disk compact fracture toughness specimens	20
Fig. 17 Fracture surfaces and test temperatures of the 10 fracture toughness specimens.	26
Fig. 18 Overlay of the load versus crack opening displacement (COD)	27
Fig. 19 Overlay of J-Integral versus Crack Extension graphs	27
Fig. 20 Fracture toughness Master Curve developed from 15 ABI tests.....	28
Fig. 21 Overlay of load versus COD graphs from 6 fracture toughness tests	29
Fig. 22 Fracture toughness master curves.....	29
Fig. 23 Fracture toughness master curves from six ABI tests	30
Fig. 24 Fracture toughness plotted versus normalized test temperature ($T - T_0$)	31
Fig. 25 Example of the use of the critical fracture stress model to determine the critical indentation depth.....	32
Fig. 26 Example of the use of the critical fracture strain model when testing a ductile material at room temperature	32

This Page Intentionally Left Blank

In-Situ Measurement of Pipeline Mechanical Properties Using Stress-Strain Microprobe® - Validation of Data for Increased Confidence & Accuracy

Executive Summary

Most pipeline operators carry infrastructure that spans a wide range of vintages including pipelines that were built in 1950s to the 2000s. Some of the pipelines have changed hands, and in many cases, more than once, resulting in a loss of the operating history and of pertinent pipeline data relating to the grade or mechanical properties. In the case of pipelines of unknown grades, OPS/DOT stipulates the assumption of a 24 ksi yield strength, regardless of its construction. OPS also allows the establishment of the Specified Minimum Yield Strength (SMYS) of the pipeline by verifying its yield strength by carrying out a statistically valid number of sampling. Conventional tensile testing requires the removal of samples from the pipeline for testing which results in temporary line shut down and loss of transmission service. The constructability issues around this are complex, and it requires line repair after sample extraction. In addition, this will result in a loss of throughput and consequently disrupting the hydrocarbon supply.

Stress-Strain Microprobe® (SSM) testing using the Automated Ball Indentation (ABI) technique has emerged as a viable nondestructive method for measuring the yield and tensile strength values (hence, determining the SMYS and SMTS) and fracture toughness (K_{Jc}) properties of in-service pipeline materials (base and welds), in-situ and without any service interruption. Advanced Technology Corporation (Oak Ridge, TN), the developer of this patented SSM system, has been offering the commercial equipment worldwide since 1991, and in-situ SSM/ABI pipeline testing services (in favor with several pipeline operators in USA and Europe) since 1999.

The two goals of this project have been successfully accomplished. The first phase generated adequate ABI-measured yield and tensile strength results that correlated accurately to actual physical tensile test data on various grades of steel including Grade B, X42, X52, X60, and X65. Multiple (6-8) destructive tensile tests and nondestructive ABI tests were conducted on the base metal of five pipelines and on the seam welds of four pipelines. The average yield strength (YS) and tensile strength (TS) values from both ABI and tensile test techniques were within 10% and 6% for the YS and TS, respectively. The standard deviation of all ABI results for each grade was very small (less than 5% or 2-5 ksi). The reliable and accurate ABI-measured tensile properties can be used to calculate a safe higher/efficient maximum transmission pressure using the ABI-determined SMYS and SMTS values from in-situ/nondestructive testing of undocumented/(unknown grades) pipelines. In the second phase of this project, the fracture toughness measurements (using the Haggag Toughness Method “HTM” of the ABI technique) were correlated with actual K_{Jc} test data from 37 fracture toughness specimens spanning several grades of pipeline base metal and seam weld materials and a tank steel material supplied by BP. The average fracture toughness values from the ABI tests were within 12% of the average values for all tested steel materials. Furthermore, crack-tip-opening displacement (CTOD) values were estimated from the ABI-determined K_{Jc} values for the nine pipeline steel materials. The ABI-determined fracture toughness values are very accurate, reliable, always valid (geometry/pipeline thickness independent), and have a very small standard deviation as compared to those from destructive fracture toughness tests. This in-situ determination of fracture toughness will be invaluable for fitness-for-service calculations of pipelines using fracture mechanics.

In brief, the adequate amount of data from the nondestructive ABI tests and the destructive tensile and fracture toughness tests provides reasonable statistical data sets to establish the validity and accuracy of the ABI technique which produces both tensile and fracture toughness properties from each single test. The ABI test (accomplished in less than two minutes) is now proven to replace both the tensile and fracture toughness tests without specimen machining or service interruption, and it requires only localized surface polishing of in-service pipelines.

This Page Intentionally Left Blank

Acknowledgement

ATC gratefully acknowledges PRCI and Shell Pipeline Company for their leadership and support of this project. ATC would like to thank Ken Lorang and Scott Thetford of PRCI for overseeing the project. Brent Byrd and Damodaran Raghu from Shell Pipeline Company initiated this project and provided pipeline materials and witnessed part of the testing at ATC's facility. Also, ATC would like to thank Mike Silverman of BP for allowing the use of BP's data on tank steel in this report.

1.0 Introduction

Our transportation networks of oil and gas pipelines are aging and their structural integrity must be monitored periodically, particularly those installed in high-consequence areas. Concerns over pipeline rehabilitation are coupled with meeting the current and future energy demands through safely increasing the transmission throughput. Most pipeline operators carry infrastructure that spans a wide range of vintages including pipelines that were built in 1950s to the 2000s. Some of the pipelines have changed hands, and in many cases, more than once, resulting in a loss of the operating history and of pertinent pipeline data relating to the grade or mechanical properties. In the case of pipelines of unknown grades, OPS/DOT stipulates the assumption of a 24 ksi yield strength, regardless of its construction. OPS also allows the establishment of the Specified Minimum Yield Strength (SMYS) of the pipeline by verifying its yield strength by carrying out a statistically valid number of sampling. Conventional tensile testing requires the removal of samples from the pipeline for testing which results in temporary line shut down and loss of transmission service. The constructability issues around this are complex, and it requires line repair after sample extraction.

Stress-Strain Microprobe® (SSM) testing using the Automated Ball Indentation (ABI) technique has emerged as a viable nondestructive method for measuring the yield and tensile strength values (hence, determining the SMYS and SMTS) and fracture toughness (K_{Ic}) properties of in-service pipeline materials (base and welds), in-situ and without any service interruption. Advanced Technology Corporation (Oak Ridge, TN), the developer of this patented SSM system, has been offering the commercial equipment worldwide since 1991, and in-situ SSM/ABI pipeline testing services (in favor with several pipeline operators in USA and Europe) since 1999. The ABI tests provide the actual/current values of the key mechanical properties for base metal, welds, and heat-affected-zones. The SSM-measured tensile and fracture toughness properties are used with other nondestructive measurements such as crack size (determined from either in-line/smart-pig runs or off-line ultrasound devices) or corrosion pits to determine the safe operating pressure of the pipeline or to necessitate certain actions of rehabilitation. In addition to fitness-for-service assessment of aging pipelines, the ABI tests are also applicable for the quality assurance/control of girth welds of newly constructed pipelines, including high strength steels such as grades X80 to X120.

The Automated Ball Indentation (ABI) test technique was invented in 1989 to measure key mechanical properties of metallic samples and structures in a nondestructive and localized fashion. A single ABI test replaces the tension test for metallic materials and the fracture toughness test for ferritic steels. The laboratory version of the patented Stress-Strain Microprobe® (SSM) technology with its ABI test technique has been in commercial use since 1991, and the portable/*in-situ* SSM version received a 1996 R&D 100 Award as one of the 100 most technologically significant new products of the year. Furthermore, in 1999, Advanced Technology Corporation (ATC) introduced a new miniature SSM system to provide even greater portability and easier field/*in-situ* applicability. The SSM technology and its ABI technique and test results have been reviewed by the office of Pipeline Safety of the US DOT and are recommended for use by the pipeline industry (see attached DOT review letter in Appendix A). The

ABI-measured tensile and fracture toughness results provide the basis for deterministic fracture mechanics assessment, allow robust fitness-for-service assessments of aged/undocumented infrastructure, and improve the effectiveness and efficiency of quality control inspections for production, new alloy development, and welding. The ABI test method procedure, data analysis, and precision values from a comprehensive round robin program are given in Appendix B.

The ABI test technique is described in details in many publications.¹⁻¹⁸ The ABI technique is nondestructive and localized and is a sophisticated mechanical test technique that can be applied to small samples as well as to metallic components, such as pipelines and storage tanks in the field. These capabilities of the ABI technique and the SSM technology are advantageous and desirable for testing aged or undocumented components and for structural integrity evaluation. Furthermore, in addition to the nondestructive and localized ABI stress-strain curve measurements, the ABI technique of the SSM system provides localized and nondestructive fracture toughness properties (highly desirable for small welds and heat affected zones where valid results might not be obtainable from the conventional destructive fracture toughness tests due to thickness/width limitation). The determination of fracture toughness properties from ABI tests is described in References 14 through 18. *Example calculations and applications of the ABI-determined fracture toughness values, using the Haggag Toughness Method (HTM), are given in details in Reference 16.*

The ABI test is based on progressive indentation at the same location with intermediate partial unloadings until the desired maximum depth (strain) is reached, and then the indenter is fully unloaded. The indentation force-depth data are collected continuously during the test using a 16-bit data acquisition system. The nonlinear/spherical geometry of the tungsten carbide indenter allows increasing strain as the indentation penetration depth is increased. Hence, the incremental values of indentation force and plastic depth (associated with each partial unloading cycle) are converted to incremental values of true-stress and true-plastic-strain according to elasticity and plasticity theories.³ Since the ABI test is multi-axial in nature, the stress triaxiality underneath the indenter increases with depth and can reach high values similar to those ahead of a crack tip; hence, fracture toughness values can be determined from the ABI tests.¹⁴⁻¹⁸ The ABI test is considered practically nondestructive because the test leaves only a small, shallow, spherical depression with a smooth surface (i.e., no sharp edges/cracks and no stress concentration sites), and it leaves a compressive residual stress (that retards crack initiation) in the test surface area. Each ABI test is very similar to a single shot peen, albeit slightly larger.

2.0 Objectives

The objectives of this project are to: (1) generate adequate amount of tensile properties from the nondestructive ABI tests to correlate with the physical results from destructive/conventional tensile tests, and (2) generate ABI-determined fracture toughness data to correlate with those from destructive fracture toughness tests in order to provide reasonable statistical data sets to increase the confidence and to establish the accuracy of the ABI technique which produces both tensile and fracture toughness properties from each single test.

3.0 Testing Procedures

3.1 ABI Testing

Multiple (6-8) ABI tests were conducted at ambient temperature, using a 0.762-mm (0.030-inch) diameter tungsten carbide indenter, on pipeline base metal and seam welds. Also, ABI tests were conducted at room and low temperatures on a storage tank steel supplied by BP. The patented *In-Situ* SSM system (Model SSM-M1000) is shown in Fig. 1 . Photograph of the bench-top SSM system (Model SSM-B4000) used to perform ABI and destructive tensile and fracture toughness tests of samples at low temperatures is shown in Fig. 2.

3.2 Tensile Testing

Multiple specimens were machined from the axial and circumferential orientations of the base metal of five grades of pipelines and from the axial orientation of seam welds of four grades of pipelines. All tests were accomplished according to ASTM Standard E8 at room temperature.

3.3 Destructive Fracture Toughness Testing

Triplicates or more compact disk fracture toughness specimens (0.18T) were machined from base metal and seam weld pipeline materials and tested at room temperature according to ASTM Standard E1820 using the single specimen unloading compliance technique. Few samples were tested at low temperatures. Ten 0.5T CT specimens were machined from the BP tank steel materials and 8 specimens were tested at low temperatures to determine the reference temperature according to the fracture toughness master curve concept (ASTM Standard E1921).

For ferritic steels (with yield strength of 275 to 825 MPa or 40-120 ksi) the fracture toughness (median value) versus temperature curve in the transition temperature region is expressed by the master curve (ASTM E-1921-97):

$$K_{Jc} (med) = 30 + 70 e^{0.019(T-T_0)} \quad \text{MPa} \sqrt{\text{m}} \quad (1)$$

Where T is the test temperature and T_0 is the reference temperature when $K_{Jc} = 100 \text{ MPa}\sqrt{\text{m}}$.

In order to obtain median dynamic fracture toughness (K_{Id}) values as a function of temperature, the ASTM Standard E1921-97 equation of the static fracture toughness (K_{Jc}) master curve (Reference 19) can be used provided that the reference temperature be shifted to a higher value that depends on the yield strength of the test material at room temperature. It is well known that the dynamic fracture toughness curve is shifted to the right hand-side of the static fracture toughness curve by a temperature shift value depending on the room-temperature yield strength of the ferritic steel material.

The median dynamic fracture toughness (K_{Id}) can be calculated from the following equation:

$$K_{Id} (med) = 30 + 70 e^{0.019(T-[T_0+T_{shift}])} \quad \text{MPa} \sqrt{\text{m}} \quad (2)$$

Where T is the test temperature in °C and T_0 is the reference temperature when $K_{Jc} = 100 \text{ MPa}\sqrt{\text{m}}$. The T_{shift} can be determined from the Barsom correlation [Ref. 20] and using the average yield strength measured from multiple ABI tests at room temperature. The Barsom correlation is given by:

$$T_{shift} (^{\circ}F) = 215 - 1.5\sigma_{ys} (ksi) \quad \text{for } 36 \text{ ksi} < \sigma_{ys} < 140 \text{ ksi} \quad (3)$$

where σ_{ys} is the room-temperature yield strength of the steel material.

3.4 Haggag Toughness Method (HTM)

The Haggag Toughness Method (HTM) determines the fracture toughness (K_{Jc}) value from the ABI test on ferritic steel materials by integrating the indentation deformation energy (compression of the two surfaces of the ball indenter and the test material instead of pulling two surfaces in a destructive fracture toughness test) from the beginning of the test up to a critical indentation depth. The latter is calculated using either the critical fracture stress model or the critical fracture strain model; depending on the flow properties of the material at the test temperature. The analysis first checks the attainment of the critical fracture stress (using the mean pressure plot as a function of normalized indentation depth) before a strain value of 12% or a normalized depth of 0.6. If this occurs then the test is analyzed according to this model and all ABI test results can be further analyzed using the fracture toughness master curve concept and a

reference temperature is determined in order to evaluate the brittle behavior of the test material at low temperatures. If the critical fracture stress is not attained prior to a normalized depth of 0.6 then the specimen is analyzed according to the critical fracture strain model and further analysis using the fracture toughness master curve becomes invalid (or if used it will produce a very conservative reference temperature since the test material is in the ductile temperature region instead of the transition region).

Indentation with a ball indenter generates concentrated stress (and strain) fields near and ahead of the contact of the indenter and the test surface, similar to concentrated stress fields ahead of a crack tip; albeit the indentation stress fields are mostly compressive. The high value of the stress under the ball indenter is an example of *plastic constraint* where the rigid material surrounding the indentation volume does the constraining. Hence, at a certain critical ball indentation depth, there is a high state of transverse and lateral stresses similar to those in front of a sharp notch in an elastic material. Although the conditions for crack initiation might be attained, the high degree of plastic constraint will prevent cracks from developing during ball indentation of ductile metallic materials. Therefore, only initiation fracture toughness, not tearing modulus, can be determined from ball indentation (Equations 6-12 on page 60 of Ref. 18). The initiation fracture toughness is calculated from the integration of the indentation deformation energy (*IDE*) up to the critical depth (when the maximum pressure underneath the ball indenter equals the critical fracture stress of the steel material at the test temperature or reaches a critical strain value of 0.12, whichever occurs first).

The ABI-measured fracture toughness capability is material-thickness independent since different size indenters can be used for all pipelines and pressure vessels in order to achieve valid results. Furthermore, its localized nature allows testing heat-affected-zones that cannot be tested destructively because of their irregular shapes and small volumes.

3.4.1 The Critical Fracture Stress (σ_f): The σ_f value as a function of test temperature was calculated using the semi-empirical Equation 4 and the fracture toughness and yield strength values of nuclear pressure vessel steel material from Oak Ridge National Laboratory (Ref. 14). Using Equation 4 and the ORNL data produces the tabulated values of critical fracture stress as a function of test temperature shown in Table 1.

$$\sigma_f = \sigma_y \left[1 + \ln \left(1 + 2360 \left(\frac{K_{Ic}}{\sigma_y} \right)^2 \right) \right] = 1.1 P_m \quad (4)$$

Where P_m is the mean pressure underneath the spherical indenter, “ln” is the natural logarithm, and K_{Ic} is the cleavage fracture toughness. The maximum stress ($1.1 P_m$) increases as the ABI depth increases and when it reaches the critical fracture stress value at the ABI test temperature before attaining a normalized depth of $d_t/D = 0.6$ (i.e., 12% strain), then the test is analyzed according to the critical fracture stress model and the concept of fracture toughness master curve is applicable where the reference temperature is determined from a minimum of 3 ABI tests. Numerous ABI tests conducted on various ferritic steels at low-test temperatures produced reference temperatures that are within 5°C from those determined from destructive fracture toughness specimens tested according to ASTM Standards E1820 and E1921.

3.4.2 Critical Fracture Strain Model: If the maximum stress (equal to the critical fracture stress at the ABI test temperature) is not reached before a normalized indentation depth of $d/D = 0.6$ (i.e., 12% strain where “d” is the indentation chordal diameter on the sample surface and “D” is the indenter diameter), then the test is analyzed using the critical fracture strain model by integrating the indentation deformation energy (mean pressure as a function of depth) up to an empirically conservative depth value of 12% strain. Since localized cooling of an ABI test area of an in-service structure (a pipeline or a storage tank, etc.) is not practical or safe, the reasonably conservative (within 10%) fracture toughness values obtained

from a minimum of 3 ABI tests, analyzed using the critical fracture strain model, can be used to determine a very conservative reference temperature (up to 70C° higher than that if the critical fracture stress model was applied on samples tested at low temperatures).

Table 1 Critical Fracture Stress of Ferritic Steels as a Function of Test Temperature

Test Temperature, (°C)	Critical Fracture Stress, σ_f (MPa)	Critical Fracture Stress, σ_f (ksi)
-100	2275	330
-90	2280	331
-80	2295	333
-70	2322	337
-60	2363	343
-50	2417	351
-40	2488	361
-30	2575	373
-20	2680	389
-10	2804	407
0	2949	428
10	3115	452
20	3304	479



Fig. 1 The testing head of the miniature SSM system (Model SSM-M1000) is mounted using electric magnets on steel pipelines.



Fig. 2 The bench-top SSM system (Model SSM-B4000) is shown above with all optional accessories including an environmental chamber for low and high temperature testing. ATC's patented SSM systems have been in use worldwide since 1991. In addition to performing the innovative ABI tests, the bench-top systems are also state-of-the-art universal testing machines that perform destructive tensile and fracture toughness tests.

3.5 Tensile and Fracture Toughness Specimen Geometries and Test Setups

Tensile specimens and fracture toughness specimens were machined according to the dimensions of Fig. 3 (tensile),

Fig. 4 (0.18T disk compact for all pipeline materials), and

Fig. 5 (0.5T compact tension specimens of BP tank steel material). The fracture toughness setup is shown in Fig. 6.

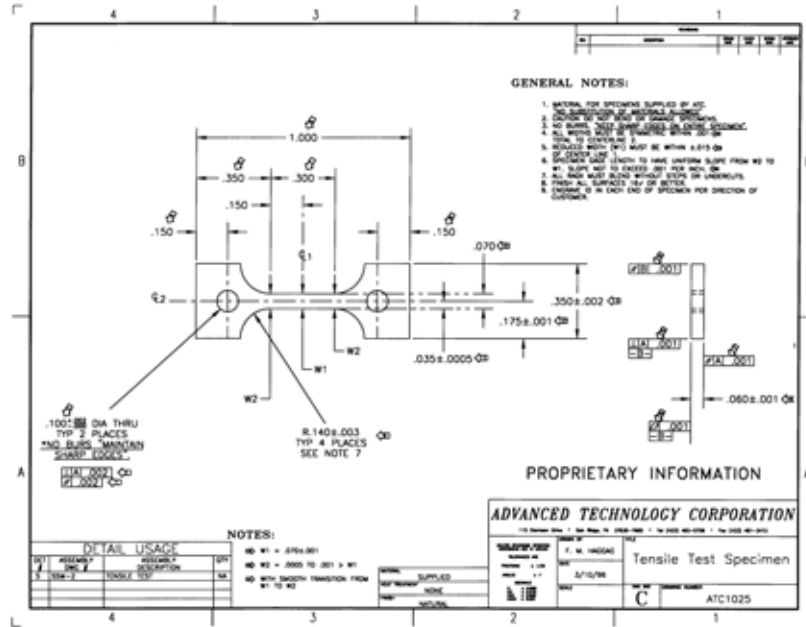


Fig. 3 Dimensions of the miniature tensile specimen.

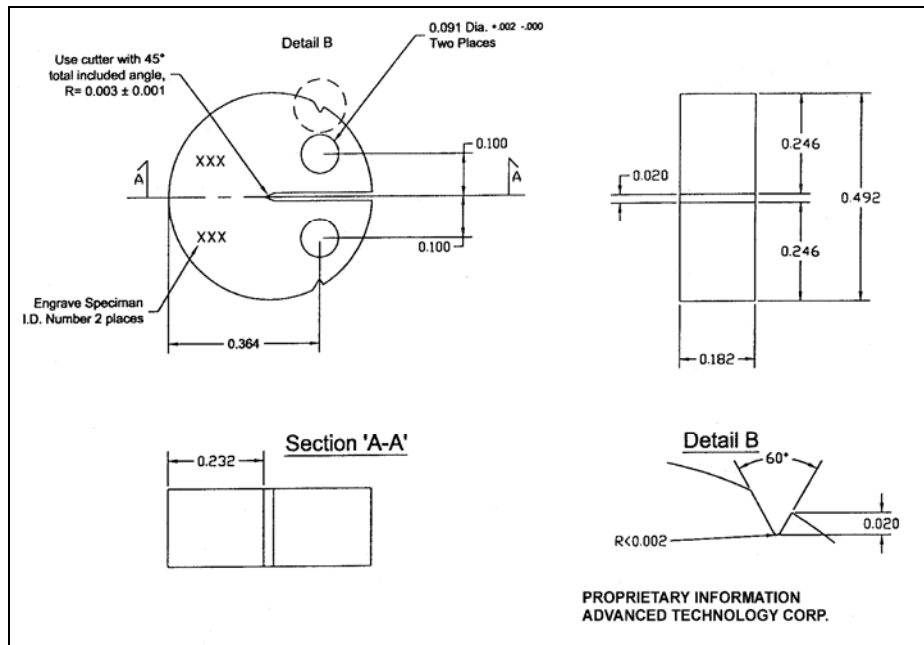


Fig. 4 Dimensions of the 0.18T disk compact fracture toughness specimen (for all pipeline materials).

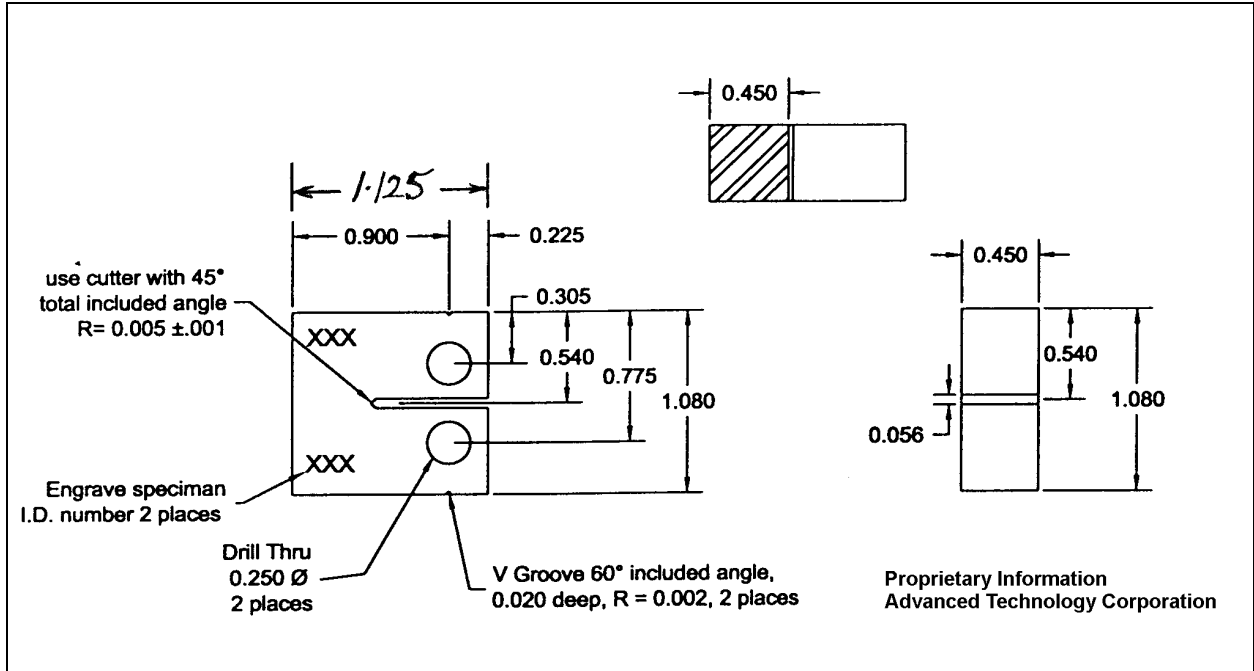


Fig. 5 Dimensions of the 0.5T compact tension fracture toughness specimen (for BP tank steel).



Fig. 6 Destructive fracture toughness testing setup using the environmental chamber of the bench-top SSM system (Model SSM-M4000).

4.0 Results

A photo of the four 6-ft long pipelines received from Shell Pipeline Company is shown in Fig. 7. The four material certificates are given in Appendix C and their tensile properties are summarized in Table 2. A small 12-inch section of an undocumented Grade B was also received from Shell. Tensile and fracture toughness specimens were machined from the base metal and seam welds of these materials. Also, small sections were cut from all long pipelines for ABI testing on these sections (see nine sections in Fig. 8). Also, 9-inch diameter x 1.25-inch thick trepan was supplied by BP from a storage tank (Fig. 9).



Fig. 7 Photo of the four pipelines received from Shell (grades X42, X52, X60, and X65).



Fig. 8 Photo of all 9 pipeline sections (Grade B base metal, X42 BM, X52 BM, X60 BM, X65 BM, X42 W, X52 W, X60 W, and X65 W).



Fig. 9 Photographs of both surfaces of the 9-inch diameter steel trepan from a BP storage tank.

Table 2 Summary of tensile properties from the certificates of pipelines received from Shell.

Grade	Heat #	Diameter	YS (ksi)	TS (ksi)	% Elongation
X42	M62657	10.75	55.5	66	41
X52	ZP1288	8.625	67.4	79.3	34
X60	ZN1653	10.75	73.5	87.5	33
X65	T42523 A	10.75	76.5	83.5	33

The average yield strength of the grade B pipeline and the BP tank steel materials were higher than 40 ksi. Extensive effort did not find a pipeline with low yield strength; hence, a thin sheet of A366 steel was procured since its average yield strength was 26.5 ksi. A sample of the range of engineering stress-strain curves of the base materials investigated in this project is shown in Fig. 10. The range of true-stress versus true-plastic-strain curves (ASTM E646) of the same materials is shown in Fig. 11.

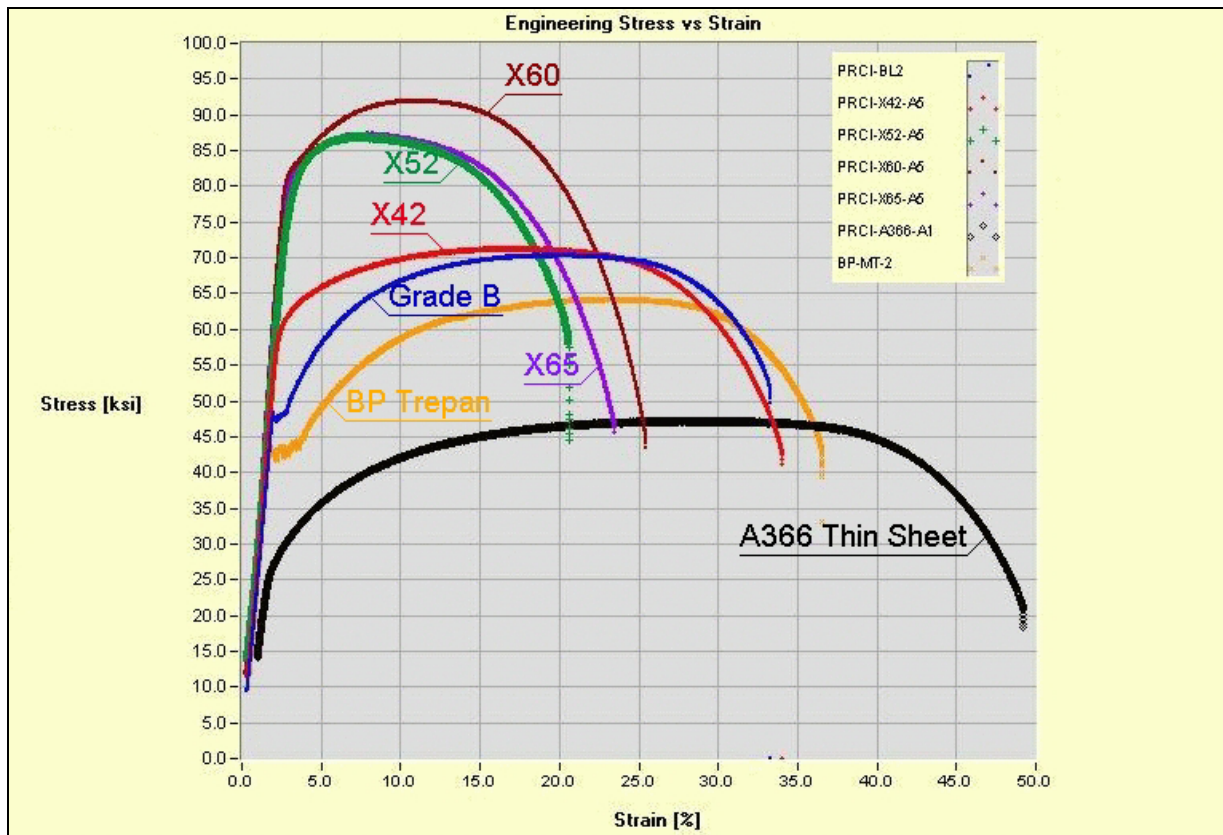


Fig. 10 Sample of the engineering stress-strain curves of five pipeline materials (Grade B, X42, X52, X60, X65), storage tank steel (BP trepan), and thin sheet steel (A366) with low yield strength.

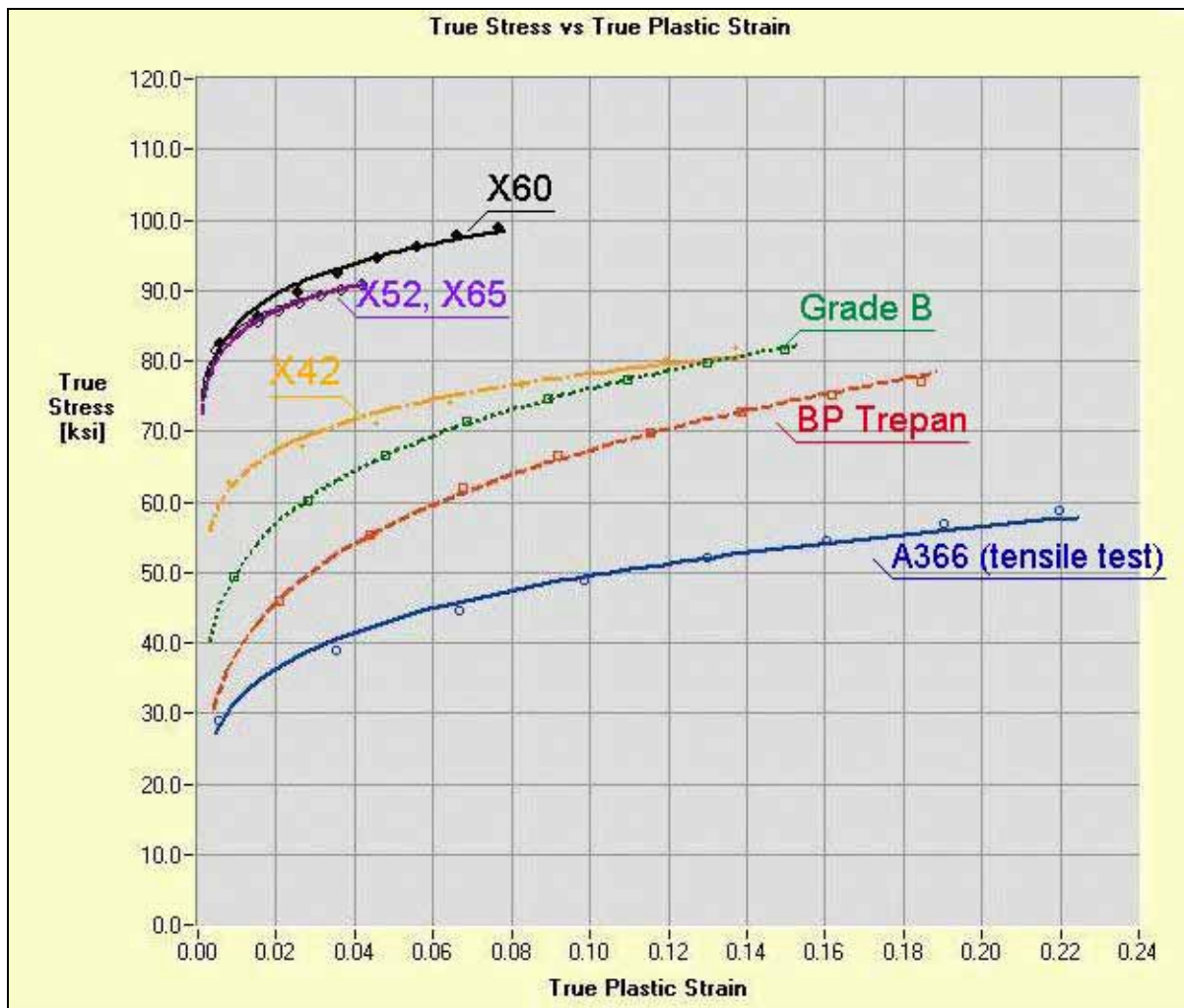


Fig. 11 Sample of the true-stress versus true-plastic-strain curves (ASTM Standard E646) of five pipeline materials (Grade B, X42, X52, X60, X65), storage tank steel (BP trepan), and thin sheet steel (A366) with low yield strength.

4.1 ABI-Measured Tensile Properties and Comparisons with Results from Destructive Tensile Tests

A sample of the ABI indentation force-depth data and true-stress/true-plastic-strain results of the seven base materials shown earlier are given in Fig. 12 and Fig. 13. Example comparisons between true-stress/true-plastic-strain curves from ABI and tensile test for two materials are shown in Fig. 14 and Fig. 15. The ABI-measured yield and tensile strength values (from ABI tests conducted on the end tabs of flat tensile specimens) and their comparisons with those from the destructive tensile tests are shown in Tables 3 and 4 (including the average values per material, standard deviation, and differences between the ABI and tensile test results. Detailed ABI test results are given in Appendix D. All ABI tests (using a 0.030-inch diameter ground tungsten carbide indenter) were analyzed using the values of 0.376, -32.5 ksi, and 1.2 for the yield strength slope, offset, and the constraint factor, respectively. The average yield strength (YS) and tensile strength (TS) values from both ABI and tensile test techniques were within 10% and 6% for the YS and TS, respectively. The standard deviation of all ABI results for each grade was very small (less than 5% or 2-5 ksi).

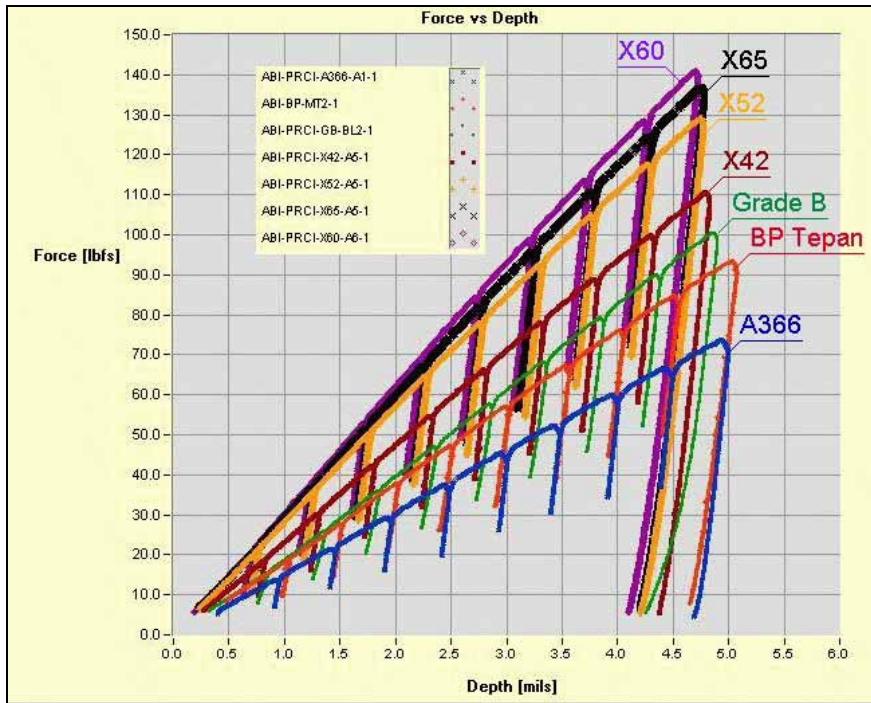


Fig. 12 Sample of ABI force-depth data from ABI tests conducted on the end tabs of seven steel base materials showing distinct differences and a wide range of force-depth data.

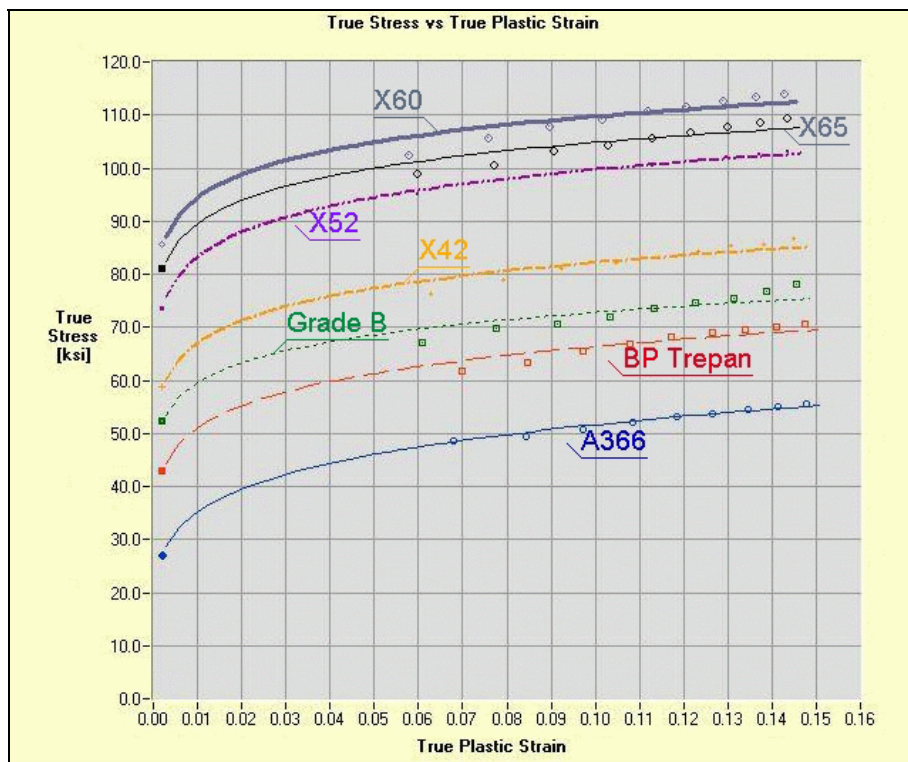


Fig. 13 Sample of ABI-measured true-stress/true-plastic-strain curves from ABI tests conducted on the end tabs of seven steel base materials showing distinct differences and a wide range of stress-strain curves (wide range of yield strength, tensile strength, uniform ductility, etc.).

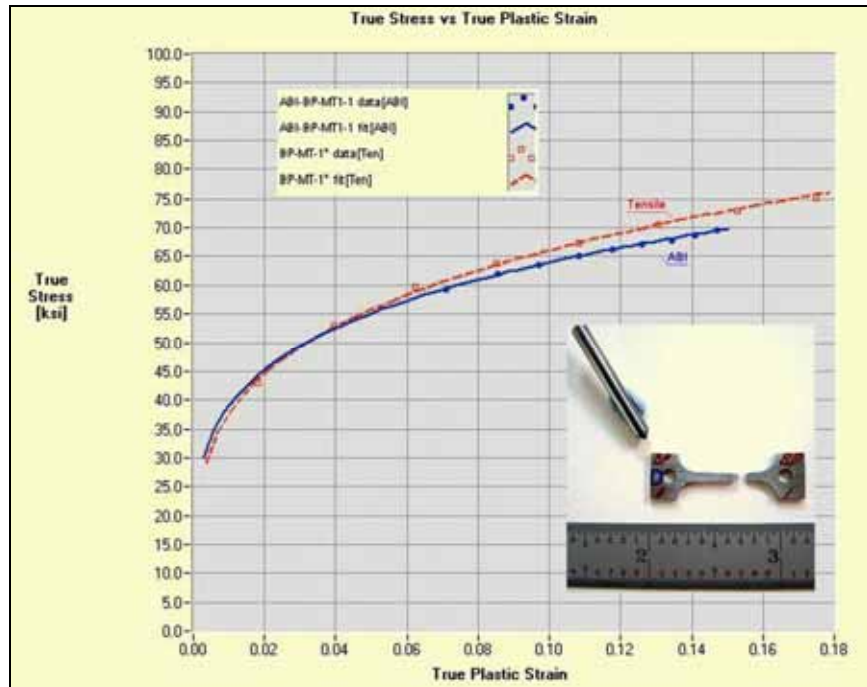


Fig. 14 Overlay of the true-stress/true-plastic-strain curves from ABI and tensile tests (BP tank steel). The ABI test was conducted on the end tab of the miniature tensile specimen as shown in the inset photo.

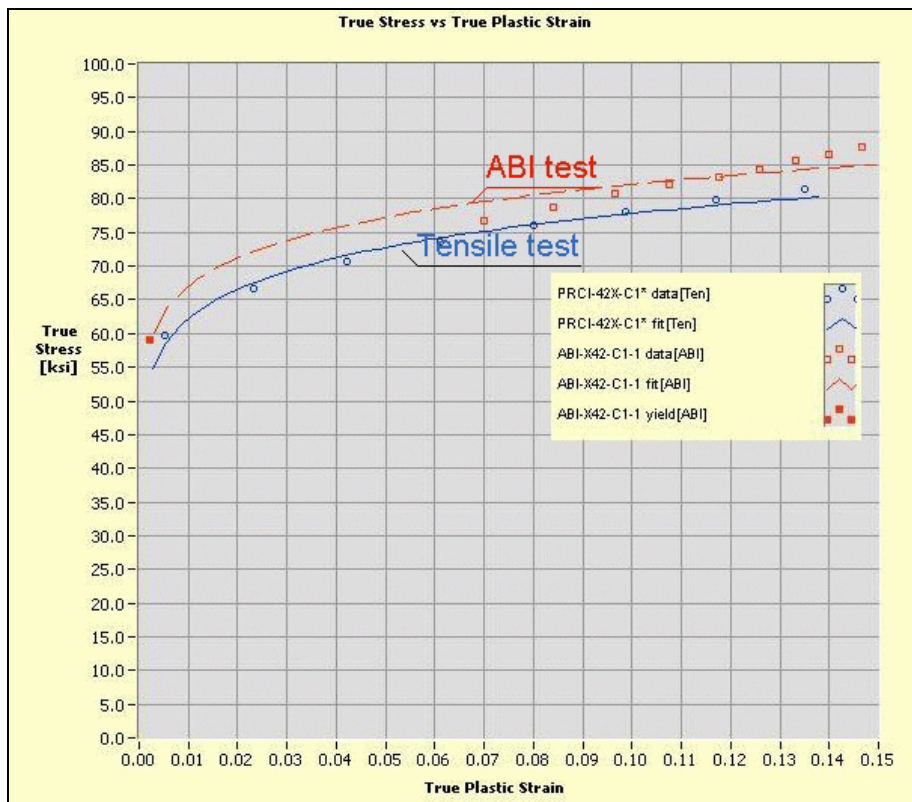


Fig. 15 Overlay of the true-stress/true-plastic-strain curves from ABI and tensile tests (X42 base metal). The difference between ABI and tensile yield and tensile properties is approximately 5%.

Table 3 Comparison between yield strength measured from ABI and tensile tests

Material	ABI-Yield Strength, ksi	Tensile-Yield Strength, ksi	Agreement between ABI-Yield Strength and Yield from Tensile Tests (%)
A366 Thin Sheet	24.8	26.9	-7.8
	24.8	26.0	-4.6
Average	24.8	26.5	-6.2
Standard Deviation	0.0	0.6	2.3
BP Storage Tank Trepan	41.7	40.2	3.7
	42.9	42.7	0.5
BP Storage Tank Trepan	39.0	41.1	-5.1
Average	41.2	41.3	-0.3
Standard Deviation	2.0	1.3	4.5
Grade B Base Metal (BM)	53.6	49.1	9.2
	52.5	47.2	11.2
Average	53.1	48.2	10.2
Standard Deviation	0.8	1.3	1.5
Grade B Seam Weld (SW)	47.3	45.5	4.0
	53.5	46.9	14.1
Average	50.4	46.2	9.1
Standard Deviation	4.4	1.0	7.2
X42 BM	59.0	56.2	5.0
	64.2	60.6	5.9
	65.8	62.2	5.8
	59.3	56.7	4.6
	58.8	59.4	-1.0
	65.3	63.4	3.0
	64.8	70.1	-7.6
63.1	61.4	2.8	
Average	62.5	61.3	2.1
Standard Deviation	3.0	4.4	4.6
X42 SW	68.8	69.1	-0.4
	64.1	72.0	-11.0
	68.3	69.6	-1.9
	65.3	71.1	-8.2
	63.6	70.7	-10.0
	68.4	71.8	-4.7
Average	66.4	70.7	-6.1
Standard Deviation	2.4	1.2	4.4
X52 BM	75.7	74.0	2.3
	68.0	75.1	-9.5
	76.3	76.4	-0.1
	77.1	75.6	2.0
	73.5	74.7	-1.6
	78.1	78.7	-0.8
	77.9	82.6	-5.7
73.6	79.2	-7.1	
Average	75.0	77.0	-2.6
Standard Deviation	3.3	2.9	4.3

Table 3 Comparison between yield strength measured from ABI and tensile tests (Continued)

ABI Test Name	ABI-Yield Strength, ksi	Tensile-Yield Strength, ksi	Agreement between ABI-Yield Strength and Yield from Tensile Tests (%)
X52 SW	67.7	69.8	-3.0
	70.5	74.0	-4.7
	71.2	71.9	-1.0
	64.7	63.6	1.7
	71.6	71.6	0.0
	65.8	68.3	-3.7
Average	68.6	69.9	-1.8
Standard Deviation	2.9	3.6	2.4
X60 BM	79.2	79.6	-0.5
	84.7	83.2	1.8
	83.0	82.8	0.2
	84.2	80.4	4.7
	84.3	80.3	5.0
	85.7	84.3	1.7
	82.2	83.8	-1.9
85.0	85.1	-0.1	
Average	83.5	82.4	1.3
Standard Deviation	2.1	2.1	2.5
X65 BM	80.8	83.0	-2.7
	79.1	77.2	2.5
	85.6	82.6	3.6
	76.9	76.6	0.4
	81.1	77.9	4.1
	83.3	85.0	-2.0
	83.3	85.8	-2.9
	81.2	79.9	1.6
Average	81.4	81.0	0.5
Standard Deviation	2.7	3.6	2.8
X65 SW	73.5	74.0	-0.7
	70.1	67.4	4.0
	67.9	68.1	-0.3
	73.5	73.8	-0.4
	76.1	73.4	3.7
	71.4	70.7	1.0
Average	72.1	71.2	1.2
Standard Deviation	2.9	3.0	2.1

Table 4 Comparison between tensile strength measured from ABI and tensile tests

Material	ABI-Estimated UTS, ksi	Tensile-UTS, ksi	Agreement between ABI-UTS and UTS from Tensile Tests (%)
A366 Thin Sheet	45.9	47.3	-3.0
	44.5	46.9	-5.1
Average	45.2	47.1	-4.0
Standard Deviation	1.0	0.3	1.5
BP Storage Tank Trepan	58.6	63.1	-7.1
	60.1	64.3	-6.5
	58.6	64.6	-9.3
Average	59.1	64.0	-7.7
Standard Deviation	0.9	0.8	1.4
Grade B Base Metal (BM)	68.2	71.8	-5.0
	65.9	70.4	-6.4
Average	67.1	71.1	-5.7
Standard Deviation	1.6	1.0	1.0
Grade B Seam Weld (SW)	64.3	71.7	-10.3
	68.0	69.6	-2.3
Average	66.2	70.7	-6.4
Standard Deviation	2.6	1.5	5.7
X42 BM	74.4	71.2	4.5
	77.0	72.6	6.1
	80.3	74.8	7.4
	74.1	72.1	2.8
	74.4	71.4	4.2
	79.7	74.4	7.1
	77.5	79.3	-2.3
	79.4	73.4	8.2
Average	77.1	73.7	4.7
Standard Deviation	2.6	2.6	3.4
X42 SW	82.3	78.3	5.1
	80.0	78.3	2.2
	82.9	79.8	3.9
	82.4	77.8	5.9
	78.8	77.8	1.3
	83.7	80.7	3.7
Average	81.7	78.8	3.7
Standard Deviation	1.9	1.2	1.7
X52 BM	90.1	86.4	4.3
	84.5	83.8	0.8
	90.0	86.5	4.0
	92.3	85.2	8.3
	90.4	87.0	3.9
	93.4	85.8	8.9
	90.1	87.0	3.6
Average	89.8	85.6	4.9
Standard Deviation	2.8	1.5	2.6

Table 4 Comparison between tensile strength measured from ABI and tensile tests (Continued)

Material	ABI-Estimated UTS, ksi	Tensile-UTS, ksi	Agreement between ABI-UTS and UTS from Tensile Tests (%)
X52 SW	82.1	81.0	1.4
	86.7	82.5	5.1
	86.1	80.3	7.2
	77.4	76.7	0.9
	85.6	80.6	6.2
	82.0	79.8	2.8
Average	83.3	80.2	4.0
Standard Deviation	3.5	1.9	2.6
X60 BM	93.5	96.3	-2.9
	98.3	93.8	4.8
	96.4	94.1	2.4
	96.7	96.1	0.6
	94.9	92.0	3.2
	99.9	92.9	7.5
	96.4	93.1	3.5
99.3	94.5	5.1	
Average	96.9	94.1	3.0
Standard Deviation	2.2	1.5	3.1
X65 BM	90.4	89.8	0.7
	94.0	88.8	5.9
	99.1	89.6	10.6
	87.5	87.0	0.6
	95.4	87.4	9.2
	97.3	91.0	6.9
	98.1	90.5	8.4
	91.1	87.8	3.8
Average	94.1	89.0	5.8
Standard Deviation	4.1	1.5	3.8
X65 SW	86.9	85.4	1.8
	86.6	82.3	5.2
	72.9	80.7	-9.7
	84.6	84.5	0.1
	88.7	85.9	3.3
	77.0	82.3	-6.4
Average	82.8	83.5	-0.9
Standard Deviation	6.3	2.1	5.8

4.2 ABI-Measured Fracture Toughness (K_{Jc}) Values and Comparisons with Results from Destructive Fracture Toughness Tests

The ABI-determined fracture toughness values for all tested pipeline base metal and seam weld materials were within 12% of the results from destructive tests conducted according to the single specimen unloading compliance technique of ASTM Standard E1820. All ABI tests on the pipeline materials were analyzed using the critical fracture strain model since the samples were tested at room temperature and exhibited ductile behavior. Comparisons of the K_{Jc} values from ABI tests and from destructive disk compact fracture toughness specimens are given in Table 5. Examples of detailed fracture toughness data and analysis are provided in Appendix E. The broken halves of all disk compact specimens are shown in Fig. 16 below.



Fig. 16 Fracture surfaces of all disk compact fracture toughness specimens from the base metal and seam welds of several pipeline steels and from 1018 steel plate. The 1018 steel material was used before obtaining Grade B pipeline material.

Table 5 Comparison of fracture toughness values from ABI tests (conducted on end tabs of miniature tensile specimens using the Haggag Toughness Method) and from disk compact fracture toughness specimens

Material	Destructive Fracture Toughness (KJc) from Jlc or Jb, (ksi*in ^{.5})	Destructive Standard Deviation	Nondestructive HTM Fracture Toughness (KJc) from ABI, (ksi*in ^{.5})	HTM Standard Deviation	Agreement between Average HTM and Average Destructive Results (%)
1018 Base	188.3		181.0		
	165.2		176.3		
	178.4		180.5		
	175.7		179.1		
Average	176.9	9.5	179.2	2.1	1.3
X60 Base	174.6		192.6		
	189.5		204.0		
	177.8		193.2		
Average	180.6	7.8	196.6	6.4	8.8
X42 Base	186.3		181.5		
	198.8		189.6		
Average	192.6	8.8	185.6	5.7	-3.6
X42 Weld	189.0		188.3		
	191.2		191.0		
	194.1		192.8		
Average	191.4	2.6	190.7	2.3	-0.4
X52 Base	143.0		198.5		
	150.8		203.0		
	135.8		187.3		
Average	Invalid		196.3		
X52 Weld	195.0		191.0		
	176.9		186.2		
	220.3		196.3		
Average	197.4	21.8	191.2	5.1	-3.2
X65 Base	217.1		193.3		
	203.4		184.5		
	219.8		196.9		
Average	213.4	8.8	191.6	6.4	-10.2
X65 Weld	223.7		199.1		
	226.5		199.5		
	232.1		202.0		
Average	227.4	4.3	200.2	1.6	-12.0

4. 3 ABI-Measured Tensile and Fracture Toughness Tests on Sections of Pipelines

Five ABI tests were conducted on each base metal and seam weld of X42, X52, X60, and X65 and on the base metal of Grade B pipeline materials. The results are summarized in Table 6. Also, values of the crack-tip-opening displacement (CTOD) were also estimated from the ABI-measured K_{Jc} values and are shown in the last column of Table 6.

Table 6 Summary of ABI test results on pipeline sections (5 tests conducted on each material)

Material	Calculated	ABI	Ratio	ABI Yield	ABI	Fracture	Fracture
	Uniform	Hardness	Yield	Strength	Engineering	Toughness	Toughness
	Ductility	(030G)	to		UTS	KJc from ABI	(CTOD) from ABI
	[%]		UTS	[ksi]	[ksi]	(ksi*in ^{0.5})	(mm)
Grade B Pipe, No Certificate	7.8	168	0.81	58.1	71.3	179.9	0.31
	8.4	171	0.80	58.3	72.8	183.0	0.31
	10.5	168	0.78	57.0	72.8	182.9	0.32
	10.0	167	0.79	57.0	71.9	181.6	0.32
	11.0	167	0.76	55.6	73.4	185.2	0.33
Average	9.5	168.2	0.8	57.2	72.4	182.5	0.318
Standard Deviation	1.4	1.6	0.0	1.1	0.8	2.0	0.009
Minimum from Certificate	N/A	N/A	N/A	N/A	N/A	N/A	N/A
X42 Pipe (BM)	10.3	174	0.78	59.4	75.9	188.0	0.32
	8.3	176	0.80	60.9	76.1	186.0	0.30
	10.4	174	0.78	59.6	76.1	185.3	0.31
	10.2	176	0.79	60.5	76.6	188.0	0.31
	10.4	178	0.78	60.4	77.2	189.4	0.31
Average	9.9	175.6	0.8	60.2	76.4	187.3	0.310
Standard Deviation	0.9	1.7	0.0	0.6	0.5	1.7	0.004
Minimum from Certificate	N/A	N/A	N/A	55.5	66.0	N/A	N/A
X42 Pipe (SW)	7.3	204	0.82	73.3	89.5	201.4	0.27
	6.4	201	0.87	76.6	88.0	194.8	0.25
	6.6	201	0.87	76.3	88.2	196.4	0.26
	7.2	202	0.83	74.0	89.5	198.7	0.27
	7.3	202	0.82	73.5	89.2	200.6	0.27
Average	7.0	202.0	0.8	74.7	88.9	198.4	0.264
Standard Deviation	0.4	1.2	0.0	1.6	0.7	2.8	0.009
Minimum from Certificate	N/A	N/A	N/A	N/A	N/A	N/A	N/A
X52 Pipe (BM)	6.7	208	0.85	77.7	91.1	202.4	0.26
	7.0	208	0.84	76.5	91.2	200.7	0.26
	6.8	206	0.84	76.7	90.9	201.4	0.26
	7.2	206	0.83	75.4	91.0	201.7	0.27
	7.1	207	0.83	76.2	91.7	200.9	0.26
Average	7.0	207.0	0.8	76.5	91.2	201.4	0.262
Standard Deviation	0.2	1.0	0.0	0.8	0.3	0.7	0.003
Minimum from Certificate	N/A	N/A	N/A	67.4	79.3	N/A	N/A
X52 Pipe (SW)	7.3	206	0.83	76.4	92.3	202.1	0.26
	10.4	202	0.78	73.3	93.8	200.3	0.27
	10.2	199	0.79	73.0	92.7	197.1	0.27
	10.7	200	0.76	71.6	94.4	199.1	0.28
	10.3	198	0.79	72.7	92.4	198.3	0.27
Average	9.8	201.0	0.8	73.4	93.1	199.4	0.271
Standard Deviation	1.4	3.2	0.0	1.8	0.9	1.9	0.005
Minimum from Certificate	N/A	N/A	N/A	N/A	N/A	N/A	N/A

Table 6 Summary of ABI test results from pipeline sections (5 tests conducted on each material), Continued

Material	Calculated	ABI	Ratio	ABI Yield	ABI	Fracture	Fracture
	Uniform	Hardness	Yield	Strength	Engineering	Toughness	Toughness
	Ductility	(030G)	to		UTS	KJc from ABI	(CTOD) from ABI
	[%]		UTS	[ksi]	[ksi]	(ksi*in ^{0.5})	(mm)
X60 Pipe (BM)	10.3	203	0.78	75.2	95.9	198.6	0.26
	10.4	202	0.78	74.4	95.8	198.7	0.27
	10.3	203	0.78	75.6	96.6	198.4	0.26
	10.0	197	0.79	73.8	93.0	194.7	0.26
	10.7	201	0.76	73.4	97.0	198.3	0.27
Average	10.3	201.2	0.8	74.5	95.7	197.7	0.264
Standard Deviation	0.3	2.5	0.0	0.9	1.6	1.7	0.003
Minimum from Certificate	N/A	N/A	N/A	73.5	87.5	N/A	N/A
X60 Pipe (SW)	6.5	217	0.86	82.2	95.5	203.6	0.25
	6.5	221	0.86	84.0	97.8	207.5	0.25
	6.2	219	0.88	84.8	96.4	206.0	0.24
	6.4	217	0.87	83.2	95.6	203.9	0.24
	6.5	221	0.86	84.5	97.7	207.4	0.24
Average	6.4	219.0	0.9	83.7	96.6	205.7	0.245
Standard Deviation	0.1	2.0	0.0	1.1	1.1	1.9	0.002
Minimum from Certificate	N/A	N/A	N/A	N/A	N/A	N/A	N/A
X65 Pipe (BM)	10.4	193	0.78	69.6	89.3	198.8	0.28
	11.2	184	0.73	65.4	89.7	189.2	0.29
	10.9	183	0.76	67.1	88.7	190.9	0.28
	10.9	189	0.75	67.5	90.5	197.2	0.29
	11.5	185	0.70	63.8	91.4	191.3	0.30
Average	11.0	186.8	0.7	66.7	89.9	193.5	0.289
Standard Deviation	0.4	4.1	0.0	2.2	1.1	4.2	0.006
Minimum from Certificate	N/A	N/A	N/A	76.5	83.5	N/A	N/A
X65 Pipe (SW)	11.0	198	0.74	70.4	95.3	202.0	0.29
	10.0	200	0.79	72.7	91.9	196.2	0.27
	10.2	198	0.78	71.7	91.4	199.1	0.28
	10.5	198	0.77	70.3	90.8	198.5	0.28
	9.7	201	0.79	73.0	92.1	199.9	0.27
Average	10.3	199.0	0.8	71.6	92.3	199.1	0.277
Standard Deviation	0.5	1.4	0.0	1.3	1.8	2.1	0.007
Minimum from Certificate	N/A	N/A	N/A	N/A	N/A	N/A	N/A

Note that the “Minimum from Certificate” refer to the yield (YS) and ultimate tensile (TS/UTS) values from tensile tests. The ABI values are consistently higher than the specified minimums.

4.4 Results from ABI tests and from 0.5T CT Fracture Toughness Specimens of BP Storage Tank Material

Summary tables of the tensile and the ABI test results are given in Tables 7 and 8. Also, 12 ABI tests were conducted in triplicates on both surfaces of fracture toughness specimens BP1 and BP2, which were machined across the thickness of the 1.25-inch thick trepan in order to determine the through-thickness homogeneity of the trepan. The results from these 12 ABI tests (Tables 9 and 10 in English and SI units) on fracture toughness specimens BP1 and BP2 demonstrate excellent material homogeneity. Triplicate ABI tests were conducted on fracture toughness specimens Number 5, 7, and 9 at low temperatures of -80°C , -100°C , and -100°C , respectively. Fracture toughness specimens BP1 and BP 10 were tested at room temperature while the remaining 8 specimens were tested at low temperatures. The fracture surfaces of all 10 destructive fracture toughness specimens are shown in Fig. 17. The ABI-measured tensile and fracture toughness properties from 15 room-temperature ABI tests are given in Tables 9 and 10 (in English and SI units).

Table 7 Summary of tensile test results

<div style="display: flex; justify-content: space-between;"> <div style="border: 1px solid black; padding: 2px;">Select Files</div> <div style="border: 1px solid black; padding: 2px;">English Units</div> <div style="border: 1px solid black; padding: 2px;">Exit</div> <div style="text-align: center;">Summary of Tensile Test Results</div> <div style="border: 1px solid black; padding: 2px;">PRINT</div> <div style="border: 1px solid black; padding: 2px;">JPEG</div> <div style="border: 1px solid black; padding: 2px;">Output File</div> </div>								
Test Name	Temp. [F]	CHS [in/s]	Unif. Elong. [%]	Total Elong. [%]	Yield Streng. [ksi]	Streng. Coeff. [ksi]	Strain Hard. Exp.	UTS [ksi]
BP-MT-1	72	0.0010	20.3	32.1	40.2	115.9	0.244	63.1
BP-MT-2	72	0.0010	20.4	35.0	42.7	116.7	0.239	64.3
BP-MT-3	72	0.0010	22.0	37.2	41.1	114.9	0.233	64.6

Table 8 Summary of results from 3 ABI test conducted on end tabs of the three tensile specimens

<div style="display: flex; justify-content: space-between;"> <div style="border: 1px solid black; padding: 2px;">Select Files</div> <div style="border: 1px solid black; padding: 2px;">English Units</div> <div style="border: 1px solid black; padding: 2px;">Exit</div> <div style="text-align: center;">ABI-Measured Tensile & Fracture Toughness Summary</div> <div style="border: 1px solid black; padding: 2px;">PRINT</div> <div style="border: 1px solid black; padding: 2px;">JPEG</div> <div style="border: 1px solid black; padding: 2px;">Output File</div> </div>									
Test Name	Yield Strength [A,β] [ksi]	Strength Coefficient [K] [ksi]	Strain Hardening Exponent [n]	Estimated Engineering UTS [ksi]	Calculated Engineering UTS [ksi]	Calculated Uniform Ductility [%]	Ratio Yield to UTS	ABI Hardness	Fracture Toughness [ksi*in ^{0.5}]
ABI-BP-MT1-1	44.2	109.6	0.215	63.5	61.8	13.3	0.70	136 (030G)	165.8
ABI-BP-MT2-1	45.3	106.4	0.190	64.1	63.2	13.4	0.71	138 (030G)	169.7
ABI-BP-MT3-1	41.6	92.1	0.137	61.2	61.1	12.9	0.68	134 (030G)	164.9

Table 9 Summary of all 15 ABI tests at room temperature (3 on mini-tensile and 12 on two fracture toughness specimens), English units

ABI-Measured Tensile & Fracture Toughness Summary									
Test Name	Yield Strength (A,B) [ksi]	Strength Coefficient (K) [ksi]	Strain Hardening Exponent (n)	Estimated Engineering UTS [ksi]	Calculated Engineering UTS [ksi]	Calculated Uniform Ductility [%]	Ratio Yield to UTS	ABI Hardness	Fracture Toughness (ksi*in ^{0.5})
ABI-8P-MT1-1	44.2	109.6	0.215	63.5	61.8	13.3	0.70	136 (030G)	165.8
ABI-8P-MT2-1	45.3	106.4	0.190	64.1	63.2	13.4	0.71	138 (030G)	169.7
ABI-8P-MT3-1	41.6	92.1	0.137	61.2	61.1	12.9	0.68	134 (030G)	164.9
ABI-FT-8P1-1	48.9	86.5	0.119	59.5	58.6	12.1	0.82	145 (030G)	168.8
ABI-FT-8P1-2	49.0	84.6	0.116	58.6	58.7	12.0	0.84	143 (030G)	167.4
ABI-FT-8P1-3	49.2	89.9	0.124	61.3	61.3	12.3	0.80	146 (030G)	171.4
ABI-FT-8P1-4	50.0	84.7	0.114	59.0	59.0	12.0	0.85	143 (030G)	165.8
ABI-FT-8P1-5	47.7	85.3	0.119	58.8	58.8	12.2	0.81	141 (030G)	166.2
ABI-FT-8P1-6	47.9	87.1	0.122	59.7	59.7	12.3	0.80	143 (030G)	168.9
ABI-FT-8P2-1	46.5	89.4	0.128	60.5	60.5	12.5	0.77	143 (030G)	169.0
ABI-FT-8P2-2	47.5	87.6	0.123	59.0	59.9	12.3	0.79	142 (030G)	169.6
ABI-FT-8P2-3	47.3	87.6	0.123	59.0	59.0	12.3	0.79	143 (030G)	169.4
ABI-FT-8P2-4	51.5	92.1	0.123	63.0	63.0	12.3	0.82	150 (030G)	173.2
ABI-FT-8P2-5	47.0	88.9	0.125	60.5	60.5	12.4	0.79	145 (030G)	169.2
ABI-FT-8P2-6	47.5	88.6	0.125	60.3	60.4	12.4	0.79	143 (030G)	168.0

Table 10 Summary of all 15 ABI tests at room temperature (3 on mini-tensile and 12 on two fracture toughness specimens), SI units

ABI-Measured Tensile & Fracture Toughness Summary									
Test Name	Yield Strength (A,B) [MPa]	Strength Coefficient (K) [MPa]	Strain Hardening Exponent (n)	Estimated Engineering UTS [MPa]	Calculated Engineering UTS [MPa]	Calculated Uniform Ductility [%]	Ratio Yield to UTS	ABI Hardness	Fracture Toughness (MPa*m ^{0.5})
ABI-8P-MT1-1	305	755	0.215	438	426	13.3	0.70	136 (030G)	182.2
ABI-8P-MT2-1	312	733	0.190	442	436	13.4	0.71	138 (030G)	186.5
ABI-8P-MT3-1	287	635	0.137	422	422	12.9	0.68	134 (030G)	181.2
ABI-FT-8P1-1	337	596	0.119	410	411	12.1	0.82	145 (030G)	185.5
ABI-FT-8P1-2	338	503	0.116	404	405	12.0	0.84	143 (030G)	183.9
ABI-FT-8P1-3	340	620	0.124	423	423	12.3	0.80	146 (030G)	188.3
ABI-FT-8P1-4	345	584	0.114	407	407	12.0	0.85	143 (030G)	182.2
ABI-FT-8P1-5	329	588	0.119	405	405	12.2	0.81	141 (030G)	182.6
ABI-FT-8P1-6	330	601	0.122	411	412	12.3	0.80	143 (030G)	185.7
ABI-FT-8P2-1	321	616	0.128	417	417	12.5	0.77	143 (030G)	185.7
ABI-FT-8P2-2	327	604	0.123	413	413	12.3	0.79	142 (030G)	186.3
ABI-FT-8P2-3	326	604	0.123	412	413	12.3	0.79	143 (030G)	186.2
ABI-FT-8P2-4	355	635	0.123	434	434	12.3	0.82	150 (030G)	190.3
ABI-FT-8P2-5	330	613	0.125	417	417	12.4	0.79	145 (030G)	185.9
ABI-FT-8P2-6	328	611	0.125	416	416	12.4	0.79	143 (030G)	185.5

The yield and ultimate strength values from the ABI tests conducted on the end tabs of the miniature tensile specimens are within 6% percent from those obtained from destructive tensile tests. The average fracture toughness determined from these 3 ABI tests (Table 10) is 183.3 MPa√m, which is 11% lower than the average value of 206.8 MPa√m obtained from destructive specimens BP1 and BP10 shown in Table 11 below. Overlay of the load versus crack opening displacement (COD) and the J-integral versus crack extension from specimens BP1 and BP10 are shown in Fig. 18 and Fig. 19. The fracture toughness master curve obtained from all 15 ABI tests conducted at room temperature on the miniature tensile specimens and the two fracture toughness specimens BP1 and BP 10 is shown in Fig. 20. The very conservative reference temperature determined from the 15 ABI tests is -15°C. The high degree of conservatism is because the ABI tests are conducted at room temperature and the material is ductile at that temperature and the analysis of the transition temperature region is not applicable but is used here only to provide a conservative evaluation.

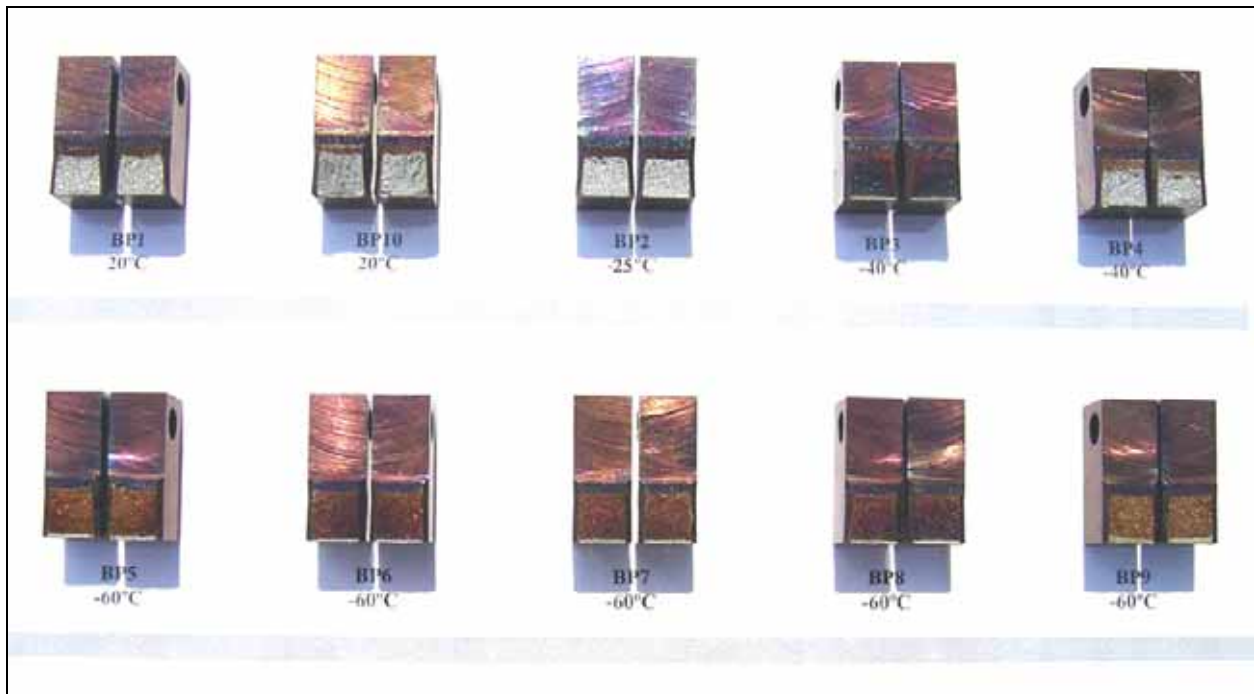


Fig. 17 Fracture surfaces and test temperatures of the 10 fracture toughness specimens.

Table 11 Summary of fracture toughness results from tests conducted at room temperature

Specimen Number	Test Temp C	Test Temp F	J _{1c} (lb/in)	Fracture Toughness (KJ _{1c}) from J _{1c} (MPa√m)	Average Fracture Toughness (KJ _{1c}) from ABI (MPa√m)
BP1	20	68	1043	203.8	183.3
BP10	20	68	1106	209.8	183.3

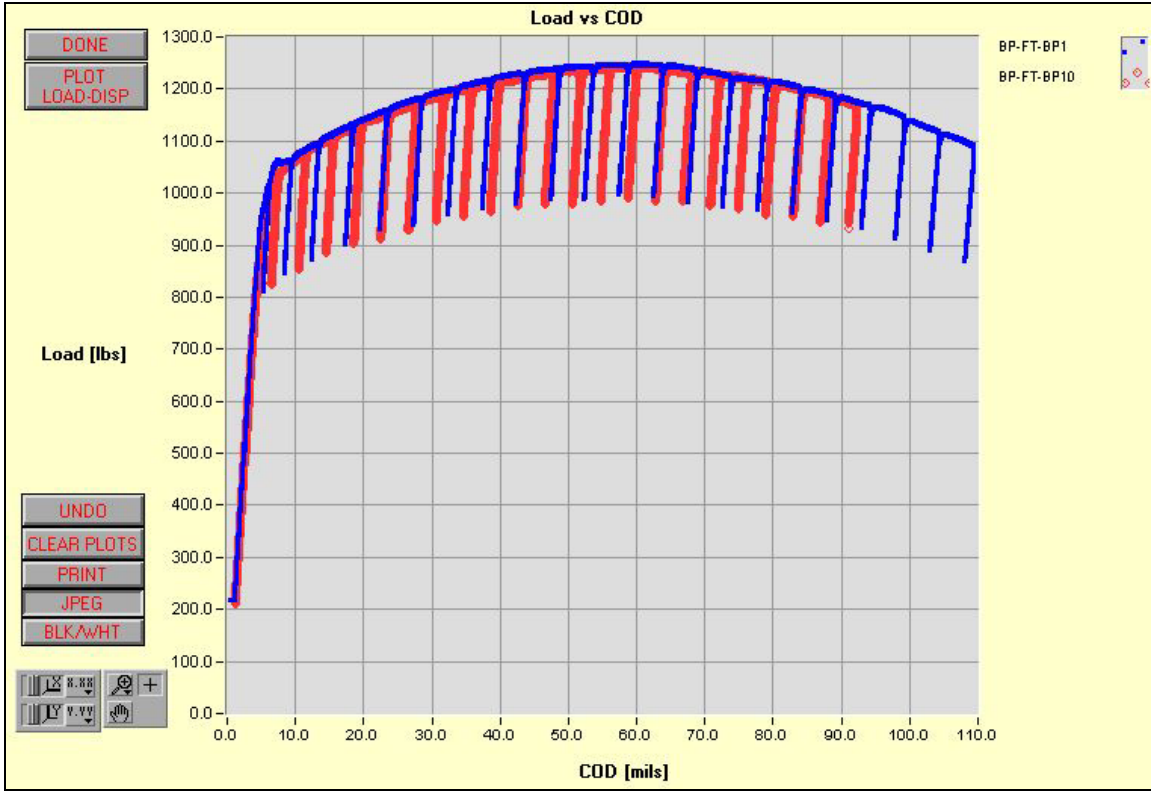


Fig. 18 Overlay of the load versus crack opening displacement (COD) from Specimens BP1 and BP10 tested at room temperature in order to compare with results from ABI tests at the same temperature.

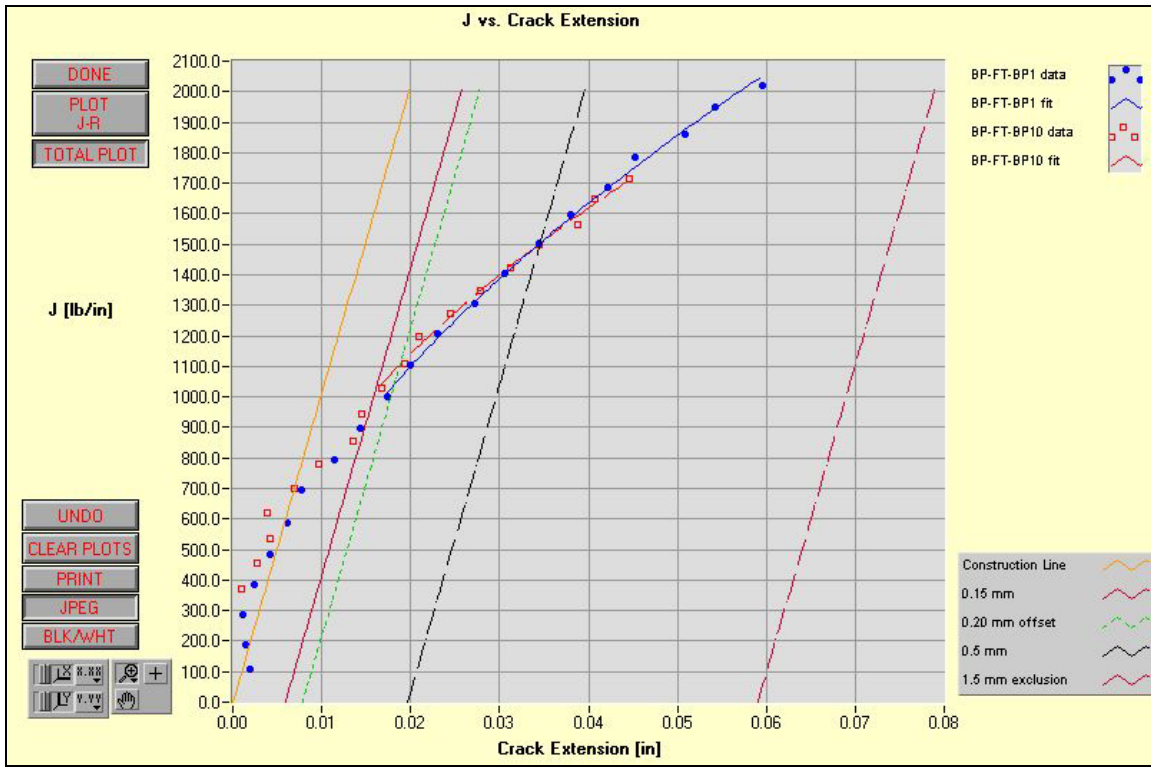


Fig. 19 Overlay of J-Integral versus Crack Extension graphs calculated from the load versus COD data shown in the previous figure for Specimens BP1 and BP10.

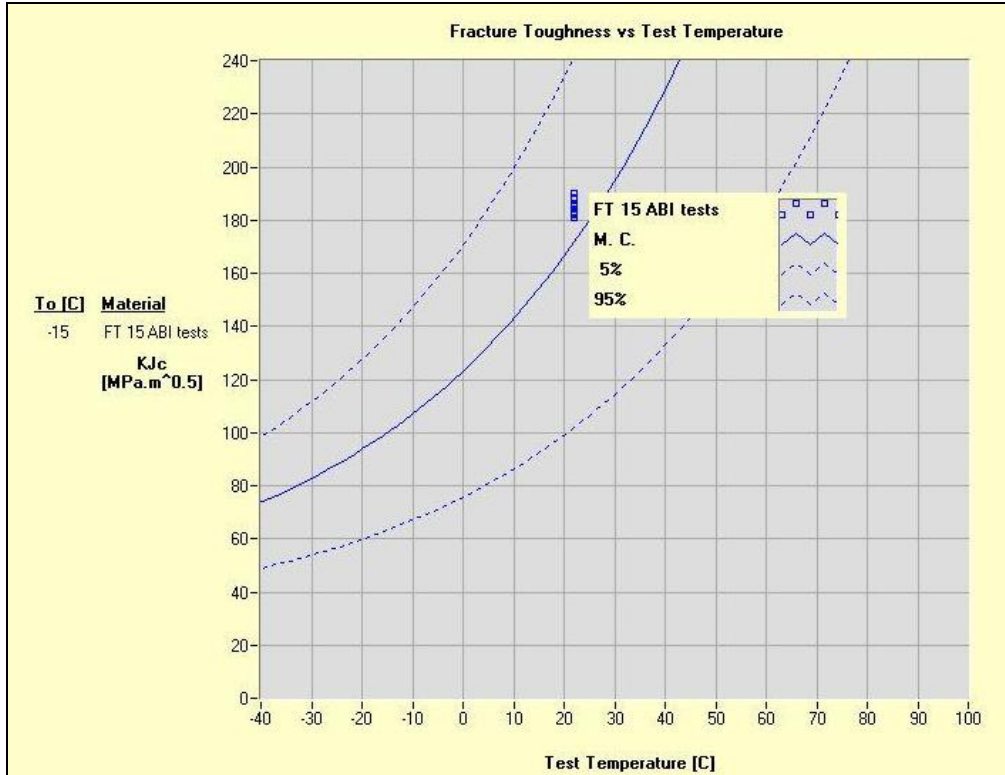


Fig. 20 Fracture toughness Master Curve developed from 15 ABI tests at ambient/room temperature using the empirical critical fracture strain model (at a critical indentation depth of 12% strain) in order to develop a very conservative reference temperature appropriate for field applications.

The results from the destructive fracture toughness tests at low temperature are shown in Table 12. Specimen BP2 tested at -25°C did not cleave and showed a pop-in after slow crack extension that rendered it invalid for fracture toughness master curve evaluation per ASTM Standard E1921. Also, specimen BP4 tested at -40°C did not cleave, hence, invalid per ASTM standard E1921. The remaining 6 specimens (BP3, BP5, BP6, BP7, BP8, and BP9) cleaved as shown in Table 12 and Fig. 21. The fracture toughness master curve and the reference temperature (-86°C) are shown in Fig. 22.

Table 12 Fracture toughness results from tests conducted at low temperatures

Specimen Number	Test Temp C	Test Temp F	Jlc (lb/in)	Fracture Toughness (KJlc) from Jlc (MPa $\sqrt{\text{m}}$)	KJc (E1921-05) (MPa $\sqrt{\text{m}}$)	Size Adjusted KJc (1T) Or KJc (limit) (MPa $\sqrt{\text{m}}$)	Comments
BP2	-25	-13	1663		262.4	218.2 (150)	Pop-in
BP3	-40	-40	1449		246.1	204.9 (154)	Cleaved
BP4	-40	-40	1073	206.7			No cleavage, Jlc
BP5	-60	-76	1091		214.9	179.4 (159)	Cleaved
BP6	-60	-76	1634		263.0	218.7 (159)	Cleaved
BP7	-60	-76	864		191.2	160.0 (159)	Cleaved
BP8	-60	-76	1318		236.2	196.8 (159)	Cleaved
BP9	-60	-76	646		165.4	138.9	Cleaved

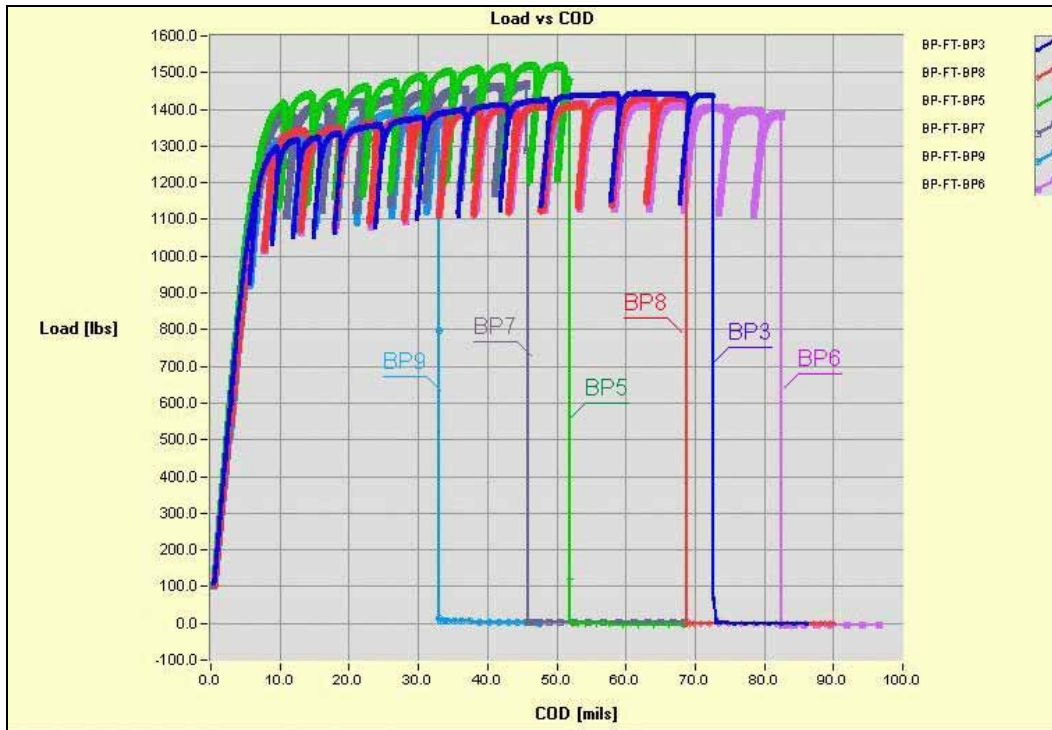


Fig. 21 Overlay of load versus COD graphs from 6 fracture toughness tests conducted at low temperatures. All 6 specimens cleaved.

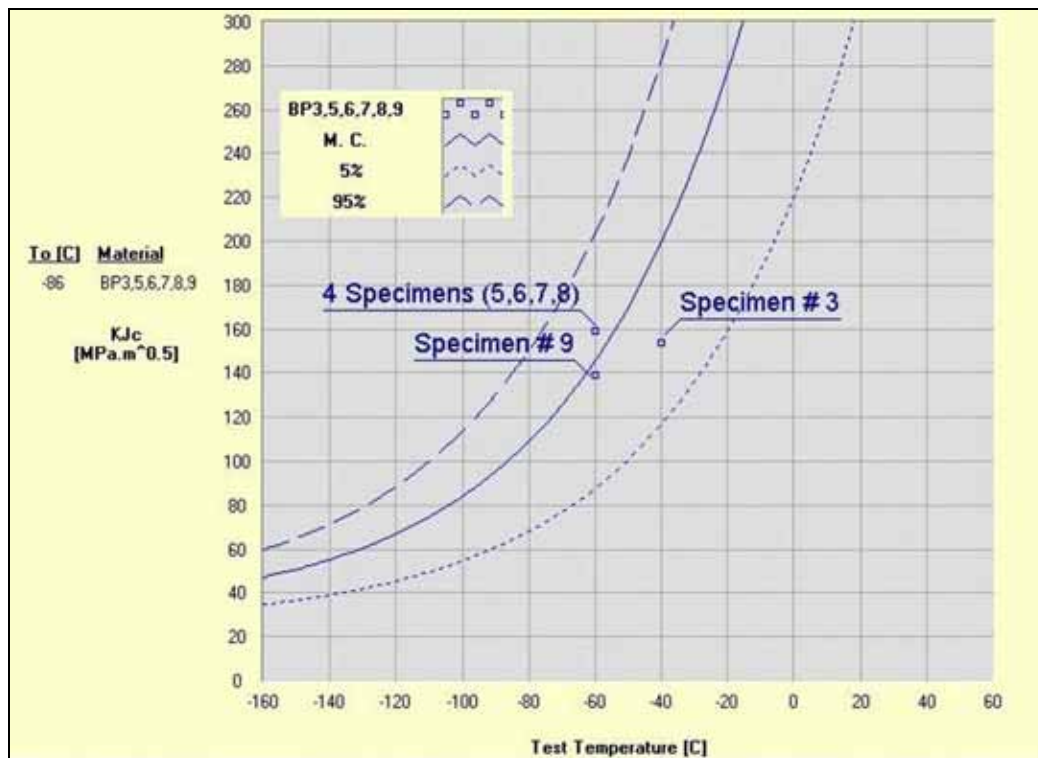


Fig. 22 Fracture toughness master curves (median, 95%, and 5% confidence curves) showing a reference temperature of -86°C .

Triplicate ABI tests were conducted on the broken halves of fracture toughness specimens BP5, BP7, and BP9 at temperatures of -60°C , -100°C , and -100°C , respectively. The test results are given in Table 13. The triplicate ABI tests conducted at -60°C did not reach the critical fracture stress corresponding to that temperature before reaching indentation depth corresponding to 12% strain. Hence, these three tests were not included in the fracture toughness master curve analysis (Fig. 23). The six ABI tests conducted at -100°C resulted in a reference temperature of -84°C , which is in excellent agreement with the -86°C obtained from the six destructive fracture toughness specimens (see comparison in Fig. 24).

Table 13 Summary of fracture toughness results from 9 ABI tests conducted at low temperatures

Summary of Fracture Toughness Test Results																
Test Name	Temp. [C]	Ind. Dia. [mm]	Load Depth Slope kn/mm	Yield Par. A [MPa]	Yield Streng. [A,β] [MPa]	Est. Eng. UTS [MPa]	Ratio Yield to UTS	ABI Hardness	Streng. Coeff. [K] [MPa]	Strain Hard. Exp. [n]	Meyer's Num. [m]	Critical Stress [MPa]	Critical Depth [H] [mic]	Critical Depth Ratio [dt/D]	WIEF [KJ/m ²]	KJc [MPa·m ^{0.5}]
Critical Fracture Stress Reached																
ABI-BP7-100-2	-100	0.7620	5.66	1975	524	685	0.76	216 (030G)	935	0.091	2.044	2639	8.915	0.21	9.6	96.7
ABI-BP7-100-3	-100	0.7620	5.28	2054	552	682	0.81	219 (030G)	892	0.075	2.127	2445	9.347	0.22	9.4	95.0
ABI-BP7-100-4	-100	0.7620	5.04	1984	527	682	0.77	215 (030G)	901	0.079	2.101	2535	5.232	0.17	5.7	60.5
ABI-BP9-100-1	-100	0.7620	5.27	1974	524	685	0.76	213 (030G)	916	0.083	2.099	2520	5.232	0.17	5.5	60.0
ABI-BP9-100-2	-100	0.7620	5.15	1901	498	685	0.73	210 (030G)	933	0.091	2.017	2481	2.997	0.12	3.2	67.8
ABI-BP9-100-3	-100	0.7620	5.29	2020	540	687	0.79	221 (030G)	914	0.081	2.066	2501	2.997	0.12	2.5	63.9
Critical Fracture Stress																
Not Reached Before 12% Strain																
ABI-BP5-60-1	-60	0.7620	3.97	1765	456	562	0.81	186 (030G)	747	0.081	2.203	2251	77.648	0.60	78.7	216.1
ABI-BP5-60-2	-60	0.7620	4.13	1787	457	552	0.83	183 (030G)	728	0.078	2.241	2212	76.200	0.60	75.5	212.3
ABI-BP5-60-3	-60	0.7620	4.44	1796	460	574	0.80	180 (030G)	762	0.081	2.103	2276	77.648	0.60	80.0	218.6

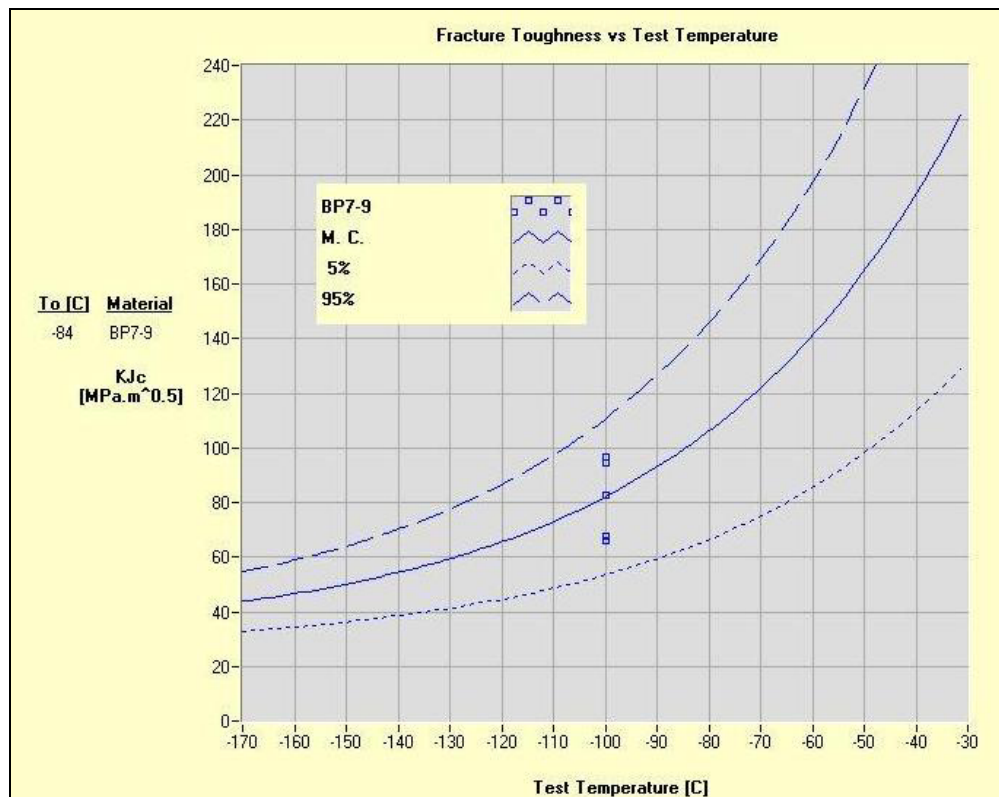


Fig. 23 Fracture toughness master curves from six ABI tests conducted in triplicates at -100°C on specimens BP7 and BP9.

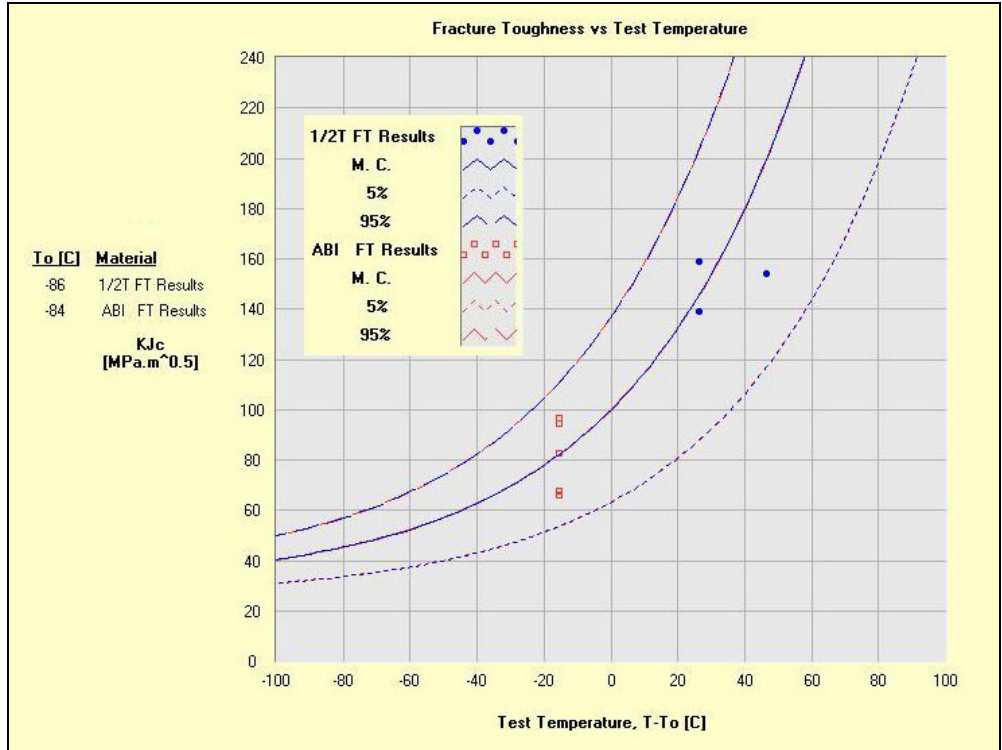


Fig. 24 Fracture toughness plotted versus normalized test temperature ($T - T_0$) showing excellent comparison of reference temperatures from six destructive fracture toughness specimens and from six ABI tests at low-test temperatures.

4.4.1 Discussion on Application of Critical Fracture Stress and Critical Fracture Strain Models

Low temperatures increase the yield and ultimate strength values of ferritic steels and decrease both the ductility and initiation fracture toughness. The measured tensile and fracture toughness properties from each ABI test conducted at -100°C are shown in Table 14 (in English units) and an example of the use of the critical fracture stress model is given in Fig. 25. At room or higher temperatures (e.g., at 20°C the critical fracture stress is 479 ksi) the maximum stress ($1.1 P_m$) is not reached before the normalized depth value of $d/D = 0.6$ (i.e., 12% strain) and then the critical depth is taken as that of $d/D = 0.6$ (12% strain) in order to calculate the fracture toughness using the critical fracture strain model since the critical fracture stress is not reached at the room or higher test temperature (see example in Fig. 26).

Table 14 ABI-measured tensile and fracture toughness properties from 6 ABI tests conducted at -100°C

ABI-Measured Tensile & Fracture Toughness Summary									
Test Name	Yield Strength (A _{0.2}) [ksi]	Strength Coefficient (K) [ksi]	Strain Hardening Exponent (n)	Estimated Engineering UTS [ksi]	Calculated Engineering UTS [ksi]	Calculated Uniform Ductility [%]	Ratio Yield to UTS	ABI Hardness	Fracture Toughness [ksi*in ^{0.5}]
ABI-BP7-100-2	76.0	135.6	0.091	99.4	99.4	10.4	0.76	216 (030G)	87.1
ABI-BP7-100-3	80.1	129.4	0.075	98.9	98.9	7.1	0.81	219 (030G)	86.5
ABI-BP7-100-4	76.5	130.6	0.079	98.9	98.8	7.5	0.77	215 (030G)	73.2
ABI-BP9-100-1	76.0	132.8	0.083	99.3	99.3	9.5	0.77	213 (030G)	72.8
ABI-BP9-100-2	72.2	135.4	0.091	99.4	99.4	10.3	0.73	210 (030G)	61.7
ABI-BP9-100-3	78.3	132.5	0.081	99.7	99.6	8.2	0.79	221 (030G)	58.1

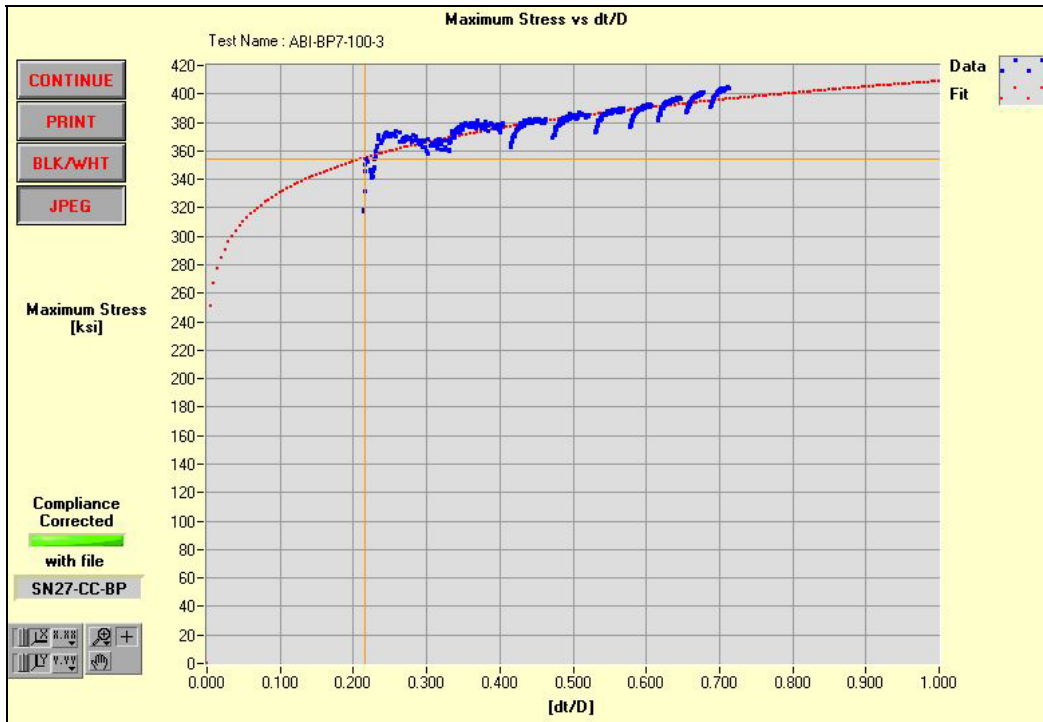


Fig. 25 Example of the use of the critical fracture stress model to determine the critical indentation depth in order to integrate the indentation deformation energy up to this critical depth to calculate fracture toughness from the multi-axis ABI test.

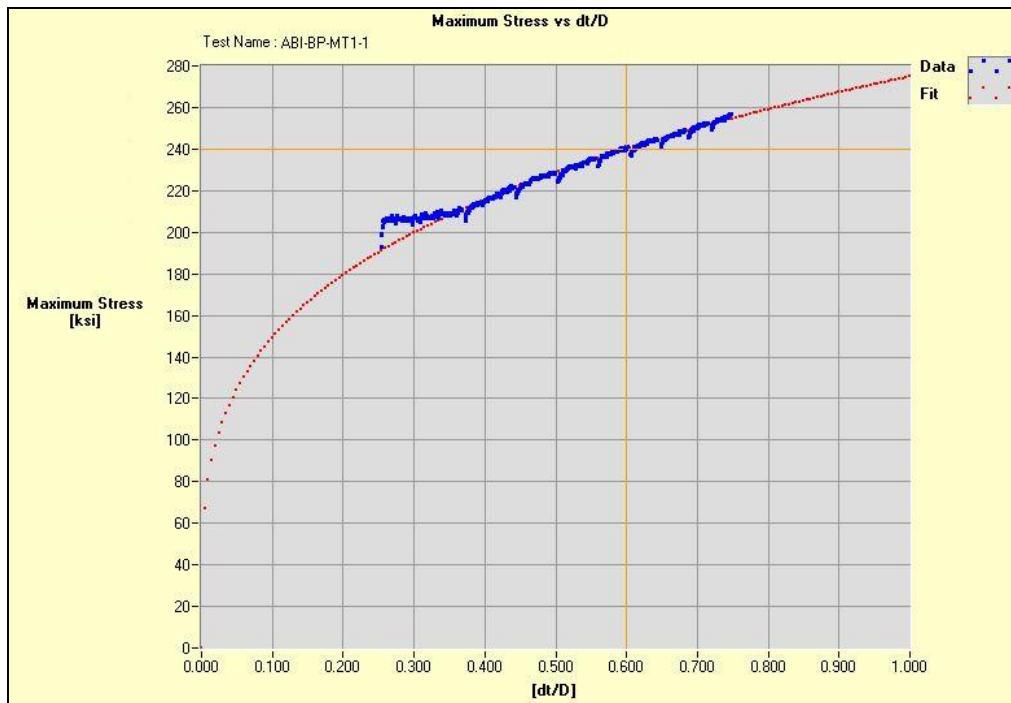


Fig. 26 Example of the use of the critical fracture strain model when testing a ductile material at room temperature where the critical fracture stress is not reached at a normalized depth of $d_i/D = 0.6$.

References

1. Haggag, F. M., "Field Indentation Microprobe for Structural Integrity Evaluation," U.S. Patent No. 4,852,397, 1989.
2. Haggag, F. M., et al., "Use of Portable/In Situ Stress-Strain Microprobe System to Measure Stress-Strain Behavior and Damage in Metallic Materials and Structures," *ASTM STP 1318*, 1997, pp 85-98.
3. Haggag, F. M., "In-Situ Measurements of Mechanical Properties Using Novel Automated Ball Indentation System," *ASTM STP 1204*, 1993, pp. 27-44.
4. Haggag, F. M., et al., "Use of Automated Ball Indentation Testing to Measure Flow Properties and Estimate Fracture Toughness in Metallic Materials," *ASTM STP 1092*, 1990, pp. 188-208.
5. Haggag, F. M. et. Al., "Indentation-Energy-to-Fracture (*IEF*) Parameter for Characterization of DBTT in Carbon Steels Using Nondestructive Automated Ball Indentation (*ABI*) Technique," *Scripta Materialia*, Vol 38, No. 4, 1998, pp 645-651.
6. Byun, T. S., et al. "A Theoretical Model for Determination of Fracture Toughness of Reactor Pressure Vessel Steels in the Transition Region from Automated Ball Indentation Test," *Journal of Nuclear Materials*, 252 (1998) pp. 187-194.
7. Byun, T. S., et al. "Measurement of Through-the-Thickness Variations of Mechanical Properties in SA508 Gr.3 Pressure Vessel Steels Using Ball Indentation Test Technique," *International Journal of Pressure Vessels and Piping*, 74 (1997) pp. 231-238.
8. Haggag, F. M., et al., "Using Portable/In-Situ Stress-Strain Microprobe System to Measure Mechanical Properties of Steel Bridges During Service," SPIE Proceedings on "Nondestructive Evaluation of Bridges and Highways," Vol. 2946, 1996, pp. 65-75.
9. Haggag, F. M., et al., "Nondestructive Detection and Assessment of Damage in Aging Aircraft Using a Novel Stress-Strain Microprobe System," SPIE Proceedings on "Nondestructive Evaluation of Aging Aircraft, Airports, and Aerospace Hardware," Vol. 2945, 1996, pp. 217-228.
10. Haggag, F. M. et al., "Structural Integrity Evaluation Based on an Innovative Field Indentation Microprobe," *ASME PVP-Vol. 170*, 1989, pp. 101-107.
11. Haggag, F. M. and Nanstad, R. K., "Estimating Fracture Toughness Using Tension or Ball Indentation Tests and a Modified Critical Strain Model," *ASME PVP-Vol. 170*, 1989, pp. 41-46.
12. Druce, S. G., et al., "The Use of Miniature Specimen Techniques for the Assessment of Material Condition," *ASME PVP-Vol. 252*, 1993, pp. 58-59.
13. Haggag, F. M., "Nondestructive Determination of Yield Strength and Stress-Strain Curves of In-Service Transmission Pipelines Using Innovative Stress-Strain Microprobe™ Technology," *ATC/DOT/990901*, September 1999.
14. Haggag, F. M., "Nondestructive and Localized Measurements of Stress-Strain Curves and Fracture Toughness of Ferritic Steels at Various Temperatures Using Innovative Stress-Strain Microprobe™

Technology,” DOE-SBIR Phase II final report *DOE/ER/82115-2*, under grant number DE-FG02-96ER82115.

15. Haggag, Fahmy M., “In-Situ Nondestructive Measurements of Key Mechanical Properties of Oil and Gas Pipelines,” *ASME PVP-Vol. 429*, 2001, pp. 99-104.

16. Haggag, Fahmy M., 2002, “In-Service Nondestructive Measurements of Stress-Strain Curves and Fracture Toughness of Oil and Gas Pipelines: Examples of Fitness-for-Purpose Applications,” *Proceedings of the 5th International Conference on Pipeline Rehabilitation & Maintenance, Det Norske Veritas, Bahrain, Paper 7*.

17. Haggag, Fahmy M. and Philips, Larry D., “Innovative Nondestructive Method Determines Fracture Toughness of In-Service Pipelines,” *ASME Proceedings of IPC 2004*, International Pipeline Conference, October 4-8, 2004, Calgary, Alberta, Canada, *IPC04-0345*, 2004.

18. Haggag, Fahmy M., “Indentation Technique Provides Pipeline Integrity Monitoring,” *Oil and Gas Journal*, August 14, 2006, p. 58-62.

19. ASTM Standard E1921-97, “Standard Test Method for Determination of Reference Temperature, T_0 , for Ferritic Steels in the Transition Range,” *Annual Book of ASTM Standards*, Vol 03.01.

20. Rolfe, Stanley T. and Barsom, John M., *Fracture and Fatigue Control in Structures: Applications of Fracture Mechanics*, Prentice-Hall, Inc., Englewood Cliffs, New Jersey, 1977, p. 129.

APPENDIX A

DOT Review Letter of ATC's SSM technology (signed by the Secretary of DOT in 1999) based on ATC's comprehensive report (Reference 13 of this report) available for downloading at:

www.atc-ssm.com/papersrepairs.html

990924-060



THE SECRETARY OF TRANSPORTATION

WASHINGTON, D.C. 20590

COPY

December 13, 1999

The Honorable Zach Wamp
U.S. House of Representatives
Washington, D.C. 20515

Dear Congressman Wamp:

Thank you for your letter and report forwarded on behalf of Dr. Fahmy M. Haggag regarding Stress-Strain Microprobe™ (SSM) technology. Dr. Haggag's report has been forwarded to the Research and Special Programs Administration (RSPA) for review.

The RSPA Administrator Kelley S. Coyner has advised me that the Office of Pipeline Safety (OPS) has been following the development of SSM technology for some time. Dr. Haggag's report has been reviewed and the technology appears to be fundamentally sound for application in the pipeline industry. Although the U.S. Government is not permitted to endorse an individual product or technology, it is RSPA's policy to encourage industry to use the latest technology, materials and practices available. RSPA is interested in and plans to follow the development of SSM technology as it is applied by the pipeline industry.

Again, thank you for bringing this information to our attention. If we can be of further assistance, please contact Michael J. Frazier, Assistant Secretary for Governmental Affairs, at (202) 366-4563.

Sincerely,

A handwritten signature in black ink, appearing to read 'Rodney E. Slater', written over a white background.

Rodney E. Slater

Get a free copy of this report at our web site:
www.atc-ssm.com

APPENDIX B

ABI Test Method (Test Procedure, Data Analysis, and Precision Values)

Standard Test Methods for Automated Ball Indentation (ABI) Testing of Metallic Materials and Structures to Determine Tensile Properties and Stress-Strain Curves

Copyright 1988-2007, Fahmy M. Haggag, Advanced Technology Corporation, Oak Ridge, TN, USA

1. Scope of the Test Methods

- 1.1. These methods cover the determination of the true-stress versus true-plastic-strain curves of metallic materials and structural components using an automated ball indentation (ABI) test technique. They can be used for any metallic material with thickness greater than 0.51 mm (0.02 in). They require a surface that is smooth and that has a minimum distance of 0.51 mm (0.02 in) between free edges. The ABI test methods can be performed using a laboratory bench-top instrument or a portable field device.
- 1.2. The ABI test can be conducted at a wide range of sample temperatures. Current experience has been shown to perform well at ranges between -196 and 427°C (-320 to 800°F). Testing at higher temperatures can be performed provided that the test surface is not severely altered by oxidation or corrosion during the test.
- 1.3. The purpose of the ABI test methods is to determine tensile properties (including true-stress versus true-plastic-strain curve, yield strength, uniform ductility, strain-hardening exponent, ultimate strength, and Lüders strain) as a nondestructive and localized alternative to the destructive tension test methods conducted according to ASTM standards E 8, E 21, and E 646.
- 1.4. *This standard does not purport to address all the safety concerns, if any, associated with its use. It is the responsibility of the user to establish appropriate safety and health practices and determine the applicability of regulatory limitations prior to use.*

2. Referenced Documents

2.1. ASTM Standards:

- E 4 Practices for Force Verification of Testing Machines
- E 6 Terminology Relating to Methods of Mechanical Testing
- E 8 Test Methods for Tension Testing of Metallic Materials
- E 21 Test Methods for Elevated Temperature Tension Tests of Metallic Materials
- E 74 Practice for Calibration of Force Measuring Instruments for Verifying the Force Indication of Testing Machines
- E 646 Test Methods for Tensile Strain-Hardening Exponents (n -Values) of Metallic Sheet Materials

3. Terminology

- 3.1. *Definitions*—The definitions of terms relating to tension testing appearing in Terminology E 6 shall be considered as applying to the terms used in these test methods of automated ball indentation (ABI) testing. Additional and new terms related to this standard are defined as follows:
 - 3.1.1 *Force-depth partial unloading slope* [FL^{-1}]*—*the ratio of spherical indentation force to indentation depth increment during the upper 50% unloading.
 - 3.1.2 *Meyer's index, m**—*a material constant related to the strain hardening of the metal.

- 3.1.3. *Yield parameter (A)* [FL⁻²]*—*a test material parameter related to the yield strength and strain hardening of the metal that expresses the resistance of metal to penetration by a spherical indenter.
- 3.1.4. *Material's yield slope (β_m)**—*a material type constant related to the yield strength of each class of metal (e.g., aluminum, ferritic steel, stainless steel, titanium, uranium alloys, etc.).
NOTE—It is an empirical value similar to the 0.2% offset value of the yield strength as defined in the uniaxial tension test.
- 3.1.5. *ABI-derived yield strength (σ_y)* [FL⁻²]*—*an ABI parameter that is related to the 0.2% offset yield strength from tension tests of most metallic materials.
- 3.1.6. *Constraint factor (α_m)**—*a material constant related to the resistance of metal to plastic spherical deformation within a specific range of strain rate or indenter speed.
- 3.1.7. *Effective ball indentation strain rate ($\dot{\epsilon}$)**—*the average strain rate from all indentation cycles performed at a single test location during a complete ABI test.
NOTE—The ball indenter strain rate ($\dot{\epsilon}$) for each cycle is the ratio of indenter velocity (v) to the indentation chordal diameter (d_i) multiplied by 0.4 ($\dot{\epsilon} = 0.4 v/d_i$).
- 3.1.8. *Strain-hardening exponent (n)**—*the exponent in the empirical relationship between true-stress (σ_t) and true-plastic-strain (ϵ_p), $\sigma_t = K\epsilon_p^n$.
NOTE—It is computed as the slope of the E 646 assumed linear relationship between logarithm true-stress and logarithm true-plastic-strain.
- 3.1.9. *Strength coefficient (K)* [FL⁻²]*—*an experimental constant, computed from the fit of the data to the assumed power law (described in E 646) that is numerically equal to the extrapolated value of true stress at a true-plastic-strain value of 1.00.
- 3.1.10 *Discontinuous yielding or Lüders strain (ϵ_L)**—*in a uniaxial tension test, a hesitation or fluctuation of force, such as is sometimes observed at or near the onset of plastic deformation, due to localized yielding (The stress-strain curve need not appear to be discontinuous.)
NOTE—In an ABI test the Lüders strain behavior is manifested in the material pile-up around the indentation. In an ABI test Lüders strain is calculated from its relationship with the material yield strength, strain-hardening exponent, and strength coefficient.

4. Summary of Test Methods

- 4.1 A spherical (ball) indenter is forced into the surface of a metallic sample or a structural component. The spherical shape of the indenter causes an increasing strain with increased indentation depth up to a maximum of 0.2 or 20% true-plastic-strain. A true strain of 20% corresponds to a penetration depth equal to the indenter radius. The penetration depth of the spherical indenter into the test surface is measured with a displacement transducer such as a spring-loaded linear variable differential transformer (LVDT). The current strain produced is a function of the penetration depth. The force required to indent the material to increased depth values is measured with a force transducer such as a load cell. The current stress at any time is a function of the current indentation force. Periodic partial unloadings during the test are used to determine the elastic strain. The elastic strain is subtracted from the total strain to give the plastic strain. The incremental values of the ABI-measured true-stress and true-plastic-strain are calculated from the indentation force-depth data (based on elasticity and plasticity theories) and plotted to form a true-stress versus true-plastic-strain curve of the material. The ABI-derived yield strength is determined from the force-depth data. Other properties, including the strain-hardening exponent (n), strength coefficient (K), Lüders strain (ϵ_L), uniform ductility, and ultimate strength (UTS), may also be estimated from the ABI test. Also, the ABI test can be performed without intermediate partial unloadings (i.e., in a single cycle of continuous loading up to the desired maximum indentation depth/strain followed by complete unloading). This approach is preferred for high temperature or high strain rate testing to avoid indentation creep

and nonlinear unloading slopes, respectively. The single cycle ABI test produces a curve of true-stress versus true-strain (i.e., total true strain since the elastic strain component cannot be subtracted due to the elimination of partial unloadings).

- 4.2 The entire test is fully automated (computer-controlled) where the spherical indenter is driven into the test surface at a desired speed which controls the strain rate of the ABI test, and the indentation force versus penetration depth are continuously collected (using a 16-bit resolution data acquisition system or better) during the entire test.
- 4.3 For laboratory specimens, the test samples can be cooled or heated to the desired ABI test temperature using an environmental chamber to bring both test sample and indenter to the desired test temperature while the force and displacement transducers are kept outside the chamber. When the depth sensor is positioned outside the environmental chamber the compliance of the testing machine shall be considered. A temperature-resistant LVDT or a clip gage can be used inside the environmental chamber. Testing at higher temperatures can be performed provided that the test surface is not severely oxidized (e.g., by utilizing an inert gas or a vacuum chamber). The test sample and the indenter shall maintain test temperature within $\pm 2.0^{\circ}\text{C}$ ($\pm 4^{\circ}\text{F}$) before conducting and during the entire ABI test.

5. Significance and Use

- 5.1 The stress-strain curve measured with the ABI test has been demonstrated to correlate with the stress-strain curve measured in a tension test. The localized ABI test is nondestructive and can be used in-situ to measure the stress-strain properties of a material sample or of a component part in service. Therefore, it can be used to measure stress-strain properties where insufficient material is available to use in a destructive tension test. The ABI test leaves a shallow spherical depression on the test surface with no sharp edges (hence, no crack initiation sites). Furthermore, it leaves a favorable compressive residual stress at the test site (similar to shot peening but on a slightly larger scale). The ABI test is also useful in testing small volumes of welds and irregularly shaped heat-affected-zones (HAZs).
- 5.2 The ABI test is particularly useful where a life extension evaluation is planned for a component and adequate materials property data are not available. Also, it can be used to measure properties for materials that may have service damage that has caused a change in tensile properties during service life (e.g. neutron embrittlement of nuclear pressure vessels). Another important application is the determination of yield strength of ferritic steel components, such as oil and gas pipelines, when no documentation exists for the original and/or repair material and when a deterministic fitness-for-service evaluation is required for safe operation at current or higher (up-rated) pressures.
- 5.3 The ABI test is a macroscopic/bulk technique that measures the properties on a small volume of material. This capability is valuable in mapping out property gradients in welds and HAZs. The minimum diameter of the indenter must be large enough such that the spherical indentation, produced at the smallest practical depth/strain, covers at least three grains of the metallic sample. This requirement is the same for the minimum thickness of a tensile specimen in order to measure macroscopic/bulk properties. The ABI technique can be used to measure the stress-strain properties of a material that may have a sharp gradient of mechanical properties. This, for example, exists in a weldment where the base metal and the weld metal have different strength and ductility and the HAZ may have a very sharp gradient of properties. Here the ABI test can measure the flow properties (true-stress versus true-plastic-strain curve) of a small volume of material and can measure the strength profile along a line traversing from one base metal through the HAZ, the weld metal and continuing through the other base metal.

- 5.4 Although the ABI test is nondestructive, the strain-hardening exponent (n) determined from the test is a function of the uniform plastic strain of many metallic materials with a power-law true-stress versus true-plastic-strain curve (e.g. nuclear pressure vessels and carbon steel materials).
- 5.5 Although there is no necking (similar to that occurring at maximum force in a tension test), the uniform ductility and ultimate tensile strength are determined from the plot of true-stress versus engineering strain.
- 5.6 The value of Lüders strain (an important property for evaluating steel sheet metals in automotive industry) is calculated from the ABI-measured yield strength, strain-hardening exponent, and strength coefficient.

6. Apparatus

- 6.1 *Testing Machines*—Machines used for ABI testing on metal samples or structures shall conform to the requirements of Practices E 4 for force verification of testing machines. The choice of bench-top or field-testing machine type depends on the application.
- 6.2 The forces used in determining the true-stress versus true-plastic-strain curve from an ABI test with a certain diameter indenter shall be within the verified loading range of the testing machine as defined in Practices E4 (Standard Practices for Force Verification of Testing Machines). The maximum ABI force depends on the indenter diameter, maximum indentation depth, and the flow properties of the metal test sample or structure. The force transducer capacity should be appropriate for the indenter diameter and the test material flow properties. The non-linearity and non-repeatability of the force transducer shall not exceed $\pm 0.1\%$ and $\pm 0.03\%$ of the full scale (maximum capacity) of the load cell, respectively. The accuracy of the force transducer shall be within $\pm 1\%$ of the full working range. The temporary attachment method (e.g., manual or electric magnets, V-blocks with mechanical clamps, etc.) shall ensure: (a) perpendicularity of the indenter axis to the test surface, and (b) enough pull force to counter the maximum indentation push force plus the weight of the load frame of the portable testing machine. The minimum components of the testing machine include a rigid load frame suitable for bench-top or field applications (for metal component testing), a driving mechanism (such as an electric motor and a mechanical actuator), an appropriate capacity force transducer such as a load cell, a gripping device for holding the indenter, a bracket for holding the displacement transducer (e.g., a spring-loaded Linear Variable Differential Transformer “LVDT”), a high resolution 16-bit data acquisition card or better, and a computer (either a desk-top or a laptop) with appropriate software and interface to the data acquisition card and the motor to provide complete control of the ABI test as well as post-test data analysis. The complete automation of the testing machine shall provide closed loop operation with continuous measurement and software limits on both the force and depth signals. The software limits prevent possible damage to the force or depth sensors and avoid violating the depth requirement for a valid ABI test.
- 6.3 *Indentation depth measurement and calibration*—a high-resolution depth sensor with a full range not greater than 1.0 mm (such as a spring-loaded LVDT) is used for ABI testing. The non-linearity of the depth sensor shall be less than 0.20% of the full range output, and the non-repeatability shall be less than 0.00010 mm (0.000004 in). The depth sensor is mounted on a bracket attached to the indenter holder. The accuracy of the depth sensor shall be within $\pm 1\%$ of the full working range. The depth sensor is calibrated using a micrometer or a similar device with an accuracy of 0.001 mm.
- 6.4 *Indenters*—The spherical indenter shall be polished and free of surface defects. The tolerance shall be ± 0.003 mm or better in any diameter of the indenter. Spherical indenters made from either tungsten carbide or silicon nitride where the spherical tip and the indenter stem are manufactured from the same material are used for ABI testing of metal samples and structural components. Spherical indenters with various diameters (e.g., 0.254-mm, 0.508-mm, 0.762-mm,

and 1.575-mm with a deviation from these values of not more than 0.003 mm in any diameter) can be used for ABI testing depending on the test volume available and the grain size of the test metal. The tungsten carbide indenter shall have an elastic modulus at room temperature greater than 620 Gpa and Vickers hardness not less than 1500. Silicon nitride indenters, with Vickers hardness of 1600 or higher and an elastic modulus at room temperature greater than 320 Gpa, are recommended for use at test temperatures above 400°C and up to 1000°C. The indenter holder, such as a stainless steel chuck, should provide easy interchangeability of indenters, solid support of the indenter stem, and ensure the perpendicularity of the indenter tip to the test surface. The indenter diameter is selected based on the test volume (thickness, final indentation depth, and available test area) and the grain size of the metal. Whenever possible the largest size indenter is selected to increase the test volume and to increase precision. Small indenters such as the 0.254-mm diameter require very smooth surface finish using at least 600-grit polishing. The maximum indentation depth shall not exceed 10% of the specimen thickness, and the indentation chordal diameter shall be enclosed within the desired test material including small welds or HAZ. Appropriate force transducer capacity should be used for each size indenter for increased resolution (e.g., 4.45 kN, 1.11 kN, 445 N, and 222 N load cells are appropriate for indenter diameters of 1.575-mm, 0.762-mm, 0.508-mm, and 0.254-mm, respectively).

6.5 *Load-frame attachments for field-testing of pipelines and pressure vessels*—Various attachment methods can be used to temporarily attach the load frame of the portable/field testing machine to structural metal components. These attachments (e.g., manual or electric magnets for magnetic components such as carbon steel pipelines and pressure vessels, V-blocks with mechanical clamps for non-magnetic materials) shall ensure: (a) perpendicularity of the indenter to the test surface, and (b) enough pull force to counter the maximum indentation push force plus the weight of the load frame of the portable testing machine.

6.6 *Furnaces or Heating Devices*—When performing an ABI test on a specimen at elevated temperature, the furnace or heating device used shall be capable of maintaining a uniform temperature of the entire test specimen and the indenter so that variation of not more than $\pm 2.0^{\circ}\text{C}$ ($\pm 4^{\circ}\text{F}$) for temperatures up to and including 427°C (800°F) occurs. Heating by self-resistance is not accepted.

7.0 Specimen/Structural Preparation

Surface finish and optional sample mounting—The ABI test location shall have a smooth machined/ground surface, or if necessary, it shall be polished to a surface finish of 1.6 μm (63 micro-inches). Care shall be taken in surface preparation to avoid overheating or cold working the surface. An irregular or very small sample shall be mounted in Bakelite or a similar hard material with the top and bottom surfaces parallel. A rigid swivel sample holder shall be used if the mounted sample does not have parallel surfaces. The ABI test area of a metal component shall be polished locally using hand held equipment. Other component areas must be prepared properly for the attachments used (e.g., any rust must be removed from carbon steel pipelines in order for the magnetic attachments to secure the load frame of the portable machine to the pipeline test location). When indentations are made on a curved surface, the minimum radius of curvature of the surface shall be not less than 25 times the diameter of the ball indenter.

8.0 Test Procedure

8.1 *Objective and Overview*—The overall objective of the test methods is to develop ABI force-depth curves that can be used to calculate the ABI-derived yield strength, true-stress versus true-plastic-strain curve, strain-hardening exponent, strength coefficient, uniform ductility, and ABI-estimated ultimate strength. Two procedures can be used: (1) a multi-cycle ABI test with

- intermediate partial unloadings or (2) a single-cycle ABI test with no intermediate partial unloadings.
- 8.2 *Locating indentation positions*—The planar spacing of indentations shall be at least three diameters from their centers and within at least two diameters from free edges.
 - 8.3 *Initial test preload*—An initial test preload is required for calculating the zero indentation point, on the ABI force-depth curve, at which the ball indenter contacts the test surface for the first time. A small indentation preload (less than 10% of the indentation force at a depth value of 30% of the indenter radius), appropriate to the indenter diameter, is applied to the sample or structure before the continuation of the ABI test. Minimum suggested preloads for the four indenter diameters of 0.254-mm, 0.508-mm, 0.762-mm, and 1.575-mm are 2 N, 5 N, 10 N, and 30 N, respectively). After the preload application, the depth transducer value, indicated on the computer screen, must be small enough to ensure that there is enough remaining range of depth measurement to complete the test up to the user-specified final indentation depth. Immediately after the application of the preload, the ABI test is continued according to either the Multi-Cycle or the Single-Cycle procedures described in 8.3 and 8.4, respectively.
 - 8.4 *Multi-Cycle ABI test*—The procedure involves progressive loading of the ball indenter into the test surface up to a final depth/strain (e.g., 30% of the indenter radius relates to approximately 15% strain). A minimum of five cycles shall be performed at a single ABI test location with equal increments of indentation depth. All intermediate cycles include partial unloading of the indenter (by a determined percentage of 30 –50% of the maximum cycle-force depending on the data acquisition rate). The specimen is fully unloaded at the end of the test. All indentation loading and unloading are performed with a constant indenter speed during the entire ABI test. The force-depth data is collected (using a 16-bit data acquisition system or better) and displayed in real-time on the computer screen during the complete ABI test. The ABI test is fully computer controlled with closed-loop software limits on both force and depth data. If during the test any limit is reached, the loading process is immediately halted and the test area is unloaded. The unloading slopes are linear because of the elastic recovery of the test volume. These slopes are not parallel and increase with increasing indentation depth as the deformation volume increases while the sample elastic modulus does not change with indentation depth. Fig.1 shows a schematic of cyclic loading and unloading of a ball indenter into the surface of test material: (a) Schematic of applied force versus indentation depth, (b) Indentation geometry during force application and after force removal (complete unloading).
 - 8.5 *Single-Cycle ABI Test*—The ABI test can be performed without intermediate partial unloadings (i.e., in a single cycle of continuous loading up to the desired maximum indentation depth/strain followed by complete unloading). This approach is preferred for high temperature or high strain rate testing to avoid indentation creep and nonlinear unloading slopes, respectively. The single cycle ABI test produces a curve of true-stress versus true-strain (i.e., total true strain since the elastic strain component cannot be subtracted due to the elimination of partial unloadings).
 - 8.6 *Field Testing Precautions*—When performing ABI field tests on metallic structures at various locations the load frame of the portable testing machine shall be moved carefully between far locations to avoid possible mechanical damage to the force and depth sensors and the indenter during shipment in an automobile or airplane.
 - 8.7 *Indenter Installation and Replacement*— When an indenter is changed, the new indenter shall be seated properly and fully in its stainless steel chuck holder. The indenter is seated by performing an ABI test at an additional test location and verifying that there is no indenter slippage inside its chuck holder (i.e., there is no horizontal force-depth behavior on the real-time force-depth display on the computer monitor).

9.0 Calculation of Results

- 9.1 *Calculation of indentation depth associated with initial test preload*—Linear regression is performed on the force-depth data of the best linear part of the first loading cycle in a Multiple-Cycle ABI test or from the early part (first 5%) of the force-depth curve in a Single-Cycle ABI test. The intersection of the extrapolation of the linear regression fit with the X-axis determines the depth value associated with the preload value. Hence, this indentation depth value is added as a correction or adjustment to all depth data of the raw force-depth curve previously collected with temporarily assuming a zero depth associated with the preload value as shown in Fig. 2. This adjustment results in a lateral shift of the raw force-depth curve to the right by the amount determined from the data regression shown in Fig. 3. The corrected/adjusted ABI force-depth data is shown in Fig. 4.

NOTE 1—The force-depth curve of an ABI test is linear because of the effect of the strain hardening behavior of metallic materials on the shape of the force-depth curve. A nonlinear/ball indenter produces increasing strain values with increasing depth while a linear indenter (Vickers, cone, etc.) produces a single value of strain regardless of depth and a nonlinear (concave) force-depth curve. Hence, a stress-strain curve can be produced only using a nonlinear indenter. ABI test results on many materials in various conditions are reported in References 1 through 16.

- 9.2 *Calculation of the plastic-depth associated with each cycle in a Multi-Cycle ABI test*—Linear regression analysis is performed on the data of each elastic partial unloading, and the calculated slope is extrapolated where its intersection with the depth axis determines the plastic depth associated with the upper force of the cycle. This is shown schematically in Fig. 1a and graphically (from an example ABI test data using a 0.762-mm diameter indenter) in Fig. 5.
- 9.3 *Calculation of true-stress and true-plastic-strain pairs*—The incremental values of the true-stress versus true-plastic-strain curve are calculated from Equations 1 through 11(3). For a single-cycle ABI test, the plastic chordal diameter is replaced by the total chordal diameter (calculated from the total depth, Equation 9). It is important to note that these equations are independent of the work-hardening behavior of the material (i.e., regardless if it follows a power law or not). The value of the constraint factor index (α_m) used in equation 6 depends on the class of material, and the test strain rate. It is determined empirically from comparison of true-stress versus true-plastic-strain curves from ABI and tension tests (values for carbon steel and aluminum alloys are given in Appendix X1). For an unknown material, a value of 1.1 should be used in Equation 6 for the constraint factor index.
- 9.4 *Calculation of the ABI-derived yield strength*—The yield strength determined from an ABI test is calculated from Equations 9 through 11 (3). Figure 6 is an example plot of Equation 10. The values of the material's yield slope (β_m) and the yield strength offset-constant (B) depend on the class of metal and the indenter diameter (slope and offset-constant values for carbon steel and aluminum alloys are given in Appendix X1). These values are empirically determined to be in close agreement with the 0.2% offset yield strength determined from uniaxial tension tests (16). For example, a recommended value for the yield strength slope (β_m) for carbon steel testing using a 0.762-mm tungsten carbide indenter is 0.22. The values of the yield parameter (A), material's yield slope (β_m), and yield strength offset-constant (B) used in the ABI-derived yield strength calculation shall be documented in the ABI test report. For an unknown material, values of 0.20 and 0.00 should be used for the material yield strength slope and yield strength offset-constant, respectively.
- 9.5 *Calculation of strain-hardening exponent (n), strength coefficient (K), Lüders strain (ϵ_L), and estimated ultimate strength (UTS)*—The true-stress versus true-plastic-strain results from the ABI test are fitted to the power law form of Equation 12 as described in Method E 646. A single power curve is fitted to the entire curve between yield and the final true strain at the end of the

test, or the yield strength point can be eliminated from the data fit, depending on the desired strain range for determining the “ n ” value. The strain-hardening exponent (n) and the strength coefficient (K) are determined from this empirical representation of the flow curve (Equation 12). An example of ABI-measured flow properties, including the yield strength value, and their power-law fitting is shown in Fig. 7. The Lüders strain is calculated from Equation 13. If the flow properties of the test material are well represented by the power law form of Equation 12 (E 646), then the ultimate strength can be estimated from Equation 14. If the ABI-measured true-stress versus true-plastic-strain curve does not follow a single power law, then it shall be calculated from the plot of true-stress versus engineering strain as explained in item 9.6 below and in Figure 8.

NOTE 2—In the ABI test there is no necking behavior similar to that occurring in a tension test. Hence the *UTS* can be estimated from Equation 14 or it can be calculated using the plot of true-stress versus engineering strain.

- 9.6 *Calculation of uniform ductility and ultimate tensile strength (UTS)*— A straight line is drawn from an engineering strain value of -1.00 to be a tangent to the true-stress versus engineering strain curve (17). The X-axis value of this line at the tangent intersection point determines the uniform ductility while the intersection of the line with the Y-axis, at the origin (0,0), determines the engineering *UTS* value. An example of the calculation of the Uniform Ductility and the Engineering *UTS* from the ABI-measured True-Stress versus Engineering Strain curve is shown in Figure 8.
- 9.7 *Indenter Diameter Selection and Data Qualification*—The indenter diameter is selected based on the test volume (thickness, final indentation depth, and available test area) and the grain size of the metal. For a Single-Cycle test, some of the force-depth data collected at very low depth (the first 5% depth of the entire test) shall be excluded from the stress-strain curve calculations if the indentation chordal diameter at such a small depth covers less than three grains. Notice that the progressive ball indentation at lowest practical depth increment should cover more than three grains in order to obtain macroscopic stress-strain properties. An example comparison between a small indentation (made using a 0.254-mm diameter indenter and a force of 2 N) and the grain size of the test material is provided in Figure 9. An example of qualified ABI force-depth data (generated using a 0.508-mm diameter indenter), test results, and comparison with tensile test results are shown in Fig. 10. An example of the geometry of a large indenter (1.575-mm diameter) is shown also in Figure 10 (inset photo).

Where:

$$\epsilon_p = \frac{0.2d_p}{D} \quad (1)$$

ϵ_p = true plastic strain,
 d_p = plastic indentation diameter,
 D = diameter of the ball indenter.

$$\sigma_t = \frac{4P}{\pi d_p^2 \delta} \quad (2)$$

Where:

σ_t = true stress,
 P = applied indentation force,
 δ = a parameter whose value depends on the stage of development of the plastic zone beneath the indenter as shown in Equation 5 below.

$$d_p = \left\{ 0.5CD \left[\frac{h_p^2 + \left(\frac{d_p}{2}\right)^2}{h_p^2 + \left(\frac{d_p}{2}\right)^2 - h_p D} \right] \right\}^{1/3} \quad (3)$$

Where h_p is the plastic indentation depth and “C” is defined in Equation 4 below.

$$C = 5.47P \left(\frac{1}{E_1} + \frac{1}{E_2} \right) \quad (4)$$

Where E1 and E2 are the elastic moduli of the indenter and the test sample, respectively.

$$\delta = \begin{cases} 1.12 & \Phi \leq 1 \\ 1.12 + \tau \ln \Phi & 1 < \Phi \leq 27 \\ \delta_{\max} & \Phi > 27 \end{cases} \quad (5)$$

$$\delta_{\max} = 2.87\alpha_m \quad (6)$$

Where α_m is the constraint factor index.

$$\Phi = \frac{\epsilon_p E_2}{0.43\sigma_t} \quad (7)$$

$$\tau = \frac{\delta_{\max} - 1.12}{\ln(27)} \quad (8)$$

Where “ \ln ” is the natural logarithm.

$$d_t = 2\sqrt{h_t D - h_t^2} \quad (9)$$

Where h_t and d_t are the total indentation depth and total indentation diameter while the force is being applied, respectively.

$$\frac{P}{d_t^2} = A \left(\frac{d_t}{D} \right)^{m-2} \quad (10)$$

Where A is the material yield parameter and m is Meyer’s index.

$$\sigma_y = \beta_m * A + B \quad (11)$$

Where σ_y is the ABI-determined yield strength, β_m is the material yield slope, and B is the yield-strength offset-constant.

$$\sigma_t = K\epsilon_p^n \quad (12)$$

Where K is the strength coefficient and n is the strain-hardening exponent.

$$\ln\left(\frac{K}{\sigma_y}\right) = \epsilon_L - n * \ln \epsilon_L \quad (13)$$

Where ϵ_L is Lüders strain.

$$UTS = K\left(\frac{n}{e}\right)^n \quad (14)$$

Where UTS is the ABI-estimated ultimate strength and $e = 2.718$.

10. Report

- 10.1 A recommended format for reporting the test parameters, equipment parameters, analysis parameters, and test results for both Multi-Cycle and Single-Cycle ABI tests is shown in Fig. 11 (a) while an additional reporting format suggested for the Multi-Cycle ABI test only is shown in Fig. 11(b).
- 10.2 Report the following information for each ABI test: test name, test material and test number, test atmosphere, test temperature, indenter diameter, indenter speed, number of unloadings, data acquisition rate, percentage of the partial unloading, maximum indentation depth (percentage of indenter radius used in final indentation), indenter material and its elastic modulus, constraint factor, yield strength slope and offset, total number of data points collected, reporting of any force or depth limits triggered during the ABI test, ABI results of ABI-derived yield strength, strain-hardening exponent, strength coefficient, ABI-estimated engineering UTS , ABI-calculated engineering UTS (from the plot of true-stress versus engineering strain), and calculated uniform ductility.
- 10.3 Report the additional data and test results for each cycle of a Multi-Cycle ABI test: cycle number, maximum total depth, plastic depth, maximum force, plastic indentation chordal diameter, unloading slope, R^2 value (regression coefficient) for the regression analysis of the partial unloading slope, total chordal diameter, true-plastic-strain, and true-stress.
- 10.4 Report the following graphs: force-depth data before and after adjustment for the depth associated with the applied preload, yield strength calculation plot, true-stress versus true-plastic-strain curve with individual points and power-law fit, and a plot of the true-stress versus engineering strain.

11. Precisions and Bias

- 11.1 *Precision*—The precision of any of the various ABI-determined flow properties cited in these test methods is a function of the precision and bias of the various measurements of indenter diameter, the precision and bias of the depth measurement, the precision and bias of the force measurement, and the precision and bias of the data acquisition system used to construct the force-depth curve. It is not possible to make meaningful statements concerning the precision and bias for all these measurements. However it is possible to derive useful information concerning the precision of the ABI-measured flow properties in a global sense from interlaboratory test programs. Values of the ABI-determined yield strength and true-stress versus true-plastic-strain curves were evaluated in (15) for several pressure vessel steels at various test temperatures. The ABI-derived yield strength and estimated ultimate strength values were evaluated in (16) for seven pipeline steels, with various grades and manufacturing dates, tested at room temperature using two indenter diameters (0.508 mm and 0.762 mm), and the ABI test results were compared to the results from tensile tests on the same materials.

An interlaboratory test program¹ gave the following values for the coefficients of variation for the most commonly ABI-measured flow properties:

	<i>Coefficient of Variation, %</i>				
	ABI-Yield Strength	ABI-Estimated Ultimate Strength	Strength Coefficient	Strain-Hardening Exponent	Uniform Ductility
CV % _r	1.4	1.5	2.6	5.8	6.9
CV % _R	1.7	2.3	3.4	6.7	7.8

CV %_r = repeatability coefficient of variation in percent within a laboratory
 CV %_R = repeatability coefficient of variation in percent between laboratories

11.1.1 The values shown are the averages from five ABI tests on each of four frequently tested metals (ferrous and non-ferrous), selected to include most of the normal range for each property listed above. Twenty ABI tests were conducted by each of six different laboratories using commercial Stress-Strain Microprobe (SSM) systems² especially designed for ABI testing. The slightly higher coefficients of variation for the strain-hardening exponent and the uniform ductility are due to the fact that these two properties depend on the shape of the stress-strain curve and the homogeneity of the metal. The values of the coefficient of variation are provided to allow potential users of these test methods to assess, in general terms, their usefulness for a proposed application. Additional precision statistics are provided in Appendix X1.

11.2 *Bias*—The procedures in the ABI test methods for measuring flow properties have no bias because these properties can be defined only in terms of the test methods. When comparing flow properties from ABI and tension tests the agreement will be closer for those tests conducted at the same strain rate. Flow properties from ABI tests may not correlate with results from uniaxial tension tests conducted on materials that exhibit different behavior under tension or compression loading, such as those fabricated from powder compacts. The ABI test results will be closer to those from compression tests on powder compacts.

12. Calibration and Standardization

12.1 The following devices should be calibrated against standards traced to national standards (in the United States, National Institute of Standards and Technology). Applicable ASTM methods are listed beside the device.

Force-measuring system	E 4 and E 74
Micrometers (for calibrating the depth sensor)	

12.2 Calibrations should be as frequent as is necessary to assure that the errors in all tests do not exceed the permissible variations listed in these test methods. The maximum period between calibrations of the force and depth sensors shall be 18 months.

¹ Supporting data are available from ATC: e-mail: info@atc-ssm.com. Request Report ATC-RR-ABI-2003.

² Advanced Technology Corporation, Oak Ridge, TN 37830, USA, website: www.atc-ssm.com is the source of bench-top and field instruments for ABI testing, and ATC's "STRESS-STRAIN MICROPROBE" patented systems are trademarked (registered on September 28, 2004).

13. Verification of Testing Machines

- 13.1 New testing machines shall be verified once prior to service use by conducting at least one ABI test on the end tab of each flat tensile specimen manufactured in triplicates from two alloys of two types of metallic materials (e.g. steels and aluminums) with a wide range of yield strength values for each material type (e.g., 200 to 700 MPa). The new machine is accepted if the following two conditions are met: (a) the average estimated yield strength from each triplicate ABI tests is within $\pm 10\%$ of the average yield strength measured from the triplicate tension tests, of each of the four alloys tested according to ASTM Standard E8, and (b) the average value of the final plastic indentation diameter, d_p , measured in two perpendicular directions shall be within $\pm 5\%$ of the corresponding value calculated using Equation 3 for each of the ABI tests conducted on the four alloys. The comparison of the optical versus calculated values of the final plastic indentation diameter is an indirect verification of the overall performance of the testing machine, including its force transducer, depth sensor, and ball indenter diameter and perpendicularity to the test surface.
- 13.2 Periodic verification is conducted according to the user's requirements and application with a minimum frequency of once per year by performing at least three ABI tests on the end tabs of three flat tensile specimens manufactured from a Ferritic steel material with yield strength greater than 500 MPa. The average value of the estimated yield strength from the ABI tests shall be within $\pm 10\%$ of the average measured yield strength from tension tests conducted according to ASTM Standard E8. Due to the possibility of damage during handling, it is strongly recommended that portable ABI testing machines be verified every day that they are used. Both lab and portable testing machines shall have a minimum verification of once per year.

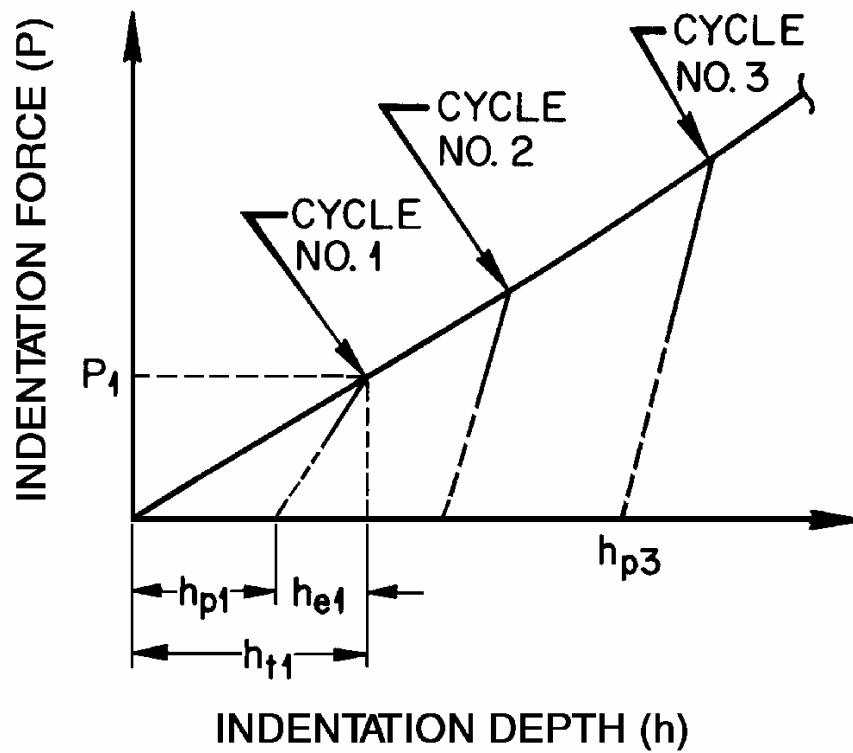
14. Keywords

- 14.1 Automated Ball Indentation, ball indenter, indenter velocity, force-depth data, partial unloading slope, yield parameter, yield strength, true-stress, true-plastic-strain, strain-hardening exponent, strength coefficient, ultimate strength, uniform ductility, Lüders strain

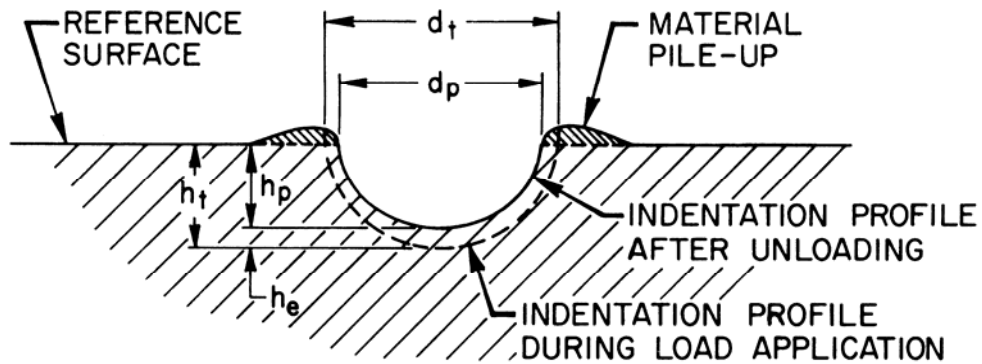
REFERENCES

- (1) Haggag, F. M., "Field Indentation Microprobe for Structural Integrity Evaluation," U.S. Patent No. 4,852,397, August 1, 1989.
- (2) Haggag, F. M., et al., "Use of Portable/In Situ Stress-Strain Microprobe System to Measure Stress-Strain Behavior and Damage in Metallic Materials and Structures," *ASTM STP 1318*, 1997, pp. 85-98.
- (3) Haggag, F. M., "In-Situ Measurements of Mechanical Properties Using Novel Automated Ball Indentation System," *ASTM STP 1204*, 1993, pp. 27-44.
- (4) Haggag, F. M., et al., "Use of Automated Ball Indentation Testing to Measure Flow Properties and Estimate Fracture Toughness in Metallic Materials," *ASTM STP 1092*, 1990, pp. 188-208.
- (5) Byun, T. S., et al. "Measurement of Through-the-Thickness Variations of Mechanical Properties in SA508 Gr.3 Pressure Vessel Steels Using Ball Indentation Test Technique," *International Journal of Pressure Vessels and Piping*, Vol. 74, 1997, pp. 231-238.
- (6) Haggag, F. M., et al., "A Novel Stress-Strain Microprobe for Nondestructive Evaluation of Mechanical Properties of Materials", *Nondestructive Evaluation and Materials Properties III*, The Minerals, Metals & Materials Society, 1997, pp. 101-106.

- (7) Haggag, F. M., et al., "Using Portable/In-Situ Stress-Strain Microprobe System to Measure Mechanical Properties of Steel Bridges During Service," SPIE Proceedings on "Nondestructive Evaluation of Bridges and Highways," Vol. 2946, 1996, pp. 65-75.
- (8) Haggag, F. M., et al., "Nondestructive Detection and Assessment of Damage in Aging Aircraft Using a Novel Stress-Strain Microprobe System", SPIE Proceedings on "Nondestructive Evaluation of Aging Aircraft, Airports, and Aerospace Hardware," Vol. 2945, 1996, pp. 217-228.
- (9) Haggag, F. M. et al., "Characterization of Strain-Rate Sensitivity of Sn-5%Sb Solder Using ABI Testing," Microstructures and Mechanical Properties of Aging Materials II, TMS, 1995, pp. 37-44.
- (10) Haggag, F. M., et al., "Application of Flow Properties Microprobe to Evaluate Gradients in Weldment Properties," *International Trends in Welding Sciences and Technology*, ASM, 1993, pp. 629-635.
- (11) Haggag, F. M., et al., "Measurement of Yield Strength and Flow Properties in Spot Welds and Their HAZs at Various Strain Rates," *International Trends in Welding Sciences and Technology*, ASM, 1993, pp. 637-642.
- (12) Haggag, F. M. et al., "Structural Integrity Evaluation Based on an Innovative Field Indentation Microprobe," *ASME PVP-Vol. 170*, 1989, pp. 101-107.
- (13) Haggag, F.M., et al., "The Use of Field Indentation Microprobe in Measuring Mechanical Properties of Welds," *Recent Trends in Welding Science and Technology*, TWR'89, ASM, 1990, pp. 843-849.
- (14) Druce, S. G., et al., "The Use of Miniature Specimen Techniques for the Assessment of Material Condition," *ASME PVP-Vol. 252*, 1993, pp. 58-59.
- (15) Haggag, F. M., *Nondestructive and Localized Measurements of Stress-Strain Curves and Fracture Toughness of Ferritic Steels at Various Temperatures Using Innovative Stress-Strain Microprobe™ Technology*, DOE/ER/82115-2, October 1999.
- (16) Haggag, F. M., *Nondestructive Determination of Yield Strength and Stress-Strain Curves of In-Service Transmission Pipelines Using Innovative Stress-Strain Microprobe™ Technology*, ATC/DOT/990901, September 1999.
- (17) Dieter, George E., *Mechanical Metallurgy*, Second Edition, McGraw-Hill Book Company, 1976, p. 344.



(a)



(b)

Fig. 1 Cyclic Loading and unloading of a ball indenter into the surface of test material: (a) Schematic of applied force versus indentation depth, (b) Indentation geometry during force application and after force removal (complete unloading).

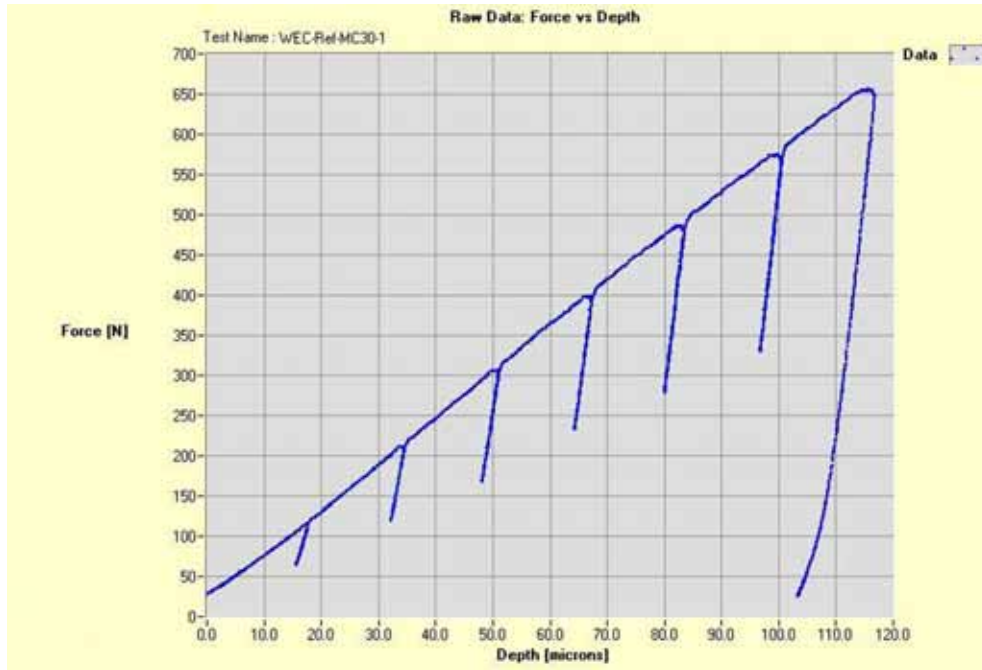


Fig. 2 Example of raw data collected using a 0.762-mm diameter tungsten carbide indenter on a ferritic steel sample. Note that a zero value is temporarily assumed for the indentation depth associated with the preload value of the ABI test. The actual indentation depth value associated with the preload value is calculated next in Fig. 3.

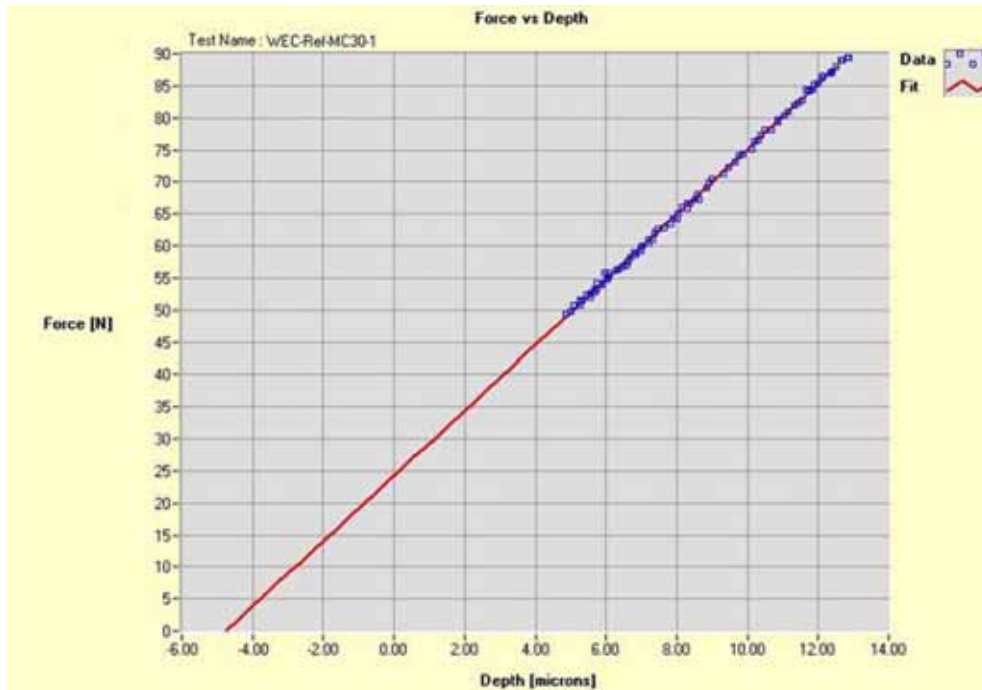


Fig. 3 Example of the linear regression of the force-depth data from the first loading cycle of the Multi-Cycle ABI test shown in Fig. 2. The solid line resulting from the linear regression is used to calculate the indentation depth associated with the indentation preload value (the intersection value of the X-axis).

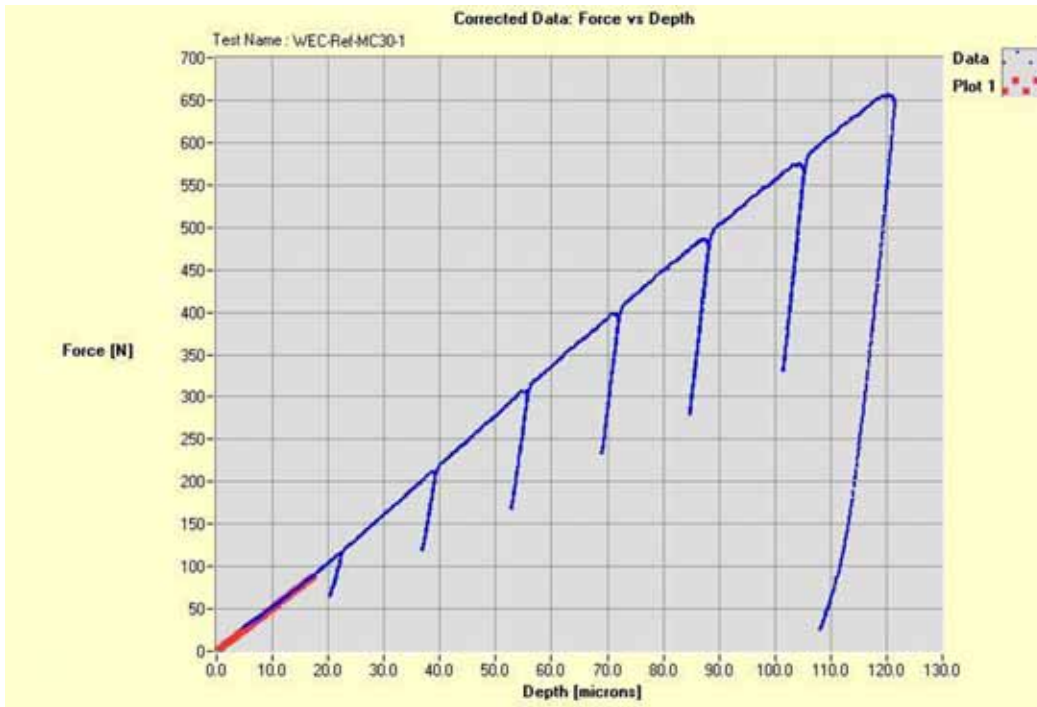


Fig. 4 Example of the corrected ABI data (after shifting the curve to the right by the amount of indentation depth associated with the indentation preload calculated in Fig. 3).

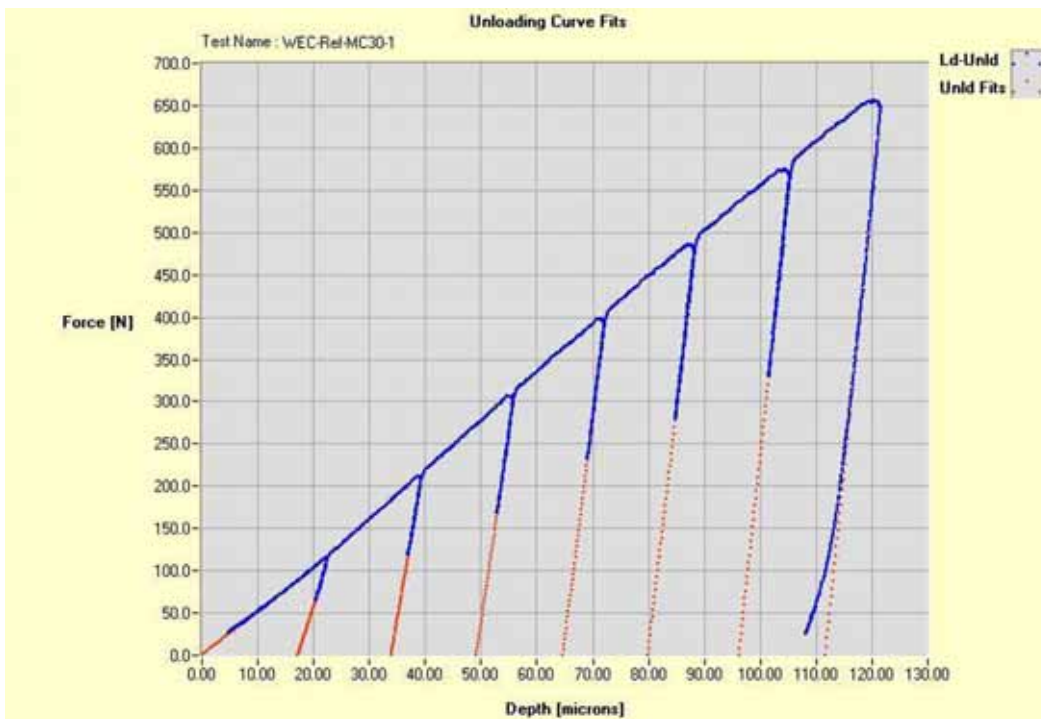


Fig. 5 Example of the corrected force-depth data showing the linear regression of the elastic unloadings (dotted lines). The intersection of the dotted lines (extrapolated from the unloadings) with the X-axis determines the plastic-depth associated with each cycle.

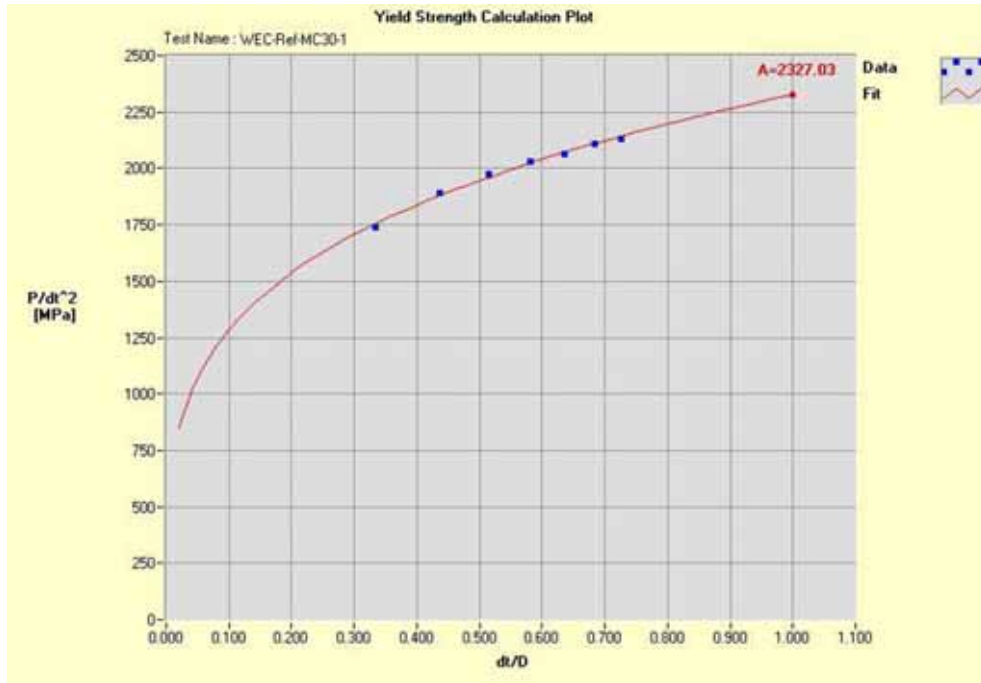


Fig. 6 Yield strength calculation plot. The extrapolation of the curve to an X-axis value of 1.00 produces the yield strength parameter “A” that is used in Equation (11) to calculate the yield strength value.

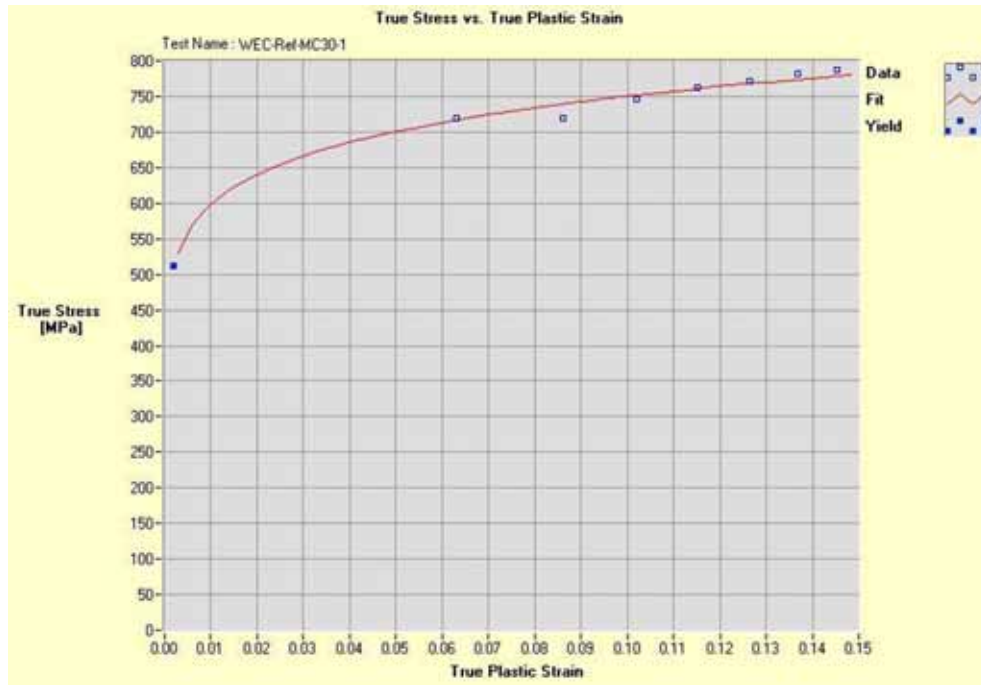


Fig. 7 Example of the true-stress versus true-plastic-strain curve determined from the ABI test. The yield strength is plotted with a different symbol (solid square instead of an open square) since it is calculated from the plot of Fig. 6 and it is not a back-extrapolation from the other points. The solid line is calculated from the power-law fitting of the data as described in ASTM Standard E 646.

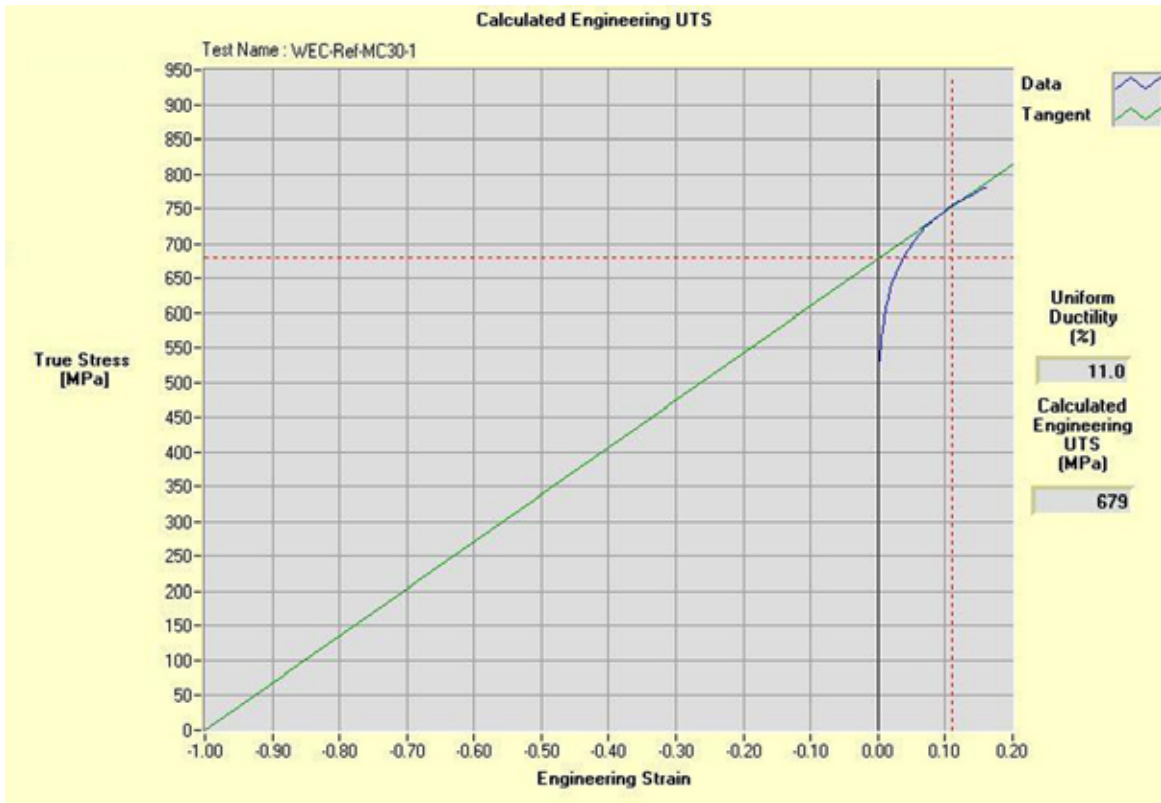


Fig. 8 Example of the calculation of the Uniform Ductility and the Engineering Ultimate Strength (*UTS*) from the ABI-measured True-Stress versus Engineering Strain curve.

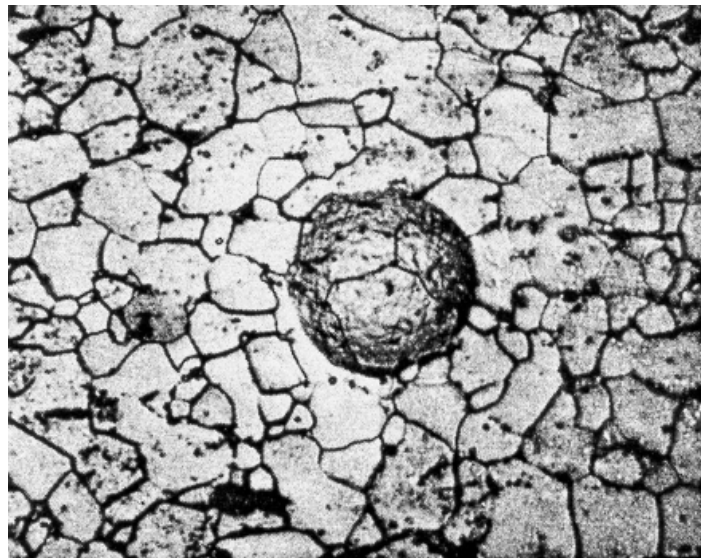


Fig. 9 Spherical indent in 1015 steel (20 μm grain size) obtained at a force of 2 N using a 254 μm (0.010 in) diameter indenter. Notice that the progressive ball indentation at lowest depth increment should cover more than three grains in order to obtain macroscopic stress-strain properties.

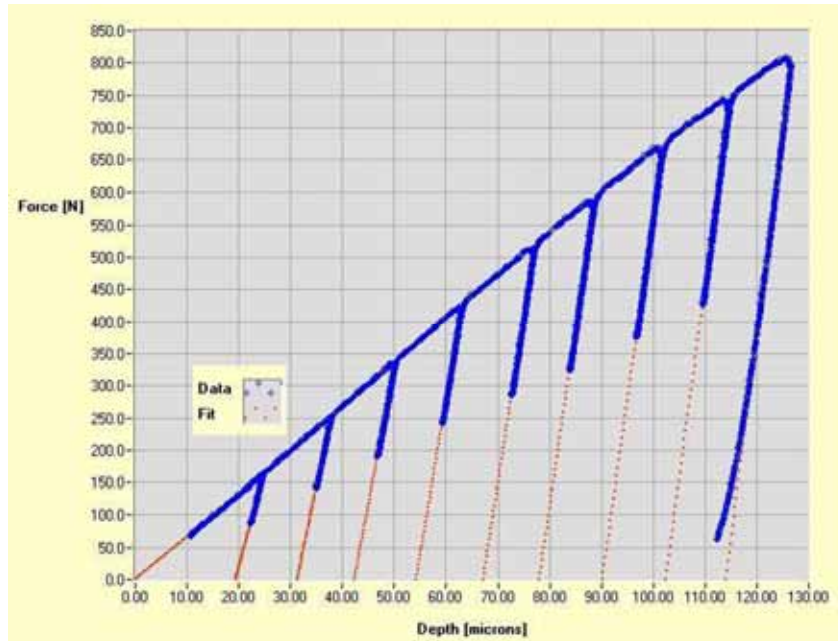


Fig. 10 (a) Indentation force versus depth in an ABI test using a 0.762-mm (0.030-in) diameter tungsten carbide indenter on a ferritic steel material.

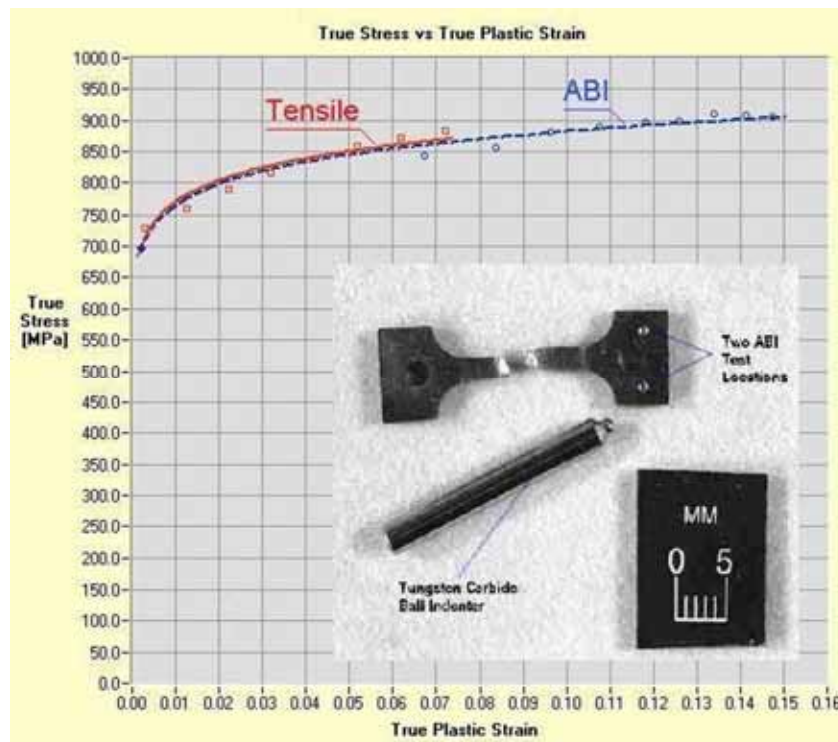


Fig. 10 (b) True-stress versus true-plastic-strain curves from ABI (using a 0.762-mm diameter indenter, data shown in Fig. 10a) and tension tests on a ferritic steel. A miniature tensile specimen is shown in the inset photo with two indentations made with a larger indenter (1.575-mm diameter).

Test Name: WEC-Ref-MC30-1		Test Date: Tuesday, March 20, 2001 4:35 PM	
Project ID:		Operator: Tom	
Material & Test No.: WEC Block, Test No.1			
Additional Info.:			
TEST PARAMETERS		ANALYSIS PARAMETERS	
Atmosphere: Air	Ind. Material: Tungsten Carbide	LVDT Correction: 0.00 [mm]	
Temperature: 22 [C]	Ind. Modulus: 641.22 [GPa]	Inclde Yield Pt.?: YES	
Indenter Speed: 0.010 [mm/sec]	Sample Modulus: 206.84 [GPa]	Yield Level : 0.2 [%]	
Indenter Diameter: 0.7620 [mm]	Initial Ld Levels: Top: 89.50 [N]	R^2 Yield Strength: 0.995	
No. of Unloadings: 7	Bot: 49.42 [N]	R^2 Stress-Strain: 0.992	
Acquisition Rate: 50 [pts/sec]	Regression Fit: Top: 30.0%	Meyer's Number: 2.258	
% Unloading: 40.00	Bot: 0.0%	Yield Par., A: 2327 [MPa]	
Pre-Load Set Point: 22.241 [N]	Constraint Factor Index(α): 1.2000	Yield Strength(A, β , B): 512 [MPa]	
Indenter Rad. Used: 30.0 [%]	Material Yield Slope(β): 0.2200	Strain Hard. Exp(n): 0.098	
	Material Yield Offset(B): 0 [MPa]	Strength Coeff.(K): 941 [MPa]	
EQUIPMENT PARAMETERS		RESULTS	
LVDT Slope: 0.05 [mm/V]	No. of Data Pts.: 3375	Yield Strength(n, K): 512 [MPa]	
LVDT Offset: 0.00 [mm]	Abort Data Pt.: 0	Est. Eng. UTS: 679 [MPa]	
LVDT CutOff Depth Lim: 0.13 [mm]	End Message: Normal	Calc. Eng. UTS : 679 [MPa]	
Load Cell Slope: 446.60 [N/V]	Ld./Depth Slope: 5.09 [kn/mm]	Calc. Unif. Duct : 11.0 [%]	
Load Cell Offset: 0.00 [N]	Pre-Ld. Depth: -4.75 [mic]		
Load Cell Cutoff Limit: 1067.57 [N]	Pre-Ld. Force: 26.39 [N]		
Load Cell Zero Reading: 51.19 [N]	Initial Ld, R^2: 0.999		
Correct For Ind. Comp: NO			

Fig. 11 (a) Suggested data reporting format for both Multi-Cycle and Single-Cycle ABI tests. Example of the first page of the ABI test report including the test parameters, equipment parameters, analysis parameters, and the test results.

ABI Analysis Results by Cycle														
Test Name: WEC-Ref-MC30-1		Test Date: Tuesday, March 20, 2001 4:35 PM												
Project ID:		Operator: Tom												
Material & Test No.: WEC Block, Test No.1														
Additional Info.:														
Cycle	Max Depth ht [mic]	PI Depth hp [mic]	Max Ld [N]	PI Dia dp [mic]	Pmax/dt^2 dt/D [MPa]	From Data	To Data	R^2	Slope [N/mic]	y-inter [N]	dt [mic]	True Plastic Strain	True Stress [MPa]	
Yield Strength												0.002	512.0	
1	21.724	17.227	112.0	239.944	0.333	1740.7	406	430	0.990	20.0	-345.1	253.630	0.063	719.1
2	38.204	33.932	208.9	327.723	0.436	1888.5	729	760	0.992	37.9	-1285.4	332.577	0.086	719.0
3	54.560	49.207	304.7	388.480	0.516	1973.5	1086	1125	0.991	44.6	-2194.5	392.926	0.102	746.4
4	70.869	64.719	397.2	439.118	0.581	2027.6	1490	1535	0.998	52.0	-3365.6	442.627	0.115	761.6
5	86.775	79.871	483.8	481.344	0.635	2064.2	1930	1990	0.995	55.8	-4453.9	484.118	0.126	771.9
6	103.130	96.199	573.7	520.936	0.684	2110.9	2425	2495	0.997	60.8	-5845.0	521.342	0.137	781.6
7	119.331	111.711	654.1	554.032	0.727	2132.4	2957	3039	0.998	64.4	-7199.4	553.860	0.145	787.9

Fig 11 (b) Suggested data reporting format for the Multi-Cycle ABI test. Example of the second page of the ABI test report including the tabulated values of the true-plastic-strain versus the true-stress data pairs from all cycles.

APPENDIX X1

Summary of the Interlaboratory Study (ILS) and Precision Statistics

X1.1 Because standard reference materials with certified ABI or tensile property values are not available, it is not possible to rigorously define the bias of ABI tests. However, by the use of carefully designed and controlled interlaboratory study, a reasonable definition of the precision of ABI test results can be obtained.

X1.2 An Interlaboratory test program was conducted in which five ABI tests were conducted on each of four widely differing ferrous and non-ferrous materials at each of six laboratories using commercial Stress-Strain Microprobe® (SSM) systems especially designed for ABI testing. The materials are two aluminum alloys (6061 and 7075) and two steel alloys (1018 and 4142) with a wide range of flow properties. Brazed 1.57-mm (0.062-inch) diameter tungsten carbide indenters were used in all 120 ABI tests. A summary of the ABI test and analysis parameters is included below. The indenter speed was fixed for all ABI tests in order to perform all tests at the same strain rate. The values of the yield strength slope (Beta) of 0.26 and 0.31 for the steel and aluminum samples, respectively, were determined empirically from comparisons with tensile test results in order to obtain very good agreement between the ABI-Determined yield strength and those from the empirical 0.2% offset method of the tension test. Similarly, the value of the constraint factor (Alpha) of 1.00 for both steel and aluminum materials was verified from overlays of the true-stress/true-plastic-strain curves from both the multi-axial ABI tests and the uniaxial tension tests. Although comparison of flow properties from ABI and tension tests is not the subject of this interlaboratory study, the overlay of true-stress versus true-plastic-strain curves from both types of tests produced very good agreement for all four materials as shown in Figures X1-1 and X1-2.

Test Parameters:

Indenter speed = 0.015 mm/s
Percentage indenter used = 20%
Pre-Load Set Point = 66.7 N
Number of Unloading Cycles = 10 (Equal Depth)
Unload (% of Cycle Maximum Force) = 40.0 %
Data Acquisition Rate = 200 Samples/sec
Indenter Elastic Modulus = 641.2 Gpa

Analysis Parameters for Steel Samples:

Elastic Modulus = 206.8 Gpa
Constraint Factor (Alpha) = 1.00
Yield Strength Slope (Beta) = 0.2600
Include Yield Parameter in Analysis = Yes

Analysis Parameters for Aluminum Samples:

Elastic Modulus = 68.9 Gpa
Constraint Factor (Alpha) = 1.00
Yield Strength Slope (Beta) = 0.3100
Include Yield Parameter in Analysis = Yes

Tables X1.1-X1.5 present the precision statistics, as defined in ASTM Standard Practice E 691, for the yield strength (YS-ABI), estimated ultimate strength (UTS-ABI), strength coefficient (K-ABI), strain-hardening exponent (n-ABI), and calculated uniform ductility (UD-ABI).

TABLE X1.1 – Precision Statistics for the ABI-Determined Yield Strength (YS-ABI), MPa

NOTE 1—X is the average of the cell averages, that is, the grand mean for the test parameter,
 S_r is the repeatability standard deviation (within-laboratory precision),
 S_r/X is the repeatability coefficient of variation in %,
 S_R is the reproducibility standard deviation (between-laboratory precision),
 S_R/X is the reproducibility coefficient of variation, %,
r is the 95% repeatability limits,
R is the 95% reproducibility limits.
CV %_r = repeatability coefficient of variation in percent within a laboratory
CV %_R = repeatability coefficient of variation in percent between laboratories

Materials	Average (X)	S_r	CV %_r=(S_r/X)%	S_R	CV %_R=(S_R/X)%	r	R
Al 6061-T651	329.97	5.41	1.64	6.28	1.90	15.15	17.58
Al 7075-T651	545.73	7.11	1.30	8.00	1.47	19.90	22.41
Steel 1018	361.90	6.10	1.69	7.21	1.99	17.07	20.18
Steel 4142	721.30	7.79	1.08	9.58	1.33	21.81	26.82
Averages:						1.43	1.67

TABLE X1.2 – Precision Statistics for the ABI-Estimated Ultimate Strength (UTS-ABI), MPa

Materials	Average	S_r	CV %_r	S_R	CV %_R	r	R
Al 6061-T651	396.20	3.82	0.96	5.73	1.45	10.69	16.04
Al 7075-T651	613.03	13.76	2.24	17.23	2.81	38.52	48.25
Steel 1018	497.00	8.22	1.65	15.52	3.12	23.02	43.46
Steel 4142	1003.90	13.29	1.32	19.93	1.99	37.21	55.80
Averages:						1.54	2.34

TABLE X1.3 – Precision Statistics for the ABI-Determined Strength Coefficient (K-ABI), MPa

Materials	Average	S_r	CV %_r	S_R	CV %_R	r	R
Al 6061-T651	514.40	8.45	1.64	10.42	2.03	23.67	29.18
Al-7075-T651	768.60	29.60	3.85	36.90	4.80	82.88	103.33
Steel 1018	706.63	17.83	2.52	28.94	4.10	49.93	81.02
Steel 4142	1434.93	31.32	2.18	40.51	2.82	87.69	113.44
Averages:						2.55	3.44

TABLE X1.4 – Precision Statistics for the ABI-Determined Strain-Hardening Exponent (n-ABI)

Materials	Average	S_r	CV %_r	S_R	CV %_R	r	R
Al 6061-T651	0.071933	0.003764	5.23	0.004026	5.60	0.010539	0.011273
Al-7075-T651	0.058900	0.005798	9.84	0.007206	12.23	0.016234	0.020177
Steel 1018	0.109567	0.004829	4.41	0.005254	4.80	0.013520	0.014711
Steel 4142	0.111967	0.004131	3.69	0.004693	4.19	0.011567	0.013142
Averages:						5.79	6.71

TABLE X1.5 – Precision Statistics for the ABI-Calculated Uniform Ductility (UD-ABI), %

Materials	Average	S_r	CV %_r	S_R	CV %_R	r	R
Al 6061-T651	7.41	0.88	11.88	0.98	13.22	2.47	2.74
Al 7075-T651	5.80	0.68	11.72	0.79	13.62	1.91	2.23
Steel 1018	10.35	0.23	2.22	0.25	2.42	0.64	0.69
Steel 4142	10.30	0.20	1.94	0.21	2.04	0.55	0.60
Averages:						6.94	7.83

X1.3 In each of Tables X1.1-X1.5, the first column lists the four materials tested, the second column lists the average of the average results obtained by all laboratories, the third and fifth columns list the repeatability and reproducibility standard deviations, the fourth and six columns list the coefficient of variation for these standard deviations, and the seventh and eighth columns list the 95% repeatability and reproducibility limits.

X1.4 The averages (below columns four and six in each table) of the coefficients of variation permit a relative comparison of the repeatability (within-laboratory precision) and reproducibility (between-laboratory precision) of the ABI test parameters. This shows that the ABI-calculated uniform ductility (UD-ABI) and the ABI-determined strain-hardening exponent (n-ABI) exhibit similar but less repeatability and reproducibility than the strength measurements. The overall ranking from the least to the most repeatable and reproducible is: % ABI-calculated uniform ductility (UD-ABI), ABI-determined strain-hardening exponent (n-ABI), ABI-determined strength coefficient (K-ABI), ABI-estimated ultimate strength (UTS-ABI), and ABI-determined yield strength (YS-ABI). Note that the rankings are in the same order for the repeatability and reproducibility average coefficients of variation and that the reproducibility (between-laboratory precision) is slightly less than the repeatability (within-laboratory precision), as would be expected.

X1.5 No comments about bias can be made for this ABI interlaboratory study due to the lack of certified test results for the these specimens. However, examination of the test results from five tests each on four materials (ferrous and non-ferrous) at six laboratories showed that the ABI test methods provide excellent repeatability within a laboratory and between laboratories for the ABI-determined yield strength (YS-ABI), estimated ultimate strength (UTS-ABI), and the strength coefficient (K-ABI). The repeatability coefficients of variation for the strain-hardening exponent (n-ABI) and the uniform ductility (UD-ABI) are slightly higher because the determination of these properties depends on the shape (curvature) of the true-stress/true-plastic-strain curve and the homogeneity of the metal. The two steel materials exhibited better repeatability and reproducibility of their strain-hardening exponent and uniform ductility than the two aluminum materials because of their better homogeneity and because their flow properties (true-stress versus true-plastic-strain curves) followed a better power-law behavior.

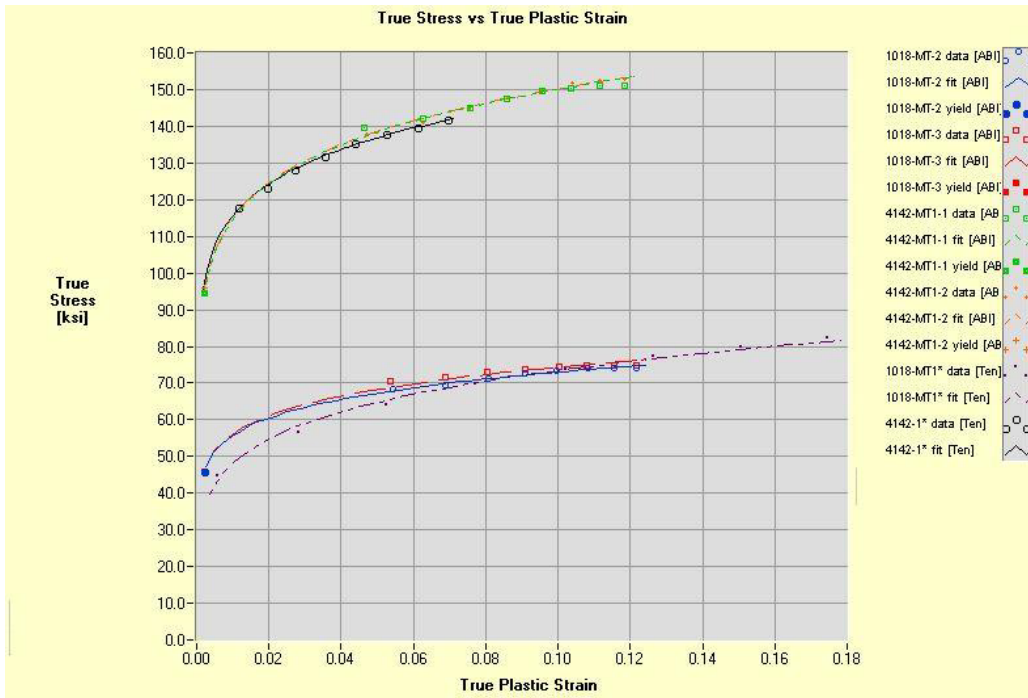


Fig. X1-1 Comparison between true-stress versus true-plastic-strain curves from ABI and tension tests of 1018 (lower curves) and 4142 steel (higher curves) samples. Two ABI tests were conducted on the end tabs of each tensile specimen.

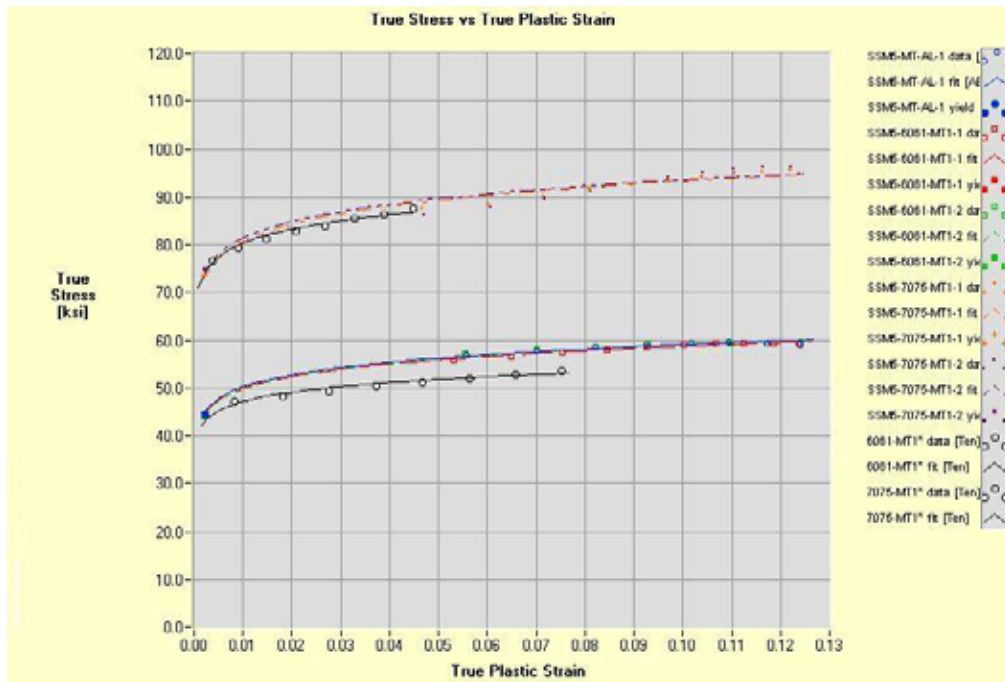


Fig. X1-2 Comparison between true-stress versus true-plastic-strain curves from ABI and tension tests of 6061 (lower curves) and 7075 aluminum (higher curves) samples. Two ABI tests were conducted on the end tabs of each tensile specimen.

APPENDIX C

Pipeline Material Certificates

X60 Certificate

鋼管検査証明書
INSPECTION CERTIFICATE

新日本製鋼株式会社
Nippon Steel Corporation

社 号: 甲 300-0071 東京都中央区東新橋二丁目 0 番 3 号
HEAD OFFICE: 1-3, JOMONCHO, CHUOH-KU, TOKYO, JAPAN
東京支店: 東京都中央区新富町 4 丁目 3 番 1 号
HIKARI PIPE & TUBE DIV. PIPE & TUBE DIVISION
〒100-0071, 東京都中央区新富町4丁目3番1号

注文者: SUMITOMO CORPORATION
注文書番号: XEE-22341/2

契約番号: 6-843-N3-5-3-E101

品名: ESW BLACK STEEL PIPE

顧客: PIONEER PIPE

規格: API SPEC 5L GRADE X60 PSL-2 (43RD EDITION MARCH 2004)

仕様: ELECTRIC-WELED TEMPERATURE FOR HEAT TREATMENT OF THE WELD SEAM: MIN 943C

備考: P. O. NO. SOC-23. HARDNESS TEST SHALL NOT BE PERFORMED, HOWEVER WE GUARANTEE

注: MATERIAL SATISFY HARDNESS REQUIREMENT (BY 238 WAY.) OF WAGE HQ0173

証明書番号: 頁 1
設計番号: 2006-03-16
DATE OF ISSUE: 2006-03-16

寸法 SIZE	数量 QUANTITY	単位 UNITS	重量 NET WEIGHT	CHEMICAL COMPOSITION %										引張強さ TENSILE TEST	延伸率 ELONGATION	断面収縮率 REDUCTION OF AREA	衝撃試験 IMPACT TEST			
				C	SI	Mn	P	S	Ni	OR	V	TI	CU					MO		
10.75 X 10.365 X 20	26	19.110	ZN1653H	0.18	0.38	1.5	3.6	2	3	1	17	3	0	P831651TK	73500	87500	33	6	6	6
12.75 X 10.315 X 40	26	23.400	ZN1653H	0.17	0.35	1.5	3.6	2	3	1	17	3	0	P828891TK	73500	87500	33	6	6	6

検査項目 ITEM	検査結果 TEST RESULT	検査方法 TEST METHOD	検査場所 TEST LOCATION
目視検査 VISUAL	良好 GOOD	目視 BY EYE	検査場 TEST SITE
引張強さ TENSILE	MIN 73500 PSI MAX 87500 PSI	引張試験機 TENSILE TESTER	検査場 TEST SITE
延伸率 ELONGATION	33%	引張試験機 TENSILE TESTER	検査場 TEST SITE
断面収縮率 REDUCTION OF AREA	33%	引張試験機 TENSILE TESTER	検査場 TEST SITE
衝撃試験 IMPACT	6 J	シャルピー試験機 CHARPY TESTER	検査場 TEST SITE
化学成分 CHEMICAL	合格 PASS	分光分析 SPECTROSCOPY	検査場 TEST SITE
硬度試験 HARDNESS	合格 PASS	リキッドペナル試験機 LIQUID PENETRANT TESTER	検査場 TEST SITE
超音波検査 ULTRASONIC	合格 PASS	超音波探傷機 ULTRASONIC TESTER	検査場 TEST SITE
放射線検査 RADIOGRAPHIC	合格 PASS	放射線探傷機 RADIOGRAPHIC TESTER	検査場 TEST SITE
磁気粉砕検査 MAGNETIC PARTICLE	合格 PASS	磁気粉砕機 MAGNETIC PARTICLE TESTER	検査場 TEST SITE

検査官: M. Koyan
検査官署名: M. Koyan
検査官印: M. Koyan
検査官職名: 検査官
検査官所属: 検査部
検査官住所: 〒100-0071, 東京都中央区東新橋二丁目 0 番 3 号
検査官電話: 03-3542-1111
検査官FAX: 03-3542-1112
検査官Eメール: m.koyan@nipponsteel.com

上記検査結果は、鋼管の規格に準拠して行われ、その結果が合格であることを証明します。
WE HEREBY CERTIFY THAT THE MATERIAL DESCRIBED HEREIN HAS BEEN
MADE IN ACCORDANCE WITH THE RULES OF THE CONTRACT.

APPENDIX D

Detailed Tensile and ABI Test Results

Table D1 Summary of tensile test results and the yield parameter “A” from ABI tests

Test Name	Uniform	Total	Strength	Strain	Yield	UTS	ABI "A"
	Elongation	Elongation	Coefficient	Hardening	Strength	[ksi]	Par.
	[%]	[%]	[ksi]	Exponent	[ksi]		(ksi)
A366/1008 Thin Sheet							
PRCI-A366-A1	26.0	47.8	77.0	0.192	26.9	47.3	152.3
PRCI-A366-A2	25.8	49.2	78.0	0.204	26.0	46.9	152.4
Storage Tank Steel (1.25-inch thick)							
XX-MT-1	20.3	32.1	115.9	0.244	40.2	63.1	197.3
XX-MT-2	20.4	35.0	116.7	0.239	42.7	64.3	200.6
XX-MT-3	22.0	37.2	114.9	0.233	41.1	64.6	190.2
1018 Ground Flat Plate							
PRCI-1018-SC2	17.4	31.9	126.5	0.188	48.9	76.3	226.0
PRCI-1018-SC3	14.4	29.6	118.0	0.149	50.9	77.0	250.0
PRCI-1018-SC4	16.0	28.4	124.1	0.189	47.9	74.7	235.7
PRCI-1018-SC5	14.9	29.2	121.6	0.156	51.1	78.3	247.7
PRCI-1018-SA6	15.7	34.1	119.9	0.153	50.3	77.8	241.3
PRCI-1018-SA7	15.9	33.1	125.5	0.187	47.6	75.9	228.9
PRCI-1018-SA8	17.1	31.7	127.3	0.181	50.2	78.1	233.0
PRCI-1018-SA9	15.6	31.7	121.5	0.165	49.2	76.6	251.1
X42 Pipeline Base Metal (Circumferential and Axial Orientation Tensile Samples)							
PRCI-X42-C1	14.5	33.3	97.3	0.097	56.2	71.2	237.8
PRCI-X42-C2	12.8	28.5	95.2	0.079	60.6	72.6	257.1
PRCI-X42-C3	12.8	29.4	98.2	0.079	62.2	74.8	261.4
PRCI-X42-C4	14.5	29.2	99.0	0.099	56.7	72.1	244.1
PRCI-X42-A5	14.7	32.4	96.8	0.093	59.4	71.4	242.7
PRCI-X42-A6	11.7	30.5	96.4	0.074	63.4	74.4	260.2
PRCI-X42-A7	4.8	23.6	97.8	0.053	70.1	79.3	260.9
PRCI-X42-A8	8.2	23.3	96.6	0.079	61.4	73.4	254.2
X42 Pipeline Seam Weld (Seam Weld Tensile Samples, Axial Orientation)							
PRCI-T-X42W-9	4.8	24.7	98.9	0.060	69.1	78.3	269.5
PRCI-T-X42W-10	3.6	23.7	94.9	0.047	72.0	78.3	256.9
PRCI-T-X42W-11	4.3	23.7	99.7	0.057	69.6	79.8	268.0
PRCI-T-X42W-12	3.5	21.7	94.7	0.048	71.1	77.8	260.1
PRCI-T-X42W-13	3.7	25.0	95.4	0.051	70.7	77.8	255.7
PRCI-T-X42W-14	4.4	25.1	99.3	0.052	71.8	80.7	268.3
X52 Pipeline Base Metal (Circumferential and Axial Orientation Tensile Samples)							
PRCI-X52-C1	4.7	19.3	108.5	0.058	74.0	86.4	287.8
PRCI-X52-C2	3.3	20.1	102.1	0.047	75.1	83.8	278.3
PRCI-X52-C3	4.2	18.4	107.3	0.054	76.4	86.5	289.0
PRCI-X52-C4	3.6	18.9	103.5	0.047	75.6	85.2	292.8
PRCI-X52-A5	4.1	18.5	109.2	0.058	74.7	87.0	281.9
PRCI-X52-A6	2.7	17.5	102.0	0.040	78.7	85.8	295.7
PRCI-X52-A7	2.3	21.7	97.1	0.023	82.6	87.0	293.7
PRCI-X52-A8	2.4	20.0	93.0	0.024	79.2	83.1	282.3
X52 Pipeline Seam Weld (Seam Weld Tensile Samples, Axial Orientation)							
PRCI-T-X52W-10	6.2	22.8	105.2	0.073	69.8	81.0	266.5

PRCI-T-X52W-11	4.7	19.7	102.7	0.058	74.0	82.5	273.9
PRCI-T-X52W-12	4.8	19.1	98.1	0.052	71.9	80.3	275.9
PRCI-T-X52W-13	8.2	25.2	101.4	0.081	63.6	76.7	258.6
PRCI-T-X52W-14	5.6	22.7	102.6	0.066	71.6	80.6	276.9
PRCI-T-X52W-15	6.1	22.6	103.0	0.071	68.3	79.8	261.4

Test Name	Uniform Elongation [%]	Total Elongation [%]	Strength Coefficient [ksi]	Strain Hardening Exponent	Yield Strength [ksi]	UTS [ksi]	ABI "A" Par. (ksi)
X60 Pipeline Base Metal (Circumferential and Axial Orientation Tensile Samples)							
PRCI-X60-C1	6.8	19.8	123.6	0.069	79.6	96.3	293.6
PRCI-X60-C2	4.3	18.6	114.4	0.050	83.2	93.8	311.6
PRCI-X60-C3	5.5	19.9	115.4	0.052	82.8	94.1	307.3
PRCI-X60-C4	6.2	20.5	122.6	0.067	80.4	96.1	310.4
PRCI-X60-A5	8.3	24.0	117.6	0.070	80.3	92.0	310.6
PRCI-X60-A6	6.8	23.7	113.0	0.051	84.3	92.9	314.3
PRCI-X60-A7	6.0	22.0	114.3	0.054	83.8	93.1	305.0
PRCI-X60-A8	4.8	20.5	112.8	0.043	85.1	94.5	310.5
X65 Pipeline Base Metal (Circumferential and Axial Orientation Tensile Samples)							
PRCI-X65-C1	1.8	17.4	104.2	0.033	83.0	89.8	301.3
PRCI-X65-C2	5.9	22.4	110.7	0.058	77.2	88.8	296.8
PRCI-X65-C3	2.2	17.9	105.2	0.036	82.6	89.6	314.2
PRCI-X65-C4	5.9	23.6	107.8	0.056	76.6	87.0	286.9
PRCI-X65-A5	5.2	21.9	106.4	0.050	77.9	87.4	302.0
PRCI-X65-A6	2.6	19.8	104.3	0.031	85.0	91.0	308.1
PRCI-X65-A7	2.9	19.5	102.8	0.028	85.8	90.5	307.9
PRCI-X65-A8	4.8	22.0	106.0	0.047	79.9	87.8	300.8
X65 Pipeline Seam Weld (Seam Weld Tensile Samples, Axial Orientation)							
PRCI-T-X65W-09	9.3	25.8	110.8	0.074	74.0	85.4	282.0
PRCI-T-X65W-10	11.4	29.6	110.2	0.087	67.4	82.3	272.9
PRCI-T-X65W-11	12.9	29.8	115.3	0.114	68.1	80.7	267.0
PRCI-T-X65W-12	9.8	28.1	113.5	0.088	73.8	84.5	282.5
PRCI-T-X65W-13	9.6	26.9	114.7	0.085	73.4	85.9	288.9
PRCI-T-X65W-14	10.9	30.9	105.7	0.070	71.6	82.3	276.3
Grade B Pipeline Steel, Base Metal (BL1, BL2) and Seam Weld (BW1, BW2), Axial Orientation							
PRCI-BL1	16.8	33.7	113.2	0.164	49.1	71.8	228.9
PRCI-BL2	17.8	31.2	115.4	0.181	47.2	70.4	226.0
PRCI-BW1	18.5	33.9	118.6	0.189	45.2	71.7	212.3
PRCI-BW2	16.7	30.5	113.6	0.180	46.9	69.6	228.8

Table D2 Summary of ABI-measured tensile properties (ABI tests conducted on end tabs of miniature tensile specimens)

Test Name	Est.	Calc.	Calc.	Ratio	ABI
	Eng.	Eng.	Unif.	Yield	Hardness
	UTS	UTS	Duct.	to	
	[ksi]	[ksi]	[%]	UTS	
A366 Thin Sheet					
ABI-PRCI-A366-A1-3	45.9	45.4	13.3	0.54	108 (030G)
ABI-PRCI-A366-A2-2	44.5	44.1	13.3	0.56	105 (030G)
BP Storage Tank					
ABI-BP-MT1-1	58.6	58.7	11.9	0.71	136 (030G)
ABI-BP-MT2-1	60.1	60.2	11.9	0.71	138 (030G)
ABI-BP-MT3-1	58.6	58.6	12.4	0.67	134 (030G)
Grade B BM and Seam Weld					
ABI-PRCI-GB-BL1-1	68.2	68.2	10.5	0.79	159 (030G)
ABI-PRCI-GB-BL2-1	65.9	65.9	9.9	0.8	154 (030G)
ABI-PRCI-GBW-BW1-1	64.3	64.3	11.4	0.74	150 (030G)
ABI-PRCI-GBW-BW2-2	68	67.9	10.4	0.79	158 (030G)
X42 BM					
ABI-X42-C1-1	74.4	74.4	9.9	0.79	170 (030G)
ABI-PRCI-X42-SC2-3	77	77	7.3	0.83	180 (030G)
ABI-PRCI-X42-C3-1	80.3	80.3	7.5	0.82	185 (030G)
ABI-PRCI-X42-C4-1	74.1	74.1	9.7	0.8	172 (030G)
ABI-PRCI-X42-A5-1	74.4	74.4	10.1	0.79	172 (030G)
ABI-PRCI-X42-A6-1	79.7	79.7	7.5	0.82	184 (030G)
ABI-X42-A7-1	77.5	77.5	7.2	0.84	177 (030G)
ABI-PRCI-X42-A8-1	79.4	79.4	9.8	0.79	182 (030G)
X42 Seam Weld					
ABI-X42W-9-1	82.3	82.3	7.1	0.84	189 (030G)
ABI-X42W-10-1	80	80	8.3	0.8	182 (030G)
ABI-X42W-11-1	82.9	82.9	7.3	0.82	187 (030G)
ABI-X42W-12-1	82.4	82.4	9.9	0.79	183 (030G)
ABI-X42W-13-1	78.8	78.8	8.3	0.81	178 (030G)
ABI-X42W-14-1	83.7	83.7	7.5	0.82	189 (030G)
X52 BM					
ABI-PRCI-X52-C1-1	90.1	90.1	6.9	0.84	205 (030G)
ABI-X52-C2-1	84.5	84.4	9.4	0.8	188 (030G)
ABI-X52-C3-2	90	90	6.8	0.85	203 (030G)
ABI-X52-C4-2	92.3	92.3	7	0.84	208 (030G)
ABI-PRCI-X52-A5-1	90.4	90.4	7.5	0.81	203 (030G)
ABI-X52-A6-2	93.4	93.4	6.9	0.84	207 (030G)
ABI-PRCI-X52-A7-1	90.1	90.2	6.5	0.86	206 (030G)
ABI-PRCI-X52-A8-1	87.5	87.6	6.9	0.84	200 (030G)
X52 Seam Weld					
ABI-X52W-10-1	82.1	82.1	7.4	0.82	187 (030G)
ABI-X52W-11-1	86.7	86.7	7.6	0.81	195 (030G)

Test Name	Est.	Calc.	Calc.	Ratio	ABI
	Eng.	Eng.	Unif.	Yield	Hardness
	UTS	UTS	Duct.	to	
	[ksi]	[ksi]	[%]	UTS	
ABI-X52W-12-1	86.1	86.1	7.2	0.83	193 (030G)
ABI-X52W-13-1	77.4	77.4	7.2	0.84	179 (030G)
ABI-X52W-14-1	85.6	85.6	7	0.84	194 (030G)
ABI-X52W-15-1	82	81.9	8.3	0.8	184 (030G)
X60 BM					
ABI-X60-C1-2	93.5	93.5	6.8	0.85	208 (030G)
ABI-PRCI-X60-C2-1	98.3	98.4	6.4	0.86	221 (030G)
ABI-PRCI-X60-C3-1	96.4	96.5	6.5	0.86	218 (030G)
ABI-PRCI-X60-C4-1	96.7	96.8	6.3	0.87	218 (030G)
ABI-PRCI-X60-A5-1	94.9	94.9	6.1	0.89	216 (030G)
ABI-PRCI-X60-A6-1	99.9	99.9	6.5	0.86	224 (030G)
ABI-PRCI-X60-A7-1	96.4	96.4	6.6	0.85	217 (030G)
ABI-X60-A8-1	99.3	99.3	6.6	0.86	220 (030G)
X65 BM					
ABI-PRCI-X65-C1-1	90.4	90.4	6	0.89	207 (030G)
ABI-PRCI-X65-C2-1	94	94.1	6.8	0.84	211 (030G)
ABI-PRCI-X65-C3-1	99.1	99.1	6.4	0.86	222 (030G)
ABI-X65-C4-1	87.5	87.6	6.3	0.88	200 (030G)
ABI-PRCI-X65-A5-1	95.4	95.5	6.7	0.85	215 (030G)
ABI-PRCI-X65-A6-1	97.3	97.3	6.5	0.86	219 (030G)
ABI-PRCI-X65-A7-1	98.1	98.1	6.6	0.85	219 (030G)
ABI-X65-A8-2	91.1	91.1	6	0.89	207 (030G)
X65 Seam Weld					
ABI-X65W-9-1	86.9	86.9	6.8	0.85	194 (030G)
ABI-X65W-10-1	86.6	86.5	7.7	0.81	195 (030G)
ABI-X65W-11-1	72.9	73	5.6	0.93	175 (030G)
ABI-X65W-12-2	84.6	84.6	6.5	0.87	194 (030G)
ABI-X65W-13-1	88.7	88.8	6.6	0.86	202 (030G)
ABI-X65W-14-2	77	77	5.7	0.93	180 (030G)
1018 Ground Flat Stock					
ABI-PRCI-1018-SC2-3	65.6	65.6	10.2	0.8	155 (030G)
ABI-PRCI-1018-SC3-1	75.2	75.2	7.8	0.82	176 (030G)
ABI-PRCI-1018-SC4-1	69.1	69	8.3	0.81	163 (030G)
ABI-PRCI-1018-SC5-1	72.7	72.7	7.4	0.83	170 (030G)
ABI-1018-SA6-3	72.9	72.8	8.8	0.8	167 (030G)
ABI-PRCI-1018-SA7-1	66.5	66.4	9.8	0.81	159 (030G)
ABI-PRCI-1018-SA8-1	64.7	64.7	7.2	0.85	157 (030G)
ABI-PRCI-1018-SA9-1	72.4	72.4	6.9	0.85	171 (030G)

Table D3 Summary of ABI-measured tensile and fracture toughness from tests on end tabs of miniature tensile specimens

Test Name	Yield Strength	Strength Coefficient (K)	Strain Hardening Exponent (n)	Estimated Engineering UTS [ksi]	Calculated Engineering UTS [ksi]	Calculated Uniform Ductility [%]	Ratio Yield to UTS	ABI Hardness	Fracture Toughness (ksi*in ^{0.5})
ABI-PRCI-A366-A1-3	24.8	74.4	0.177	45.9	45.4	13.3	0.54	108 (030G)	151.4
ABI-PRCI-A366-A2-2	24.8	71.1	0.169	44.5	44.1	13.3	0.56	105 (030G)	147.0
ABI-BP-MT1-1	41.7	84.4	0.116	58.6	58.7	11.9	0.71	136 (030G)	165.0
ABI-BP-MT2-1	42.9	86.3	0.114	60.1	60.2	11.9	0.71	138 (030G)	167.6
ABI-BP-MT3-1	39.0	86.7	0.129	58.6	58.6	12.4	0.67	134 (030G)	167.5
ABI-PRCI-GB-BL1-1	53.6	93.1	0.092	68.2	68.2	10.5	0.79	159 (030G)	178.0
ABI-PRCI-GB-BL2-1	52.5	89.0	0.087	65.9	65.9	9.9	0.80	154 (030G)	172.8
ABI-PRCI-GBW-BW1-1	47.3	90.7	0.106	64.3	64.3	11.4	0.74	150 (030G)	173.5
ABI-PRCI-GBW-BW2-2	53.5	92.5	0.091	68.0	67.9	10.4	0.79	158 (030G)	177.1
ABI-X42-C1-1	59.0	100.6	0.088	74.4	74.4	9.9	0.79	170 (030G)	183.3
ABI-PRCI-X42-SC2-3	64.2	101.2	0.076	77.0	77.0	7.3	0.83	180 (030G)	187.2
ABI-PRCI-X42-C3-1	65.8	106.0	0.079	80.3	80.3	7.5	0.82	185 (030G)	192.3
ABI-PRCI-X42-C4-1	59.3	99.8	0.086	74.1	74.1	9.7	0.80	172 (030G)	186.1
ABI-PRCI-X42-A5-1	58.8	100.7	0.088	74.4	74.4	10.1	0.79	172 (030G)	186.9
ABI-PRCI-X42-A6-1	65.3	105.5	0.079	79.7	79.7	7.5	0.82	184 (030G)	191.9
ABI-X42-A7-1	64.8	101.5	0.075	77.5	77.5	7.2	0.84	177 (030G)	183.5
ABI-PRCI-X52-A8-1	73.6	113.7	0.072	87.5	87.6	6.9	0.84	200 (030G)	197.0
ABI-X42W-9-1	68.8	107.6	0.075	82.3	82.3	7.1	0.84	189 (030G)	191.5
ABI-X42W-10-1	64.1	107.1	0.084	80.0	80.0	8.3	0.80	182 (030G)	191.6
ABI-X42W-11-1	68.3	108.9	0.077	82.9	82.9	7.3	0.82	187 (030G)	192.8
ABI-X42W-12-1	65.3	111.0	0.086	82.4	82.4	9.9	0.79	183 (030G)	189.2
ABI-X42W-13-1	63.6	105.3	0.083	78.8	78.8	8.3	0.81	178 (030G)	186.4
ABI-X42W-14-1	68.4	110.6	0.079	83.7	83.7	7.5	0.82	189 (030G)	194.7

Test Name	Yield	Strength	Strain	Estimated	Calculated	Calculated	Ratio	ABI	Fracture
	Strength	Coefficient	Hardening	Engineering	Engineering	Uniform	Yield	Hardness	Toughness
		(K)	Exponent	UTS	UTS	Ductility	to		
	[ksi]	[ksi]	(n)	[ksi]	[ksi]	[%]	UTS		(ksi*in ^{0.5})
ABI-PRCI-X52-C1-1	75.7	117.0	0.072	90.1	90.1	6.9	0.84	205 (030G)	201.9
ABI-X52-C2-1	68.0	113.1	0.084	84.5	84.4	9.4	0.80	188 (030G)	191.5
ABI-X52-C3-2	76.3	116.3	0.070	90.0	90.0	6.8	0.85	203 (030G)	199.6
ABI-X52-C4-2	77.1	120.1	0.073	92.3	92.3	7.0	0.84	208 (030G)	203.0
ABI-PRCI-X52-A5-1	73.5	119.3	0.078	90.4	90.4	7.5	0.81	203 (030G)	202.4
ABI-X52-A6-2	78.1	121.1	0.071	93.4	93.4	6.9	0.84	207 (030G)	203.0
ABI-PRCI-X52-A7-1	77.9	114.9	0.065	90.1	90.2	6.5	0.86	206 (030G)	199.2
ABI-PRCI-X52-A8-1	73.6	113.7	0.072	87.5	87.6	6.9	0.84	200 (030G)	197.0
ABI-X52W-10-1	67.7	108.1	0.077	82.1	82.1	7.4	0.82	187 (030G)	191.0
ABI-X52W-11-1	70.5	114.7	0.079	86.7	86.7	7.6	0.81	195 (030G)	194.1
ABI-X52W-12-1	71.2	113.0	0.076	86.1	86.1	7.2	0.83	193 (030G)	193.8
ABI-X52W-13-1	64.7	101.3	0.075	77.4	77.4	7.2	0.84	179 (030G)	186.2
ABI-X52W-14-1	71.6	111.4	0.073	85.6	85.6	7.0	0.84	194 (030G)	196.3
ABI-X52W-15-1	65.8	109.7	0.084	82.0	81.9	8.3	0.80	184 (030G)	192.1
ABI-X60-C1-2	79.2	120.4	0.069	93.5	93.5	6.8	0.85	208 (030G)	201.2
ABI-PRCI-X60-C2-1	84.7	125.2	0.065	98.3	98.4	6.4	0.86	221 (030G)	208.1
ABI-PRCI-X60-C3-1	83.0	122.9	0.065	96.4	96.5	6.5	0.86	218 (030G)	205.2
ABI-PRCI-X60-C4-1	84.2	122.4	0.062	96.7	96.8	6.3	0.87	218 (030G)	207.1
ABI-PRCI-X65-A5-1	81.1	122.6	0.068	95.4	95.5	6.7	0.85	215 (030G)	204.5
ABI-PRCI-X65-A6-1	83.3	124.4	0.066	97.3	97.3	6.5	0.86	219 (030G)	206.2
ABI-PRCI-X65-A7-1	83.3	126.0	0.068	98.1	98.1	6.6	0.85	219 (030G)	208.3
ABI-X60-A8-1	85.0	127.0	0.066	99.3	99.3	6.6	0.86	220 (030G)	204.0
ABI-PRCI-X65-C1-1	80.8	113.0	0.058	90.4	90.4	6.0	0.89	207 (030G)	198.3
ABI-PRCI-X65-C2-1	79.1	121.3	0.070	94.0	94.1	6.8	0.84	211 (030G)	204.7
ABI-PRCI-X65-C3-1	85.6	125.8	0.064	99.1	99.1	6.4	0.86	222 (030G)	207.2
ABI-X65-C4-1	76.9	111.1	0.063	87.5	87.6	6.3	0.88	200 (030G)	193.1
ABI-PRCI-X65-A5-1	81.1	122.6	0.068	95.4	95.5	6.7	0.85	215 (030G)	204.5
ABI-PRCI-X65-A6-1	83.3	124.4	0.066	97.3	97.3	6.5	0.86	219 (030G)	206.2

Test Name	Yield	Strength	Strain	Estimated	Calculated	Calculated	Ratio	ABI	Fracture
	Strength	Coefficient	Hardening	Engineering	Engineering	Uniform	Yield	Hardness	Toughness
		(K)	Exponent	UTS	UTS	Ductility	to		
	[ksi]	[ksi]	(n)	[ksi]	[ksi]	[%]	UTS		(ksi*in ^{0.5})
ABI-PRCI-X65-A7-1	83.3	126.0	0.068	98.1	98.1	6.6	0.85	219 (030G)	208.3
ABI-X65-A8-2	81.2	113.8	0.058	91.1	91.1	6.0	0.89	207 (030G)	198.6
ABI-X65W-9-1	73.5	112.3	0.070	86.9	86.9	6.8	0.85	194 (030G)	193.8
ABI-X65W-10-1	70.1	115.0	0.081	86.6	86.5	7.7	0.81	195 (030G)	196.9
ABI-X65W-11-1	67.9	89.6	0.052	72.9	73.0	5.6	0.93	175 (030G)	178.5
ABI-X65W-12-2	73.5	107.6	0.064	84.6	84.6	6.5	0.87	194 (030G)	192.0
ABI-X65W-13-1	76.1	113.9	0.068	88.7	88.8	6.6	0.86	202 (030G)	198.4
ABI-X65W-14-2	71.4	95.0	0.054	77.0	77.0	5.7	0.93	180 (030G)	181.0
ABI-PRCI-1018-SC2-3	52.5	88.8	0.088	65.6	65.6	10.2	0.80	155 (030G)	174.5
ABI-PRCI-1018-SC3-1	61.5	99.9	0.081	75.2	75.2	7.8	0.82	176 (030G)	186.9
ABI-PRCI-1018-SC4-1	56.1	92.5	0.084	69.1	69.0	8.3	0.81	163 (030G)	179.4
ABI-PRCI-1018-SC5-1	60.6	95.8	0.077	72.7	72.7	7.4	0.83	170 (030G)	182.0
ABI-1018-SA6-3	58.2	98.0	0.086	72.9	72.8	8.8	0.80	167 (030G)	180.2
ABI-PRCI-1018-SA7-1	53.6	89.6	0.087	66.5	66.4	9.8	0.81	159 (030G)	174.7
ABI-PRCI-1018-SA8-1	55.1	84.9	0.076	64.7	64.7	7.2	0.85	157 (030G)	172.5
ABI-PRCI-1018-SA9-1	61.9	93.9	0.072	72.4	72.4	6.9	0.85	171 (030G)	180.5

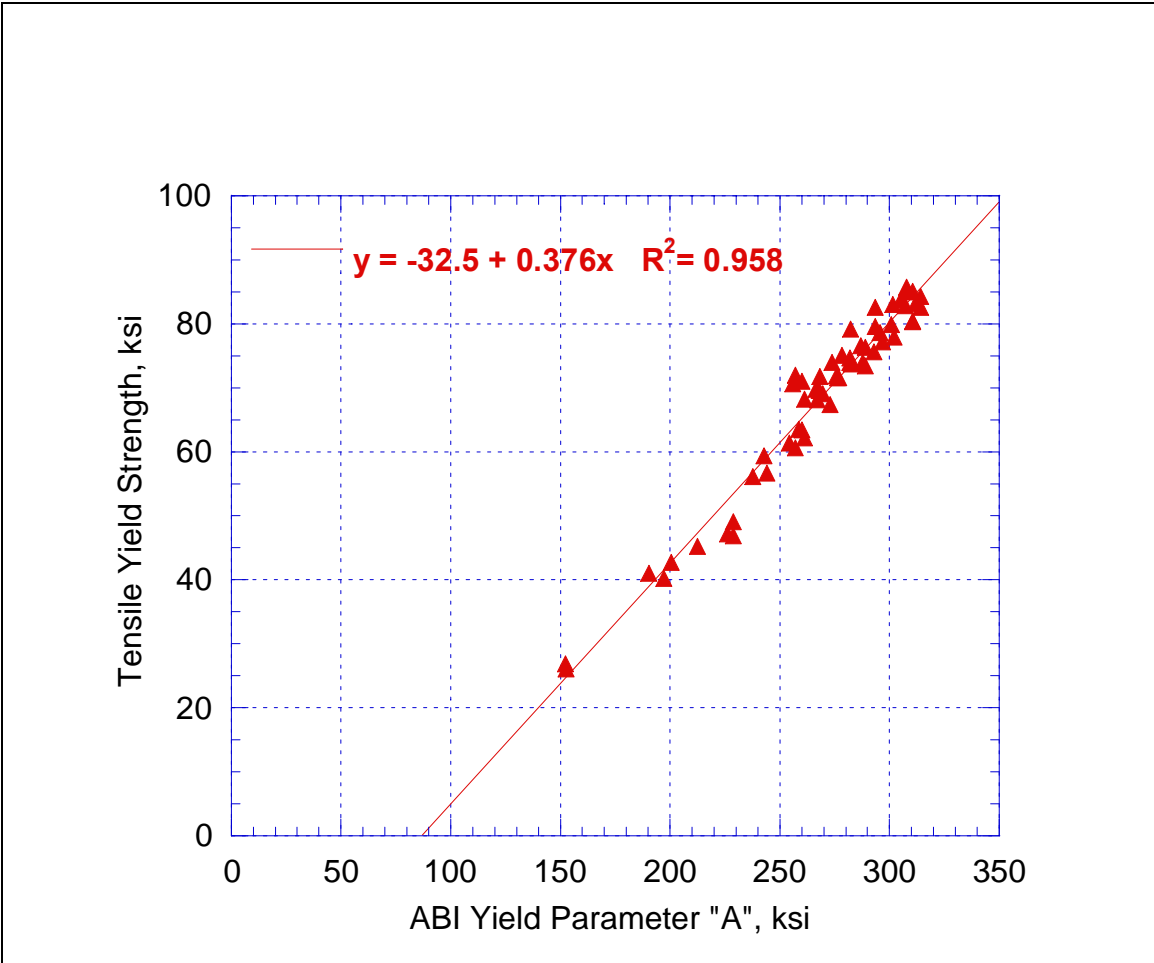


Fig. D1 Yield strength from miniature tensile versus the yield parameter “A” from ABI tests on the end tabs of these miniature tensile specimens.

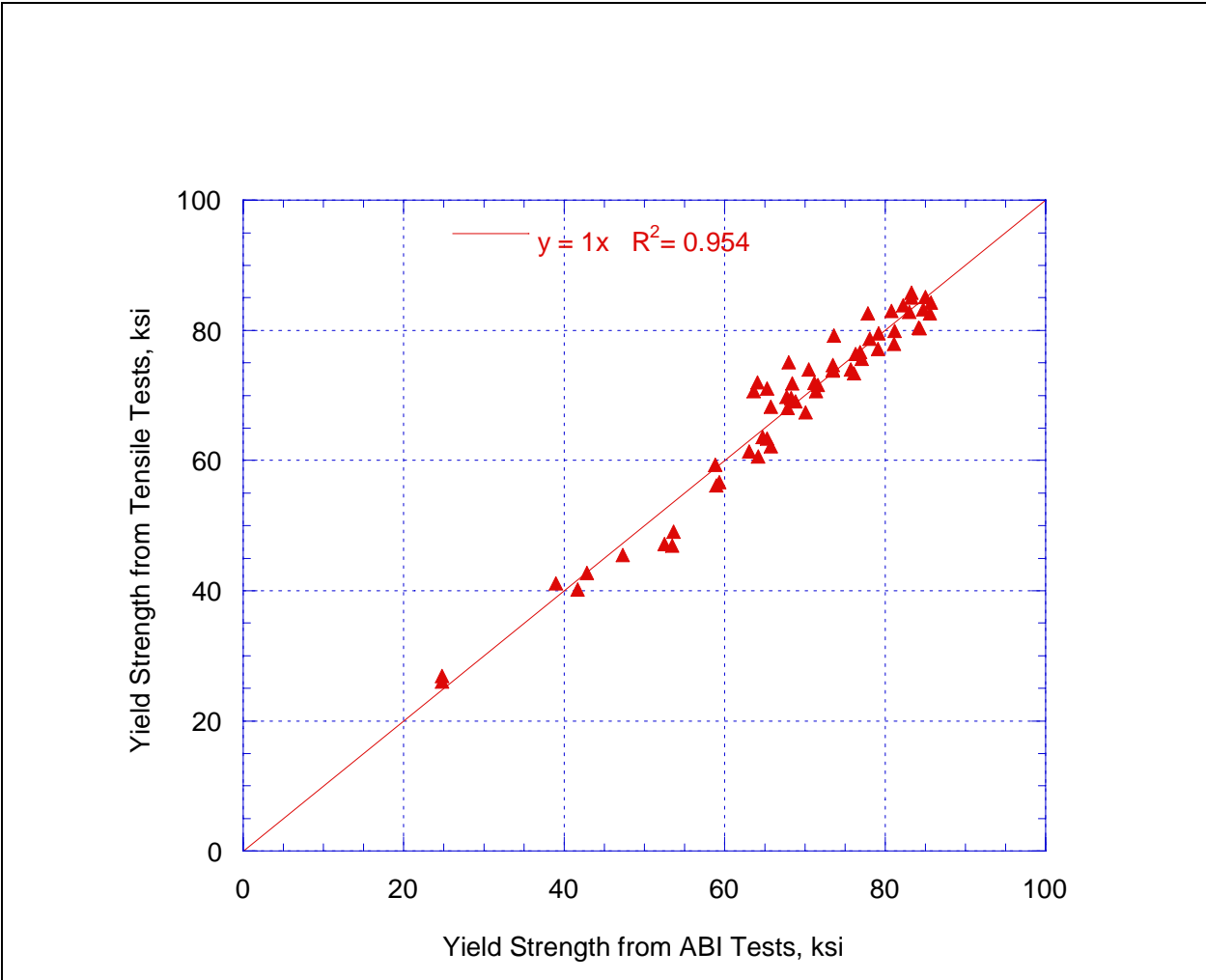


Fig. D2 Comparison of yield strength values from tensile and ABI tests.

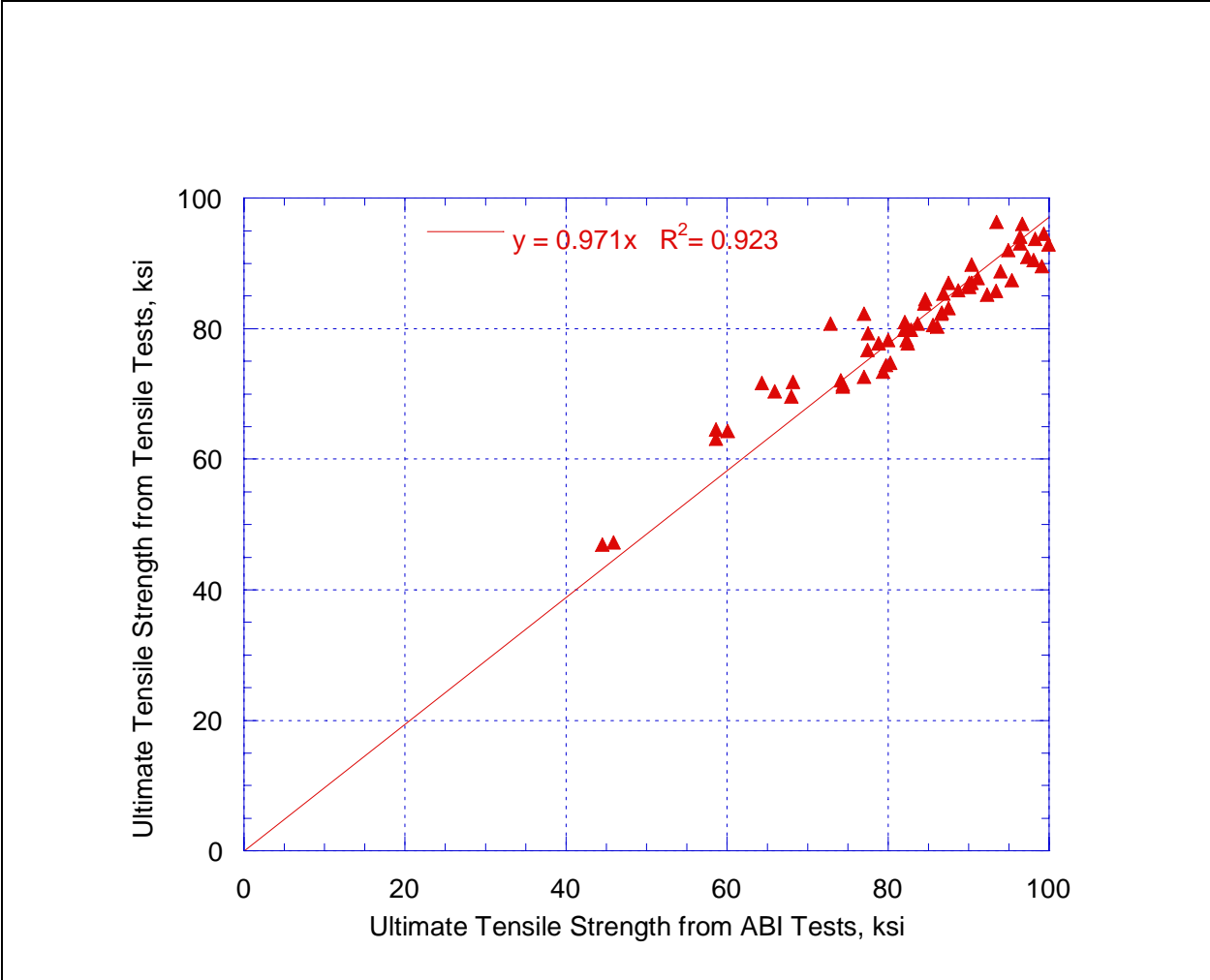


Fig. D3 Comparison of ultimate tensile strength (TS) values from tensile and ABI tests.

APPENDIX E

Fracture Toughness from Destructive Tests and from ABI Tests

Table E1 Detailed Summary of Destructive Fracture Toughness Test Results and Comparison with Nondestructive Haggag Toughness Method (HTM)

Material	Test Name	Test Temp., (F)	J _{1c} or J _b (lb/in)	Destructive Fracture Toughness (KJc) from J _{1c} or J _b , (ksi*in ^{.5})	Nondestructive HTM Fracture Toughness (KJc) from ABI, (ksi*in ^{.5})	Initial Crack Measured (in)	Initial Crack Calculated (in)	Final Crack Measured (in)	Final Crack Calculated (in)	Comments ^a
1018 Base	PRCI-1018-FT-1	70	1075.3	188.3	181.0	0.2010	0.2181	0.2470	0.2510	
1018 Base	PRCI-1018-FT-2	70	828.3	165.2	176.3	0.1960	0.2027	0.2380	0.2477	
1018 Base	PRCI-1018-FT-3	70	965.0	178.4	180.5	0.2070	0.2116	0.2660	0.2558	
1018 Base	PRCI-1018-DC-4	70	936.5	175.7	179.1	0.2020	0.2011	0.3010	0.2752	No side grooving, J _b , C10
X60 Base	PRCI-X60-FT-1	70	924.9	174.6	192.6	0.2040	0.2063	0.2470	0.2465	
X60 Base	PRCI-X60-FT-3	70	1089.4	189.5	204.0	0.2030	0.2056	0.2530	0.2509	
X60 Base	PRCI-X60-FT-4	70	959.2	177.8	193.2	0.2020	0.2074	0.2610	0.2567	
X60 Base	PRCI-X60-DC-2	-22	842.7	166.7	N/A	0.2050	0.2036	0.2920	0.2681	No cleavage, J _b , C4
X42 Base	PRCI-X42-FT-1	-118	1113.0	191.6	N/A	0.2021	0.2062	0.2021	0.2060	Cleaved, Invalid, J _c
X42 Base	PRCI-X42-FT-2	-4	1129.5	193.0	N/A	0.2010	0.2055	0.2740	0.2628	No cleavage, J _b , C10
X42 Base	PRCI-X42-FT-3	70	1053.1	186.3	181.5	0.2040	0.2069	0.2670	0.2684	
X42 Base	PRCI-X42-FT-4	70	1198.6	198.8	189.6	0.2130	0.2124	0.2560	0.2553	
X42 Weld	PRCI-X42W-5	70	1083.2	189.0	188.3	0.2040	0.2102	0.2510	0.2480	
X42 Weld	PRCI-X42W-6	70	1108.8	191.2	191.0	0.2100	0.2046	0.2700	0.2609	J _b , C6
X42 Weld	PRCI-X42W-7	70	1142.5	194.1	192.8	0.1980	0.2100	0.2540	0.2509	
X52 Base	PRCI-X52-FT-1	70	620.7	143.0	198.5	0.2105	0.2123	0.2740	0.2647	Invalid crack shape
X52 Base	PRCI-X52-FT-2	70	689.9	150.8	203.0	0.2030	0.2056	0.2670	0.2503	Invalid crack shape
X52 Base	PRCI-X52-FT-3	70	559.4	135.8	187.3	0.1930	0.2027	0.2660	0.2646	Invalid crack shape
X52 Weld	PRCI-X52W-5	70	1153.9	195.0	191.0	0.2100	0.2044	0.2720	0.2627	
X52 Weld	PRCI-X52W-6	70	948.8	176.9	186.2	0.2040	0.2113	0.2750	0.2629	
X52 Weld	PRCI-X52W-7	70	1472.3	220.3	196.3	0.1940	0.2050	0.2560	0.2533	J _b , C9

X65 Base	PRCI-X65-FT-1	70	1430.1	217.1	193.3	0.2100	0.2148	0.2560	0.2574	Jb, C11
X65 Base	PRCI-X65-FT-2	70	1255.5	203.4	184.5	0.2120	0.2174	0.2620	0.2613	Jb, C8
X65 Base	PRCI-X65-FT-3	70	1465.0	219.8	196.9	0.2000	0.2000	0.2520	0.2515	Jb, C6
X65 Weld	PRCI-X65W-4	70	1518.4	223.7	199.1	0.1950	0.2078	0.2320	0.2643	Jb, C8
X65 Weld	PRCI-X65W-5	70	1556.6	226.5	199.5	0.2000	0.2129	0.2630	0.2687	Jb, C9
X65 Weld	PRCI-X65W-6	70	1634.5	232.1	202.0	0.2000	0.2054	0.2600	0.2473	Jb, C6

^aJb is the J-integral at the test cycle (e.g, C6, C8, etc.) where the blunting process is at its end before commencing of slow crack extension. This new analysis method is more conservative than the standard/empirical 0.008-inch crack extension (E1820). Furthermore, this method provides reasonable initiation fracture toughness since the ductility of the material and the specimen small thickness resulted in severe lack of constraint despite the side grooving of the specimens. The results from the X52 specimens were invalid because of the shape of the fatigue crack front as well as of the final crack front shape. The result from Specimen PRCI-X42-FT-1 (cleaved at -118°F) is invalid because of exceeding the specimen capacity according to Equation 1 of ASTM Standard E1921-05.

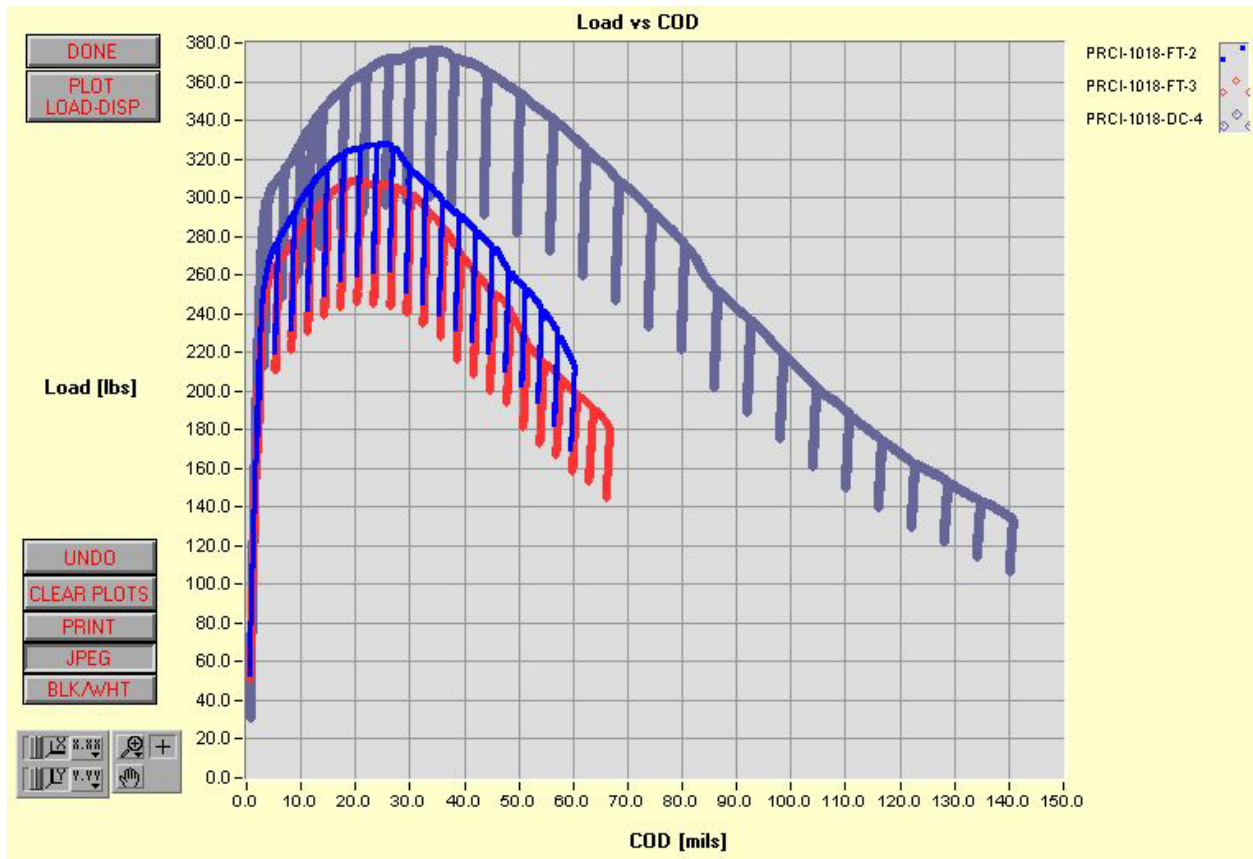


Fig. E1 Example of load versus crack opening displacement (COD) data from the disk compact specimens of the 1018 steel material.

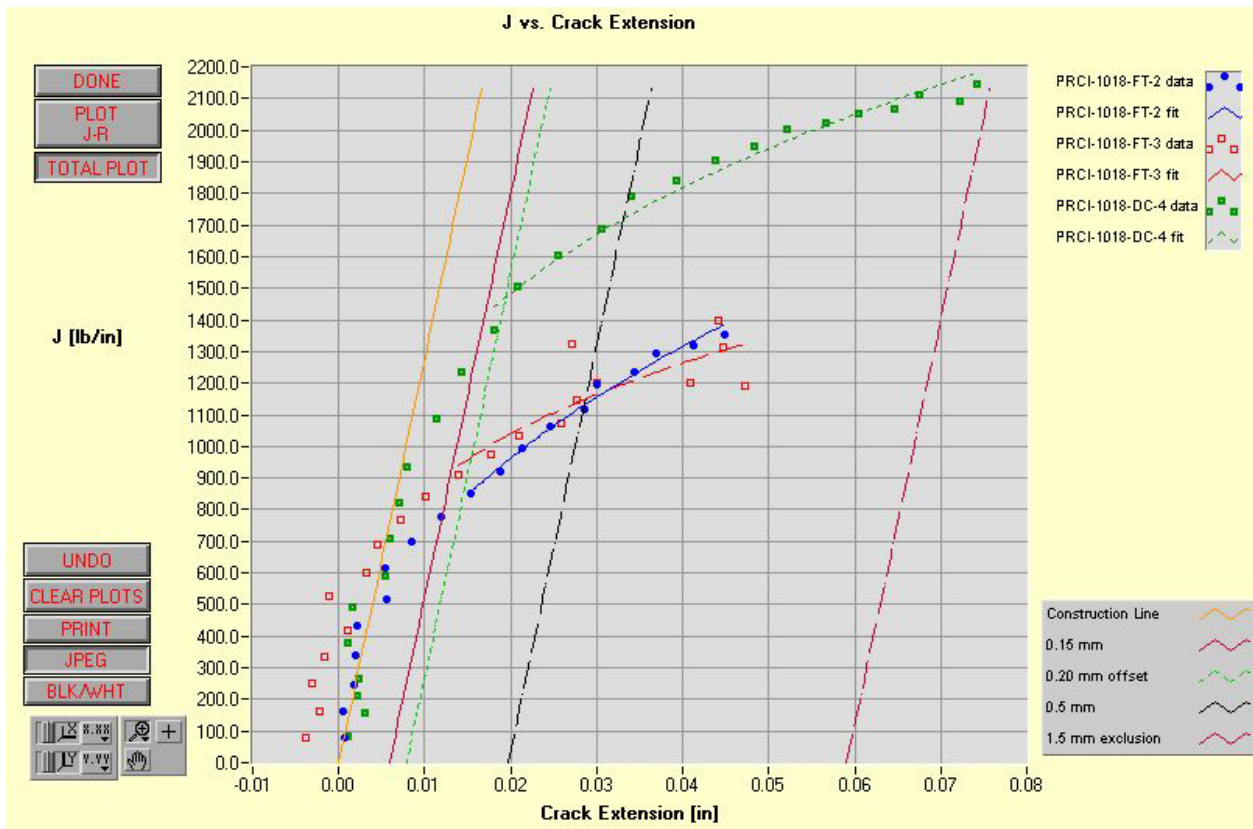


Fig. E2 Example of the J-R curves from the previous data of the 1018 steel material.



Fig. E3 Example of load versus crack opening displacement (COD) data from the disk compact specimens of the X42 pipeline steel material. Specimen Number “PRCI-X42-FT-1” cleaved since it was tested at -118°F. The other three specimens were tested at room temperature.

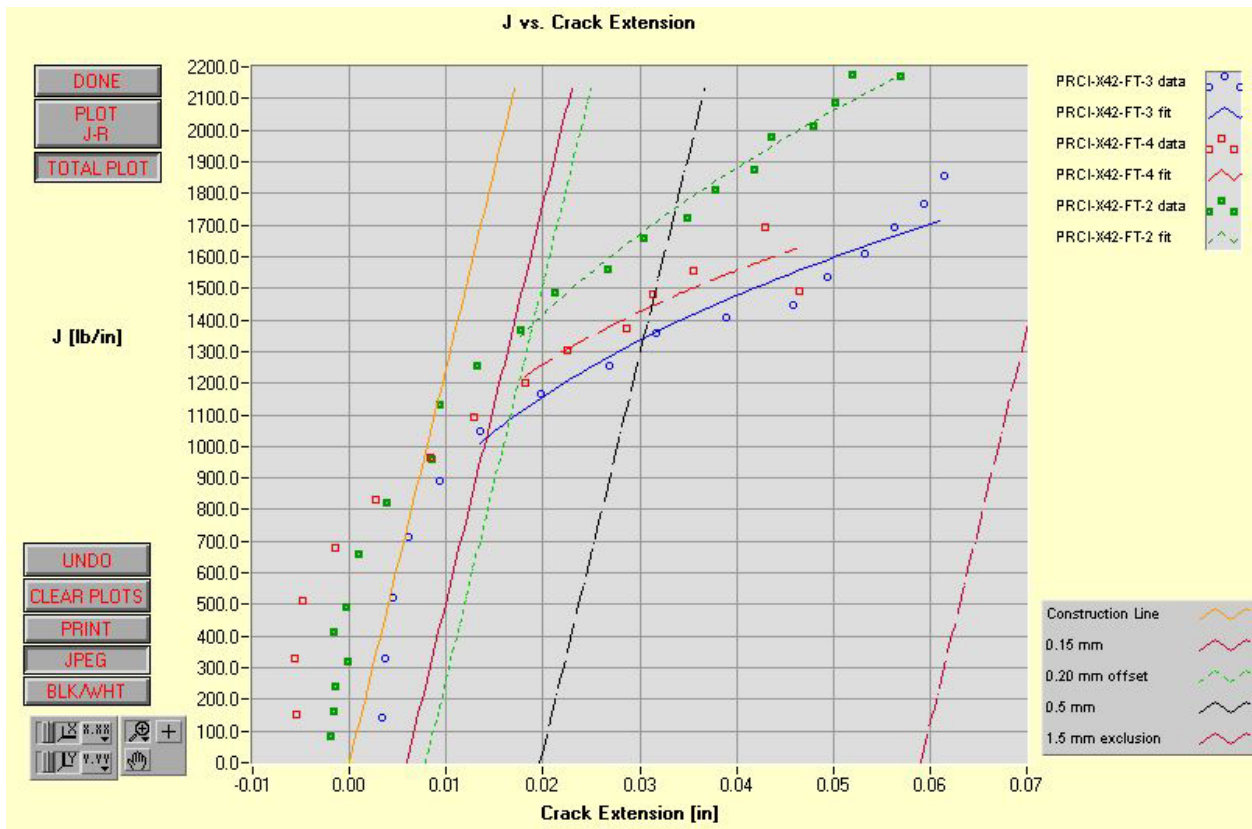


Fig. E4 Example of the J-R curves from the previous data of the X42 pipeline steel material. Specimen PRCI-X42-FT-1 did not generate an R-curve since it cleaved.

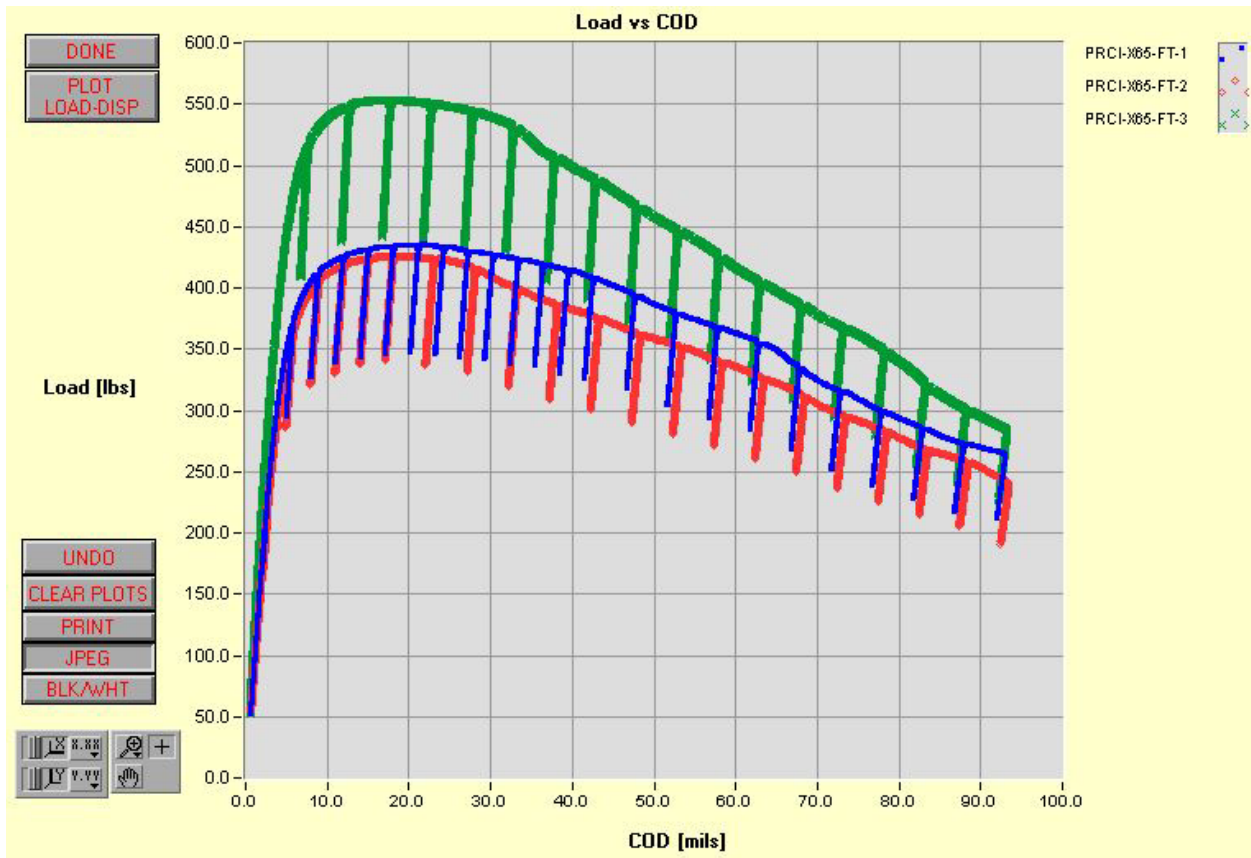


Fig. E5 Example of load versus crack opening displacement (COD) data from the disk compact specimens of the X65 pipeline steel material.

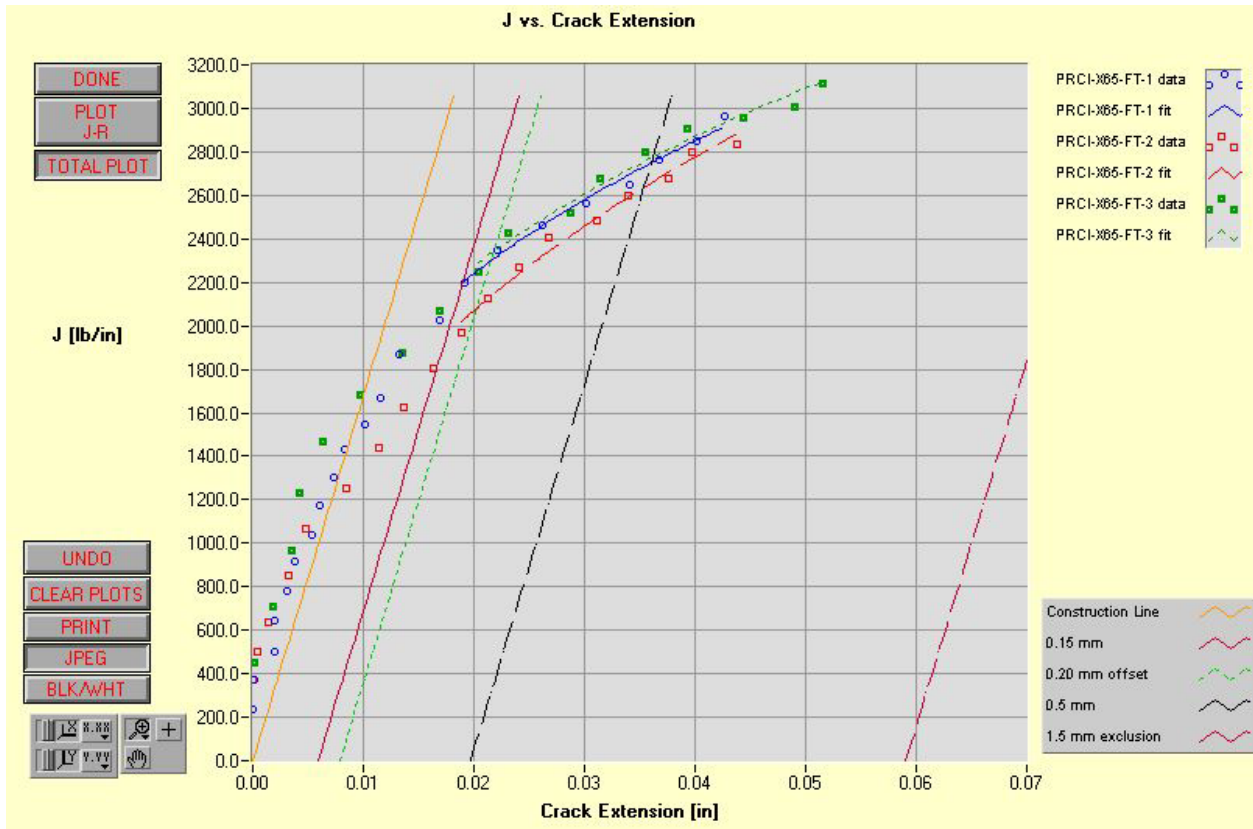


Fig. E6 Example of the J-R curves from the previous data of the X65 pipeline steel material.

This Page Intentionally Left Blank

Copyright, 2007
All Rights Reserved by Pipeline Research Council International, Inc.

PRCI Reports are Published by **Technical Toolboxes, Inc.**



3801 Kirby Drive, Suite 340
Houston, Texas 77098
Tel: 713-630-0505
Fax: 713-630-0560
Email: info@ttoolboxes.com